PHYSIOLOGICAL AND BEHAVIORAL CHANGES IN A ROTENONE MODEL OF DOPAMINE NEUROTOXICITY AND NEURODEGENERATION IN ZEBRAFISH

Jonathan Keow

A thesis submitted to the Faculty of Graduate and Postgraduate Studies in partial fulfillment of the requirements for the degree of

DOCTOR OF PHILOSOPHY IN BIOLOGY

Ottawa-Carleton Institute for Biology
University of Ottawa
Ottawa, Canada

September, 2016

Dedication

I would like to dedicate this thesis to my beautiful wife, Kara. It is with your constant love, encouragement and support that I am the best version of myself, and it is because of you that I am where I am today.

Much love, forever.

Abstract

Rotenone is a commercially available pesticide with a variety of industrial applications. However, occupational exposure to rotenone has been implicated in the development of Parkinson's disease. To explore the mechanism of dopamine neuron death secondary to rotenone exposure, the zebrafish was used as a live animal screening tool for environmentally-induced Parkinson's disease. After testing a variety of small molecule compounds on embryonic zebrafish for their potential to cause dopamine neuron loss, we identified that rotenone exposure induces a bradykinetic dopamine neuron loss phenotype. This phenotype was characterized by decreased locomotion, sensory insensitivity, and a transient but marked decrease in the number of dopamine neurons in embryos exposed to 100nM rotenone, with a concomitant decrease in *dopamine transporter* mRNA levels. The dopamine neuron deficits were observed in the subpallium, pretectum, olfactory bulb, but these losses were most pronounced in the ventral diencephalon after rotenone exposure. Rotenone damages the mitochondria, generating reactive oxygen species (ROS), and subsequently induces ROS-mediated apoptosis in these dopamine neurons. The rotenone-induced dopamine neuron loss and locomotion phenotypes could be partially rescued in zebrafish larvae with ascorbic acid co-treatment during rotenone exposure. Adults raised from zebrafish embryos exposed to rotenone did not show any deficits to their dopamine neuron distribution, but did show anxiety-like behaviors and upregulation of dopamine receptor D1 mRNA levels. These results suggest that rotenone exposure can cause dopamine neuron death through ROS-mediated apoptosis, and supports an environmental cause of Parkinson's disease.

La roténone est un pesticide disponible dans le commerce et utilisé pour une variété d'usages industriels. Cependant, l'exposition à la roténone a été impliquée dans le développement de la maladie de Parkinson. Afin d'explorer le mécanisme menant à la perte de neurones dopaminergiques suite à une exposition à la roténone, le poisson-zèbre (*Danio rerio*) a été utilisée comme modèle animal du développement de la maladie de Parkinson attribuable à des causes environnementales. Après avoir testé une série de petites molécules sur des embryons de poisson-zèbre pour déterminer leur capacité à causer une perte de neurones dopaminergiques, nous avons identifié la roténone comme causant un phénotype de perte de neurones associée à une bradykinésie. Ce phénotype était caractérisé par une perte de la locomotion, une insensibilité sensorielle, et une diminution transitoire mais marquée du nombre de neurones dopaminergiques chez des embryons exposés à une concentration de roténone de 100nM. Ceci coïncidait avec une réduction des niveaux d'expression du gène du transporteur de la dopamine (*dat*). Des pertes de neurones dopaminergiques furent observés dans le sub-pallium, le pré-tectum et le bulbe olfactif mais étaient plus prononcées dans le diencéphale ventral. La roténone cause des dommages aux mitochondries en générant des dérivés réactifs de l'oxygène (ROS) et, subséquemment, induit une apoptose attribuable aux ROS dans les neurones dopaminergiques. La perte de neurones dopaminergiques due à la roténone ainsi que les déficits locomoteurs ont pu être partiellement empêchés par un co-traitement à l'acide ascorbique. Les poissons adultes ayant été exposés à la roténone au stade embryonnaire ne montrèrent pas de déficits quant à la distribution des neurones dopaminergiques mais présentaient des comportements indiquant un plus haut niveau d'anxiété ainsi qu'une

augmentation des ARNm du récepteur D1 de la dopamine. Ces résultats suggèrent que l'exposition à la roténone peut causer la mort des neurones dopaminergiques via une apoptose médiée par les ROS et pourrait constituer une cause environnemental de la maladie de Parkinson.

Table of contents

List of Figures

List of Tables

List of Abbreviations

Alpha-synuclein	SNCA
Central nervous system	CNS
Complementary DNA	cDNA
Days post-fertilization	dpf
Diencephalic cluster	DC
Dimethylsufoxide	DMSO
Dopamine receptor	dr
Dopamine transporter	dat
Enhanced green fluorescent protein	EGFP
Fluorescence-activated cell sorting	FACS
Gamma amino-butyric acid	GABA
Glutamic acid decarboxylase	GAD
Green fluorescent protein	GFP
Hours post-fertilization	hpf
Hypothalamic clusters	Hc
Messenger RNA	mRNA
1-methyl-4-phenyl-1,2,3,6-tetrahydropyridine	MPTP
1-methyl-4-phenyl-1,2,3,6-tetrahydropyridium	MPP+
Oxidopamine	6-OHDA
Phosphate-buffered saline	PBS
Polymerase chain reaction	PCR
Pretectum	Pr
Quantitative polymerase chain reaction	qPCR
Reactive oxygen species	ROS
Ribonucleic acid	RNA
Risk ratio	RR
Subpallium	SP
Telencephalon	Tel
Transgenic	Tg
Tyrosine hydroxylase	TH
Ventral diencephalon	vDC

Acknowledgements

This thesis is a compilation of the scientific findings spread over a number of years, and originate from the hard work and dedication of a number of very talented individuals. I would like to acknowledge the hard work of two very talented honors research students, Maris Young and Daphnée Tosoni, as well as Eyal Podolsky and Simon Martel. Numerous complex techniques were used in this body of work, and their success was only possible with the technical expertise of Ana Giassi at the University of Ottawa Core Histology Laboratory, Andrew Ochalski and Christopher Clouthier at the University of Ottawa Cellular Imaging and Cytometry Facility and Berezovsky Laboratory, as well as Mirela Hasu at the Animal Core Behavior Laboratory, and Vera Tang at the University of Ottawa Flow Cytometry & Virometry Core Facility. I would also like to acknowledge both Christine Archer and William Fletcher for their stewardship of the Animal Care facilities at the University of Ottawa, as well as research associates Gary Hatch and Vishal Saxena for their help and continued guidance. I would also like to thank Canadian Institute for Health Research for funding my research project, as well as for the CIHR Frederick Banting and Charles Best Doctoral Award. Most importantly, I would like to acknowledge the omnipresence of support and encouragement from my parents, my sister and my beloved wife Kara, without whom I would have never found the inner strength to complete this project. Lastly, I would like to thank both my research supervisor Marc Ekker, and my program director Michael Schlossmacher for their mentorship, guidance and continued effort in pushing me to succeed and thrive throughout this journey.

Statement of Contributions

A portion of the results in this thesis was only made possible with the tireless work and cooperation of Simon Martel, an extremely talented undergraduate student. As co-lead authors, these results were synthesized and published in the University of Ottawa Journal of Medicine as Martel *et al.* (2015).

Introduction

Parkinson's disease is a neurodegenerative disorder that results from the loss of dopamine-producing neurons in the *substantia nigra* of the brain. Amongst neurodegenerative nervous system disorders, Parkinson's disease is the second most common neurodegenerative disorder after Alzheimer's disease, and it is estimated that Parkinson's disease affects over 1% of the population above the age of 65 (Van Den Eeden *et al.*, 2003). Parkinson's disease is classified by a clinical diagnosis of movement difficulty, tremor at rest, and other fine motor control loss, which are classified collectively as a parkinsonism phenotype (reviewed in Massano and Bhatia, 2012). Ultimately, the underlying pathology of this disease is caused by the loss of dopamine-producing neurons in the *substantia nigra*, a deep midbrain structure responsible for modulating the motor control in the basal ganglia (Damier *et al.*, 1999).

1.1 Dopamine synthesis and metabolism

Dopamine is a catecholaminergic neurotransmitter that plays an integral role in many neurological pathways in vertebrate biology. These dopamine-dependent pathways are primarily responsible for learning and reward-seeking behaviors, but are also involved in the regulation of hormone secretion and most importantly to Parkinson's disease, motor control (reviewed in Elsworth *et al.*, 1997). Dopamine is first synthesized in these dopaminergic neurons by the conversion of the amino acid tyrosine into the dopamine precursor L-DOPA. This reaction results in the addition of a hydroxyl group into the *ortho*- position of the hydroxyphenyl ring, and uses the enzyme tyrosine hydroxylase

(TH) to catalyze this reaction (figure 1.1). This initial chemical conversion is the rate limiting step in *de novo* dopamine synthesis because the conversion of the 4-hydroxyphenyl R-group on tyrosine into a 3,4-dihydroxyphenyl R-group is stereochemically challenging and electronegatively unstable (reviewed in Daubner *et al.*, 2011). It is also hypothesized that dopamine synthesis may also be oxidatively stressful due to the involvement of oxygen molecules as a substrate for this synthesis reaction (reviewed in Miyazaki and Asanuma, 2008). L-DOPA is then converted to dopamine by the removal of the terminal carboxy- moiety on L-DOPA using the enzyme dopa decarboxylase (figure 1.1). This allowed the newly synthesized dopamine molecules to be imported into synaptic vesicles with the enzyme vesicular monoamine transporter 2 for secretion into the synaptic cleft in response to the propagation of a neurotransmitted signal. Dopamine can also be reabsorbed back into the neuron from the synaptic cleft using the dopamine transporter (dat), a process that leads to the conservation and reuse of expended dopamine and reduction in the need for *de novo* dopamine synthesis. Each of these proteins confers dopaminergic properties to these neurons (reviewed in Meiser *et al.*, 2013). A normal and healthy dopaminergic pathway therefore functions to release dopamine into the synaptic cleft, which subsequently results in neurotransmitter signaling in the postsynaptic neuron through D_1-like and D_2-like family of dopamine receptors. These dopamine receptors are G-protein coupled receptors that effect downstream physiological changes responsible for cognition, memory, emotion, learning and motor function (reviewed in Beaulieu and Gainetdinov, 2011). The D_1-like family of dopamine receptors often act as a positive regulator of addictive behavior, and a net increase in this

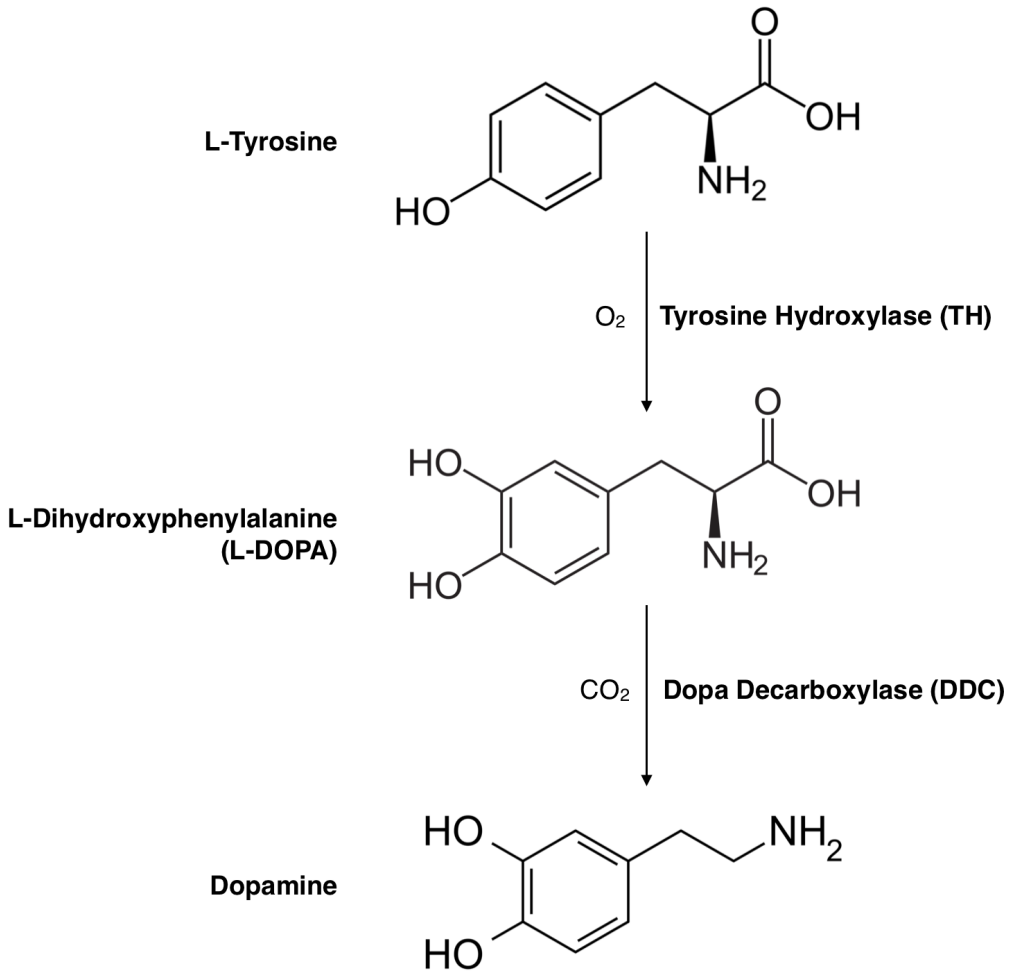

Figure 1.1: Dopamine synthesis pathway
The major components of the de novo dopamine synthesis pathway are listed above. De novo dopamine synthesis originates with the conversion of L-tyrosine to L-DOPA (L-dihydroxyphenylalanine) using the enzyme tyrosine hydroxylase (TH). This step is commonly recognized as the rate limiting step in the synthesis of dopamine. L-DOPA is then quickly converted into dopamine by dopa decarboxylase (DDC). Dopamine is then packaged into vesicles for neurotransmission or used as a staring product for the synthesis of norepinephrine.

dopamine receptor signaling in the *nucleus accumbens* modulates the reward-based learning pathway. However, D_2-like family of dopamine receptors are responsible for the neurocognitive effects of dopamine signal modulation (reviewed in Beaulieu and Gainetdinov, 2011).

1.2 The four main dopamine pathways

There are four main dopamine pathways in the human central nervous system: the mesolimbic, mesocortical, tuberoinfundibular and nigrostriatal pathways (reviewed in Beaulieu and Gainetdinov, 2011). The mesolimbic pathway is responsible for the connection between the ventral tegmentum of the midbrain to the *nucleus accumbens septi* in the basal forebrain. This pathway is important for the processing of reward stimuli, releasing dopamine as a positive signal in the *nucleus accumbens septi* in response to pleasure and reward-related learning. Upon stimulation, the *nucleus accumbens septi* then communicates to the prefrontal cortex, amygdala and hippocampus to influence behavioral decision-making, emotional responses and memory respectively. Since dopamine release in this pathway is important for processing reward stimuli, this pathway is not only involved in the governance of pleasure-seeking behavior, but also in the underlying pathophysiology for diseases of addiction (reviewed in Le Foll *et al*., 2009). The mesocortical pathway is closely associated with the functions of the mesolimbic pathway and primarily controls the cognitive effects of reward-based learning. By connecting the ventral tegmentum to the frontal lobes, this pathway appears to regulate the emotional and affective aspects of motivational learning, and its

misregulation can lead to the cognitive symptoms of schizophrenia (reviewed in Davis *et al.*, 1991). Hormonal control is primarily regulated by the tuberoinfundibular pathway, which connects the arcuate nucleus in the hypothalamus to the neuroendocrine system in the pituitary gland. This pathway primarily modulates the dopamine-dependent secretion of prolactin, a hormone important in reproduction, mammary function and gestational regulation in mammals (reviewed in Fitzgerald and Dinan, 2008). Lastly, the nigrostriatal pathway is a series of dopaminergic neurons connecting the *substantia nigra* to the neurons of the dorsal striatum in the basal ganglia, and primarily involved in the modulation of extrapyramidal motor signals by acting on the secretion of inhibitory gamma aminobutyric acid (GABA) neurotransmitter secretion in the basal ganglia (Tritsch *et al.*, 2012).

The basal ganglia are a group of primitive basal forebrain structures that play a critical role in modulating cortical motor signals through the thalamus (reviewed in Groenewegen, 2003). The *substantia nigra* acts to control the basal ganglia through the direct and indirect motor movement pathways to facilitate wanted and unwanted thalamic motor signals from the motor cortex. Through the direct pathway, the *substantia nigra* promotes the acceptance of cortico-thalamic signals by decreasing the amount of inhibitory signaling released by the striatum. The dopaminergic nigrostriatal projections synapse onto the GABAergic neurons in the *globus pallidus interna*, GABAergic neurons which normally act to suppress cortico-thalamic signals. Secretion of dopamine will decrease the amount of GABA produced by the *globus pallidus interna* via D_1-like

dopamine receptors, so inhibition of the suppressive signals from the *globus pallidus interna* neurons will therefore increase the acceptance of thalamic motor signals. The indirect pathway has the opposite effect, and acts to exclude cortico-thalamic signals by increasing the inhibitory activity of the striatum. Dopaminergic nigrostriatal projections synapse onto GABAergic neurons in the *globus pallidus externa*, which typically acts to silence the subthalamic nucleus in the ventral striatum. The subthalamic nucleus typically acts to promote signaling in the *globus pallidus interna* via excitatory glutamatergic connections. Therefore, secretion of dopamine causes inhibition of the *globus pallidus externa* via D_2-like dopamine receptors, allowing the subthalamic nucleus to freely excite the *globus pallidus interna.* This then promotes the transmission of suppressive signals from the the *globus pallidus interna* neurons exclude thalamic motor signals. These pathways work in parallel to refine the overall net signal transmission from the motor cortex, and select for specific motor pathways from the motor cortex. The loss of the dopamine neurons in the *substantia nigra* (and subsequently the nigrostriatal pathway) causes an overall net increase in the inhibitory effect of basal ganglia on cortico-thalamic motor signal modulation (reviewed in Calabresi *et al.*, 2014) by failing to promote the direct pathway and disinhibiting the indirect pathway. This increase in thalamocortical pathway inhibition therefore suppresses movement, giving rise to the motor symptoms of Parkinson's disease.

1.3 Etiology and Pathophysiology of Parkinson disease

Parkinson's disease can occur through both genetic mutations (hereditary/monogenic), exposure to environmental and neurotoxins (sporadic/secondary), or through a combination of both (complex disease). Pathologically, there are 2 major neuropathologic findings in Parkinson disease: the presence of alpha-synuclein (SNCA) aggregates known as Lewy bodies in the dopamine neurons of the *substantia nigra* (Braak *et al.*, 1999) and the loss of dopamine neurons most prominently in the ventral lateral *substantia nigra* (reviewed in Massano and Bhatia, 2012). Without these dopamine neurons, the *substantia nigra* loses its pigmented appearance, and this becomes visible in the midbrain during autopsy. This loss of nigrostriatal control of the basal ganglia causes thalamic overinhibition of the signals from the motor cortex, leading to the characteristic stiffness and rigidity seen in patients with Parkinson's disease (reviewed in Sulzer *et al.*, 2016). Approximately 60-80% of dopaminergic neurons are lost before the motor signs of Parkinson disease emerge (reviewed in Cheng *et al.*, 2010). Exposure to environmental agents and neurotoxins can also cause mitochondrial dysfunction and impairment, which may release ROS and lead to apoptosis or disruption of protein degradation pathways.

The etiology for Parkinson's disease as a whole is poorly understood, with an equally poorly understood etiology of the neurodegeneration and loss of dopaminergic neurons in the *substantia nigra* of the brain. A small percentage of Parkinson's disease patients may present with a family history of Parkinson's disease, thus implying a hereditary monogenetic component to their disease. Recessive loss-of-function mutations in genes

such as parkin, DJ-1, and PINK1 can cause mitochondrial dysfunction and accumulation of reactive oxidative species (ROS), which may cause premature degeneration of these neurons (reviewed in Dodson and Guo, 2007). Dominant missense mutations in SNCA and LRRK2 affect protein degradation pathways, leading to protein aggregation and formation of Lewy bodies (reviewed in Shulman *et al.*, 2011). Regardless of the gene affected, a common feature to these mutations is an impairment in dopamine production, release or transmission. However, the vast majority of Parkinson's disease tends to affect patients over the age of 50 without a clear hereditary genetic component (reviewed in Lang and Lozano, 1998). Current treatment for Parkinson's disease is symptomatic, and act by supplementing the low levels of dopamine responsiveness with dopamine precursors (*e.g.* levodopa) or dopamine receptor agonists (*e.g.* pramipexole) (reviewed in Radad *et al.*, 2005). Virtually all drugs that act on the central nervous system (CNS) target a small number of well-understood neurotransmitter pathways, but the real challenge to developing a cure for Parkinson's disease rests in the migration of the goals of therapy from symptomatic management to preventing the progression of further neurodegeneration.

1.4 Environmental causes of Parkinson's disease

As mentioned previously, the majority of cases of Parkinson's disease have no known associated hereditable aspect. Since most cases of Parkinson's disease are not linked to a monogenetic defect, this suggests that the development of Parkinson's disease is multifactorial, and therefore dependent on a number of secondary factors (Kitada *et al.*,

2012). These non-genetic factors associated with development of Parkinson's disease included leading a farming lifestyle (Moisan *et al.*, 2015), recurrent head injury (Taylor *et al.*, 2016), chronic pesticide exposure (Pezzoli and Cereda, 2013). We therefore sought to develop a platform with the goal of exploring potential environmental causes of Parkinson's disease.

One of the first chemicals discovered to be associated with Parkinson's disease was MPTP (1-methyl-4-phenyl-1, 2, 3, 6-tetrahydropyridine). This neurotoxin was first created as an accidental contaminant in the production of the illicit drug desmethylprodine. Drug users who self-injected this contaminated batch of desmethylprodine developed parkinsonism, which was unusual since desmethylprodine has opioid-like characteristics, and typically causes central depressant effects such as analgesia and respiratory depression (Sian *et al.*, 1999). Following this discovery, it was demonstrated that MPTP is selectively taken up by dopamine neurons, and becomes converted by the enzyme monoamine oxidase-B into its active metabolite MPP+ (1-methyl-4-phenylpyridinium), which then fastidiously binds to mitochondrial complex I, interfering with cellular respiration and leading to dopamine neuron cell death (Eberhart and Schulz, 2003). MPTP has since been used to create a reproducible model of Parkinson's disease in mice (reviewed in Meredith and Rademacher, 2011), zebrafish (Sallinen *et al.*, 2009) and apes (Porras *et al.*, 2012) with a single neurotoxin exposure.

Another chemical neurotoxin used in other animal models of Parkinson's disease is oxidopamine (6-hydroxydopamine), a structural analog of dopamine with strong oxidant properties (Simola *et al.*, 2007). Since this is a structural analog of dopamine, oxidopamine is readily taken up by dopamine transporter channels and quickly concentrates in dopamine neurons. Once inside dopamine neurons, the additional hydroxyl functional group on oxidopamine readily dissociates into a hydroxyl radical, causing free radical damage within these dopamine neurons, leading to cell death and neurodegeneration.

However, many of the chemicals that have been linked to the development of Parkinson's disease in humans according to retrospective and longitudinal studies are currently and widely used as commercial pesticides, herbicides and insecticides (table 1.1). Longitudinal studies of these environmental toxins have indicated that development of Parkinson's disease later in life is statistically increased with lifetime occupational exposures to pesticides (summary risk ratio, or sRR of 1.62), herbicides (sRR of 1.40) and insecticides (sRR of 1.50) (van der Mark *et al.*, 2012). Specifically, the herbicide paraquat, the fungicide ziram, the insecticide rotenone and methicone-containing opioids that are rich in manganese, are also linked to dopamine degeneration and Parkinson's

Name	Structure	Molecular weight	Description
MPTP (1-methyl-4-phenyl-1,2,3,6-tetrahydropyridine)	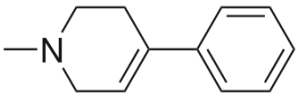	173.26 g/mol	Neurotoxin compound Byproduct of MPPP synthesis
MPP+ (1-methyl-4-phenylpyridinium)	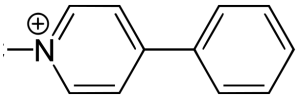	170.25 g/mol	Neurotoxin compound Active form of MPTP
Manganese(II) chloride ($MnCl_2$)	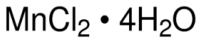	197.91 g/mol	Chronic exposure is linked to manganese poisoning and symptoms resembling Parkinson's disease
Paraquat (*N*,*N*′-dimethyl-4,4′-bipyridinium dichloride)	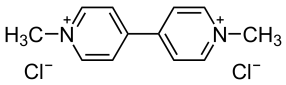	257.16 g/mol	Commercially available herbicide occupationally linked to the development of Parkinson's disease
Oxidopamine (6-hydroxydopamine)	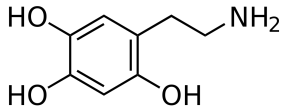	169.18 g/mol	Neurotoxin compound
Ziram (zinc dimethyldithiocarbamate)	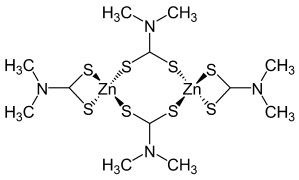	305.84 g/mol	Commercially available fungicide occupationally linked to the development of Parkinson's disease
Rotenone	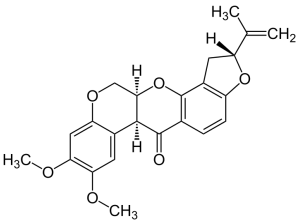	394.42 g/mol	Commercially available insecticide and piscicide occupationally linked to the development of Parkinson's disease

Table 1.1: Compounds associated with the development of Parkinson's disease
Listed above are a the names, structures, molecular weights and a brief description of compounds associated with the development of Parkinson's disease that were used in our study.

disease. Rotenone is one of the pesticides that has been associated with the development of Parkinson's disease, and can induce cytotoxicity through a powerful oxidative effect by inhibiting mitochondrial complex I (Li *et al.*, 2003). During oxidative phosphorylation, NADH (nicotinamide adenine dinucleotide, reduced form) is oxidized into NAD^+ causing the excess electrons to become shuttled onto mitochondrial complex I. These electrons are then typically shuttled onto mitochondrial complex III via coenzyme Q for controlled oxidation at complex IV with protons imported using the ATPase proton pump and free oxygen molecules (reviewed in Sazanov, 2015). However, inhibition of mitochondrial complex I prevents the electron transport chain from shuttling electrons onto complex III, and electrons accumulate in excess on mitochondrial complex I. Free oxygen can then radicalize by acquiring an electron from the electron-rich complex I, and become a superoxide radical (Li *et al.*, 2003). We hypothesize that this abundance of superoxide radicals, in addition to the oxidative stress of *de novo* dopamine synthesis can then overwhelm the cellular peroxisomes in dopamine neurons, which act as endogenous free radical buffer mechanisms. Subsequently, this abundance of free radicals can then cause ROS-mediated damage such as DNA-cross linking and protein misfolding, which can lead to apoptosis and cell death. The only published mammalian model of rotenone-induced PD involves the Lewis rat (Betarbet *et al.*, 2000) where Lewy body formation was observed, in addition to dopamine neuron loss and a motor phenotype consistent with the motor symptoms of PD (parkinsonism). Other milder phenotypes with no apparent parkinsonism after rotenone-exposure were also seen in mouse models (Thiffault *et al.*, 2000; Pan-Motojo *et al.*, 2010; Inden *et al.*, 2011).

Although small scale neurotoxin screens (including rotenone) using behavioral analysis have been performed on zebrafish to identify potential PD inducing agents, MPTP was the only toxin to yield conclusive results in zebrafish (Bretaud *et al.*, 2004).

1.5 Zebrafish models of various diseases

The majority of disease research in the last century has been focused primarily on mammalian systems, or systems that attempt to simulate mammalian pathology, such as tissue cultures or *in vitro* assays using mammalian gene products. However, experiments on mammalian systems are usually expensive, subject to stringent ethical constraints, are time-consuming and/or technically demanding. Furthermore, techniques that involve imaging are difficult, and usually impossible to perform *in vivo* with rats, mice, monkeys or humans. This challenge is further compounded by the extensive sample preparation required to visualize the brain through the considerably opaque skull, thus leading us to use tissue culture to answer our biological questions about neurophysiology.

Tissue culture cells are typically derived from tumor cells and often possess an abnormal cell cycle, an abnormal number of chromosomes, or are unresponsive to a large variety of biological signals in order to grow *in vitro*, away from the host organism. This unusual trait is not shared by other cells, and thus tissue culture cells may not always accurately represent an *in vivo* system depending on the experimental question. Changes observed within this simulated microenvironment may not always be biologically relevant, and the knowledge gained may be misleading with respect to processes involving a living animal.

These substantial limitations call for an alternative model for answering biological questions about physiology and disease. As a result, we have turned to using zebrafish to answer these questions, and as such, develop disease models in these zebrafish.

The zebrafish (*Danio rerio*) is a small tropical fish that has become a model organism for biology. This model organism was developed in the late 1970s by George Streisinger at the University of Oregon as an alternative model organism to the well-established mouse and *Drosophila* systems (but with shared characteristics) amenable to large scale mutagenesis experiments for studying functional genetics. The reproductive cycle of the zebrafish combines benefits from both previously mentioned organisms (Ma *et al.*, 2003). Zebrafish zygotes are functionally transparent, and can mature to an adult form within 96 hours post-fertilization. Since development occurs entirely *ex utero*, we can perform gross assessment of organ function and fluorescent epitope imaging. Often, a healthy breeding pair of zebrafish can produce upwards of 300 eggs in a clutch size with excellent survival rates, far surpassing the litter size of a murine breeding pair (Westerfield, 1995).

Since zebrafish embryos develop *ex utero* into an adult form within 96 hours, are transparent and amenable to continued, non-destructive observation of developmental processes in a living organism, embryos may be easily exposed to different chemicals with their effects observed in real time. Fortunately, the high embryo yield can be combined with high throughput techniques to mass screen the *in vivo* effects of chemical

treatments on observable phenotypes. Embryos can be distributed in multi-well plates, maintained for up to 7 days without feeding, and treated with minimal concentrations of small molecule compounds. Furthermore, the genome of the common zebrafish has been sequenced and annotated (Broughton *et al.*, 2001; Howe *et al.*, 2013) allowing us to perform forward and reverse genetic analyses. Therefore, the zebrafish provides an excellent model organism for answering many outstanding questions in chemical biology.

Within the past decade, a number of disease models have been developed in zebrafish, ranging from hematologic (Berman *et al.*, 2012) to neurologic (Linney *et al.*, 2004). The research depicted in these papers accurately models a variety of systems, such as the effect of low dose bisphenol A on learning deficits (Saili *et al.*, 2012) or characterization of the effects of LSD on the endocrine system (Grossman *et al.*, 2010). These projects serve as a proof-of-concept of the utility of zebrafish for studies in neurobiology, and demonstrate with ease the effects of exogenous compounds on these animals (Kyzar *et al.*, 2012). Furthermore, the high fecundity of zebrafish permits rapid and robust validation of observations, and allows us to elucidate cause-and-effect relationships.

1.6 Behavioral phenotypes can be used as reporters of physiological stress

Zebrafish exhibit a rich repertoire of behaviors, such as anxiety/fear-related behavior, cognitive behavior, social behavior, reward-related behavior, sexual behavior, pain-related behavior, sensory behavior, and sleep behavior, all of which can be altered in neurological phenotypes (reviewed in Kalueff *et al.*, 2013). These behaviors can be

assessed with a variety of assays, such as an acoustic startle assay, simple learning task (habituation training), locomotion assessment, or by fear response. The results of these assays may not be individually translatable to a specific behavioral phenotype observed in humans or other mammalian models of disease, but these diverse assays can generate a behavior barcode that provides an idea of the alteration in behaviors that are caused by exposure to a given environmentally administered compound. In combination with the observable morphological alterations as mentioned above, these behavioral and morphological data could be combined to establish a profile for each phenotype, and similarities in phenotypes could be assessed for chemical similarity. The locomotor phenotype of Parkinson's disease has been established by exposing zebrafish embryos to MPTP, a potent neurotoxin described above which is selective to dopaminergic neurons. Exposure to MPTP caused bradykinesia and an impaired touch-response in zebrafish embryos, implicating the loss of dopamine neurons with a hypomotility behavior phenotype in this animal model (Xi *et al.*, 2011b).

1.7 Dopaminergic areas of the zebrafish brain

The zebrafish provides a powerful platform for examining changes to neuronal patterning, and researchers have been able to leverage the transparency of zebrafish embryos to map the network of catecholaminergic neurons. The catecholaminergic system in zebrafish is very similar to that of other vertebrates, containing regions within the brain corresponding to homologous structures in more complex vertebrates (Rink and Wullimann, 2001). As mentioned previously, dysregulation of motor signals in the basal

ganglia is responsible for the movement disorder symptoms seen in patients with Parkinson's disease. The basal ganglia are a site of confluence between dopaminergic and GABAergic neurons, which act cooperatively to regulate afferent signals from the motor cortex. Comparative studies have established a homology between subpallium of the zebrafish to the striatum of the basal ganglia in humans (Rink and Wullimann, 2004), and these subpallial neurons express both GAD (glutamic acid decarboxylase) and TH, which are markers for GABAergic and dopaminergic neurons respectively (Filippi *et al.*, 2014). Efferent projections from the subpallium innervate the anterior commissure and hypothalamus. The subpallium sits posterior to the olfactory bulb, and is located in the ventral telencephalon, recapitulating the anatomical position of the striatum in humans. Projections to the dorsal thalamus from the subpallium also suggest a regulatory aspect of efferent signals from the forebrain, supporting the theory that the striatum and subpallium possess similar functions (reviewed in Schweitzer *et al.*, 2012). In humans, the striatum receives dopaminergic innervation from neurons that form the nigrostriatal pathway, originating from nuclei in the *substantia nigra* of the midbrain. Although the loss of dopamine neurons in the *substantia nigra* of the human midbrain is responsible for the pathophysiology of Parkinson’s disease, zebrafish do not have dopaminergic neurons in the mesencephalon (midbrain). Instead, there is a population of dopamine neurons in the posteroventral aspect of the forebrain known as the ventral diencephalon that sends ascending projections to the subpallium in zebrafish (Tay *et al.*, 2011). Several dopaminergic populations in the ventral diencephalon were first described by Rink and Wulliman (2001), and were independently named as CA 8, 9, 12, and 13 according to

Sallinen *et al.* (2009), or DC groups 2-6 according to Rink and Wullimann (2001). The dopaminergic neurons in DC groups 2 and 4 [or CA 12 according to Sallinen *et al.* (2009)] appear large and pear-shaped, and primarily innervate the subpallium (Tay *et al.* 2011). These ventral diencephalic neurons demonstrate susceptibility to the dopaminergic neurotoxin MPTP, resulting in an observable and reproducible motor phenotype (Sallinen *et al.*, 2009; Lam *et al.*, 2005; McKinley *et al.*, 2005). Although Tay *et* al. (2011) suggests that dopamine secreted in the subpallium originates from a local telencephalic source, we suggest that the neurons in DC groups 2 and 4 are homologous to the nigrostriatal pathways in humans. This is based on our own interpretation of the function of an afferent dopaminergic pathway mapping to the subpallial neurons, providing a neuronal pathway homologous to the nigrostriatal pathway seen in humans. Therefore, we hypothesize that the dopaminergic neurons of the ventral diencephalon are homologous to the mammalian *substantia nigra* as previously described by Rink and Wullimann (2002). The ventral diencephalic dopaminergic neurons in DC groups 5 and 6 [or CA 9 and 13 respectively according to Sallinen *et al.* (2009)] send efferent projections into the hypothalamus of the zebrafish brain (Tay *et al.*, 2011) and may recapitulate the tuberoinfundibular dopaminergic pathway in mammalian brains.

1.8 Markers of dopamine neurons in zebrafish

Tyrosine hydroxylase (TH), the enzyme involved in the rate-limiting step of dopamine synthesis, is typically employed as a biomarker of catecholaminergic neurons. Zebrafish express two paralogs of TH (TH and TH2), with each paralog originating from a teleost-

specific genome-wide duplication. Although the substrates and origin of TH2 may be disputed (Ren *et al.*, 2013), TH2 is mainly expressed in the hypothalamus in late larval stages and early adulthood (Filippi *et al.*, 2010; Yamamoto *et al.*, 2010, 2011), whereas TH is generally expressed throughout the dopaminergic neuron network throughout early embryo development and well into adulthood (Rink and Wullimann, 2002). Dopaminergic neurons can then typically be distinguished from noradrenergic neurons using the presence of dopamine transporter (dat), whereas noradrenergic neurons express dopamine beta hydroxylase (dbh). The distribution of these markers of catecholaminergic neurons has then demonstrated that dopamine neurons localize to the telencephalon and diencephalon of the zebrafish forebrain, and that noradrenergic neurons primarily localize to the sympathetic ganglia, locus coeruleus and medulla oblongata of the rhombencephalon (hindbrain) (reviewed in Schweitzer *et al.*, 2012).

1.9 Zebrafish as a model of environmentally-acquired Parkinson's disease

Currently, there are a number of environmental and genetic models for neurodegeneration in zebrafish (reviewed in Xi *et al.*, 2011a). After the publication of the first comparative analysis of dopamine neuron anatomy by Rink and Wulliman (2001), there have been a number of studies exploring the potential for pharmacological disruption of dopamine neurons that recapitulate the nigrostriatal neurons in zebrafish. This attempt to model environmentally-induced Parkinson's disease resulted in the creation of a well-studied zebrafish model of MPTP-induced Parkinson's disease. However, there does not appear to be a consensus on a standard dosing regimen for MPTP exposure to elicit a dopamine

neuron loss phenotype. Vastly different concentrations of MPTP have been used in numerous studies to elicit various physiological effects, ranging from a 50µM concentration causing mild dopaminergic neuron loss (Bretaud *et al.*, 2004) to 200µM causing the aforementioned loss of neurons in addition to serious morphological defects (own work, not published) to 500µM causing loss of whole populations of aminergic neurons (Sallinen *et al.*, 2009) to as high as 1000µM causing serious behavioral changes and neuronal loss (Xi *et al.*, 2011b). These data suggest that MPTP has a wide range of concentrations for causing biological effects (a concept similar to a therapeutic window) beginning as low as 50µM, until it causes embryonic death at 1.5mM.

Environmental toxins such as rotenone have also been previously tested in zebrafish (Bretaud *et al.*, 2004) but this study yielded no conclusive evidence for dopamine neuron loss or a motor phenotype. One recent study using rotenone in zebrafish was only able to reveal its embryotoxicity and suggest that chronic exposure may cause harmful toxicological effects (Melo *et al.*, 2015), whereas another study was only able to demonstrate its effect of inhibiting cellular respiration *in vitro* (Makhija and Jagtap, 2014). Each study appeared to encounter cytotoxic effects before any dopamine neuron death could be demonstrated. Therefore, it appears that since rotenone is such a potent commercial piscicide, its neurotoxic effects in zebrafish have not been investigated in depth.

1.10 Knockdown models of Parkinson's disease in zebrafish

Zebrafish have been used primarily to study the role of genes implicated in Parkinson's disease. These models employ antisense oligonucleotide knockdown strategies against RNAs encoding genes linked to the development of hereditary Parkinson's disease. Antisense knockdowns against genes such as *LRRK2*, *DJ-1*, *Parkin*, *PINK1* and *PARL* have been used to mimic the effects of genetic loss-of-function, and model the functional importance of these Parkinson's disease genes in zebrafish.

1.10.1 LRRK2 in zebrafish

LRRK2 is a leucine-rich repeat kinase encoded by the *PARK8* genetic locus in humans, and mutations to the *LRRK2* gene are the most common associated cause of familial Parkinson's disease. However, the normal function of *LRRK2* is poorly defined, since the 280kD peptide encoded by the *LRRK2* gene contains multiple functional domains and does not localize to any specific tissue types (Kett and Dauer, 2012). The vast number of functional domains made *LRRK2* a prime target for functional knockdown studies in zebrafish. A homologue of *LRRK2* in zebrafish was targeted in early genetic studies with antisense morpholinos (Sheng *et al.*, 2010; Ren *et al.*, 2011). *Lrrk2* knockdown embryos demonstrated severe developmental phenotypes, such as growth retardation, microcephaly and heart edema (Sheng *et al.*, 2010), as well as axis curvature and eye defects (Prabhudesai *et al.*, 2016). *Lrrk2* morphants also lost dopamine neurons in the diencephalon (Sheng *et al.*, 2010; Prabhudesai *et al.*, 2016) although these results were

not reproduced by other groups (Ren *et al.*, 2011). Furthermore, using splice-blocking morpholinos, it was further suggested that loss-of-function in the WD40 domain of *Lrrk2* is responsible for the dopamine neuron pathology seen in Parkinson's disease. Embryos missing the WD40 domain demonstrated a reduction in the number of dopaminergic neurons and also displayed axonal mispatterning. These phenotypes could be rescued with exogenous human *LRRK2* or zebrafish *Lrrk2* RNA (Sheng *et al.*, 2010). Knockdown of *Lrrk2* was also found to induce the aggregation of β-synuclein in zebrafish (Prabhudesai *et al.*, 2016). Morphant embryos also demonstrated a reduced locomotion phenotype, with shorter and less frequent episodes of movement when compared to wild-type zebrafish embryos (Sheng *et al.*, 2010).

1.10.2 Parkin in zebrafish

Parkin is a ubiquitin E3 ligase encoded by the *PARK2* genetic locus in humans. *Parkin* is responsible for the regulation of the ubiquitin-proteosome complex and mutations in this gene are linked to another form of autosomal recessive Parkinson's disease. While the relationship between loss of *parkin* function and dopamine neuron loss is not immediately obvious from a cell biology perspective, the epidemiological evidence for a causal association between genetic causes of *parkin* deficiency and the development of early onset Parkinson's disease is very clear (reviewed in Trempe and Fon, 2013). Zebrafish possess a highly conserved homologue of *parkin* that is ubiquitously expressed in all tissue types throughout development (Flinn *et al.*, 2009; Fett *et al.*, 2010). A splice-blocking morpholino knockdown of zebrafish *parkin* decreased both the dopaminergic

neuron population of the posterior tuberculum of developing embryos, as well as mitochondrial complex I activity (Flinn *et al.*, 2009), but these results were not reproducible with an alternative antisense knockdown model using peptide nucleic acids (Fett *et al.*, 2010). However, morphant embryos generated from either of these strategies did not display any observable locomotor deficits. Knockdown of *parkin* also revealed electron dense material in the muscular t-tubules along the trunk of morphant zebrafish (Flinn *et al.*, 2009). These t-tubules contain a high density of L-type calcium channels (reviewed in Brette and Orchard, 2007), and similar L-type calcium channels play an important role for neuronal pacemaking within the dopamine neurons of the mammalian *substantia nigra* (reviewed in Surmeier, 2007). In zebrafish *parkin* morphants, the dysregulation of these calcium channels results in an improper accumulation of calcium ions within t-tubules, requiring expenditure of additional cellular energy to properly modulate calcium homeostasis. This provides a possible hypothesis on the mechanism of how *parkin* deficiency may induce dopamine neuron death.

1.10.3 SNCA in zebrafish

Zebrafish lack a homologous version of alpha-synuclein (SNCA), and therefore do not experience neuronal dysfunction secondary to Lewy neurite formation unless genetic manipulation is performed to introduce an exogenous coding sequence of *SNCA* (Zharikov *et al.*, 2015). It is hypothesized that Lewy neurite formation impairs the synthesis and secretion of dopamine in the dopaminergic neurons of the *substantia nigra* of patients with Parkinson's disease, but also that this neurite formation leads to a

neuroinflammatory response and subsequent neuronal death and degeneration (reviewed in Mrak and Griffin, 2007). However, other groups have suggested that Lewy body formation may not be associated with a pathophysiological mechanism, and that Lewy body formation is a cytoprotective mechanism against free *SNCA* oligomers (Wakabayashi *et al.*, 2007). Regardless of the involvement of Lewy bodies and their contribution to neurodegeneration, the loss of dopamine neurons ultimately remains an important and independent aspect to the underlying pathophysiology of Parkinson's disease.

1.10.4 DJ-1 in zebrafish

DJ-1 is a gene encoded by the *PARK7* genetic locus in humans and responsible for the regulation of cellular oxidative stress (reviewed in Trempe and Fon, 2013). Mutations in the *DJ-1* gene are also linked to a small number of cases of autosomal recessive Parkinson's disease. A *DJ-1* homologue demonstrating remarkable functional and sequence similarity was identified in zebrafish (Bai *et al.*, 2006; Bretaud *et al.*, 2007), and is expressed in multiple tissue types from early embryonic development and into the brain of adults (Bai *et al.*, 2006). In the adult zebrafish brain, *Dj-1* localizes to the neuronal cytoplasm and neuropil, and appears in all major telencephalic and diencephalic dopamine neuron populations (Bai *et al.*, 2006). Expression of pro-apoptotic proteins p53 and Bax appeared to be increased in morpholino knockdowns of *Dj-1*, but these morphants did not yield any decrease in the number of dopaminergic neurons (Bretaud *et al.*, 2007). However, morphants that were exposed to hydrogen peroxide and proteasome

inhibitor MG132 demonstrated a decrease in dopaminergic neurons (Bretaud *et al.*, 2007) suggesting that the threshold for the effect of pro-apoptotic triggers is lowered in the absence of *Dj-1*. This model therefore suggests that pro-apoptotic factors such as Bax and p53 are involved in the pathophysiology of neuronal loss in Parkinson's disease.

1.10.5 PINK1 in zebrafish

Pink1 is a protein kinase critical to mitochondrial function, and mutations in *PINK1* have been linked to the development of autosomal recessive early-onset Parkinson's disease (reviewed in Pickrell and Youle, 2015). *Pink1*-null drosophila mutants demonstrated defects in mitochondrial cristae formation and reduced ATP production (Clark *et al.*, 2006; Park *et al.*, 2006), and zebrafish *pink1* morphants demonstrated developmental delays (Anichtchik *et al.*, 2008), as well as tactile insensitivity and decreased locomotion (Xi *et al.*, 2010), a phenotype consistent with MPTP-treated zebrafish larva (McKinley *et al.*, 2005; Xi *et al.*, 2011b; Noble *et al.*, 2015), and larva with nitroreductase-ablated dopamine neurons (Godoy *et al.*, 2015). These morphants also displayed axonal mispatterning, reductions to their spinal motor neuronal populations (Anichtchik *et al.*, 2008), and impaired neuronal patterning within DC groups 2, 4 and 5 of the ventral diencephalon (Xi *et al.*, 2010), regions that we hypothesize are homologous to the nigrostriatal pathways in humans. Specifically, in embryos with tactile insensitivity, these diencephalic neurons demonstrated shortened or absent projections to the subpallium of the forebrain (Xi *et al.*, 2010), supporting the hypothesis that these neurons and their projections play a modulatory role for efferent motor cortex signals. *Pink1* morphant

embryos also demonstrated increased apoptosis when compared to wild-type siblings (Anichtchik *et al.*, 2008), suggesting that improper *pink1* function may lead to a loss of mitochondrial integrity and overproduction of ROSs leading to programmed cell death.

1.10.5 PARL in zebrafish

PARL is a mitochondrial inner membrane protease that has also been linked to the development of Parkinson's disease (Shi *et al.*, 2011). *PARL* catalyses the proteolysis of many substrates (Koonin *et al.,* 2003), including the proteolytic activation *OPA1*, an anti-apoptotic protein on the inner mitochondrial membrane. Murine *PARL*-null mutants are embryonic lethal, and the loss of *PARL* results in cristae remodeling and cytochrome *c* release, which triggers widespread apoptosis (Cipolat *et al.*, 2006). Furthermore, *PARL* interacts with both *pink1* and *parkin*, another gene linked to an autosomal recessive form of early-onset Parkinson's disease (Whitworth *et al.*, 2008). Zebrafish *PARL* morphants displayed similarly mispatterned dopamine neurons as *pink1* morphants, and decreased embryonic survival (Noble *et al.*, 2012).

1.11 Mitochondrial dysfunction and Parkinson's disease

Many of the above models suggest a strong link between mitochondrial dysfunction, dopamine neuron death and development of Parkinson's disease. This is hypothesized to originate from inhibition of mitochondrial complex I within the mitochondria of dopamine neurons, which subsequently leads to ROS-mediated cellular damage and programmed cell death. Local ROS damage to the mitochondrial membrane would

manifest in cytochrome *c* leakage and induction of an apoptosis cascade involving caspase-9 and caspase-3 proteins (reviewed in Circu and Aw, 2011). Furthermore, pro-apoptotic protein Bax would translocate to the mitochondrial membrane in cases of ROS-mediated damage (reviewed in Fleury *et al.*, 2002), and anti-apoptotic protein Bcl-2 would become sequestered by Bad, another member of the BH3-like family of proteins (reviewed in Gross *et al.*, 1999). Since this apoptotic cascade is induced by ROS-mediated damage, this suggests that antioxidant compounds could rescue or ameliorate the programmed cell death of damaged dopamine neurons.

1.12 Using transgenic fluorescent reporter proteins in zebrafish

Zebrafish are also amenable to genetic manipulation, and our laboratory has published work describing the creation of three lines of transgenic fluorescent zebrafish embryos used to study Parkinson's disease (Xi *et al*, 2011b; Noble *et al.*, 2015; Godoy *et al.*, 2015). Each transgenic line harnessed the expression conferred from the *cis*-regulatory elements of the dopamine transporter gene to drive the expression of different transgenes.

Xi *et al.* (2011b) were able to insert a fluorescent green fluorescent protein (GFP) cassette within the *cis*-regulatory elements of the dopamine transporter gene, creating a transgenic line known as Tg(*dat:EGFP*). GFP expression was localized to dopamine neurons, and GFP was observed in the TH-positive areas of the pretectum, subpallium, telencephalon, diencephalon (DC groups 2-6) and hypothalamus, in addition to the amacrine cells of the eye and the olfactory bulb. Dopamine neuron population decreases were observed

following MPTP exposure, showing a 20% decrease in the GFP-positive ventral diencephalic dopaminergic neurons. However, the dopamine neurons in DC groups 4 and 5 were more affected by MPTP exposure than other diencephalic neurons. Larva exposed to MPTP also demonstrated impaired locomotion. MPTP-dependent GFP decrease was also seen in in the olfactory bulb in Tg(*dat:EGFP*) larva. Dopamine neuron projections to the olfactory bulb (and amacrine cells of the eye) tend to form local connections exclusively, and are thus not thought to be homologous to any of the main dopamine pathways of the brain. However, olfactory loss is also very strongly linked to the development and progression of Parkinson's disease (Haehner *et al.*, 2011; Cavaco *et al.*, 2015), and changes within the olfactory bulb in zebrafish can be easily visualized. We were able to use these transgenic zebrafish to answer questions about genetic causes of Parkinson's disease.

In a parallel project, Noble *et al.* (2015) were able to insert a fluorescent mitochondrial membrane tag within the *cis*-regulatory elements of the dopamine transporter gene, creating the Tg(*dat:tom20 MLS-mCherry*) transgenic line. This cassette contained a fluorescent recombinant mCherry protein, which was linked to a tom20 mitochondrial localization signal peptide, targeting this fluorescent protein to the mitochondrial outer membrane. The presence of mCherry fluorescence was observed in the mitochondria of dopamine neurons in the subpallium, pretectum, locus coeruleus, preoptic area, olfactory bulb, hypothalamus and some diencephalic clusters (DC groups 2 and 3). The fluorescence in these dopamine neurons appeared to be sensitive to MPTP neurotoxicity

consistent with Xi e*t al.* (2011b), and decreases in fluorescence were visualized in the olfactory bulb, pretectum, subpallium, diencephalon, and hypothalamus following exposure to MPTP. Since this transgenic line labels the mitochondria of exclusively dopamine neurons, this experimental platform allowed visualization of MPTP-induced mitochondrial damage, supporting the hypothesis that MPTP damages dopamine neurons through complex I inhibition and interference of cellular respiration.

Godoy *et al.* (2015) were able to insert a nitroreductase cassette within the *cis*-regulatory elements of dopamine transporter to induce cell-specific chemogenetic ablation of dopamine neurons. Nitroreductase expression would then be limited to cells that would otherwise express dopamine transporter (dopamine neurons), and in the presence of metronidazole, would crosslink the DNA in these cells and induce programmed cell death. This model provided a simple and robust model of dopaminergic neuron-specific ablation in zebrafish, and allowed us to characterize a number of observable phenotypes secondary to dopamine neuron death. Transgenic zebrafish larvae exposed to metronidazole demonstrated a decrease in locomotion and overall movement as a result of the ablation of dopamine neurons in the ventral diencephalon, consistent with Xi e*t al.* (2011b). This study provides evidence that the dopamine neurons in the ventral diencephalon play a role in the modulation of motor movements, and demonstrate that a locomotion loss may be a potential parkinsonism phenotype in zebrafish.

1.13 Statement of inquiry

We sought to create a model of environmentally-induced Parkinson disease using larval zebrafish, and use this model for the discovery of neurotoxic compounds that generate a phenotype similar to these established parkinsonism-causing agents. Our project has focused particularly on investigating environmental contributions on the development of dopamine neuron pathology and death. We therefore sought to identify and describe a set of behavioral and morphologic criteria for selecting compounds that cause parkinsonism-like symptoms in zebrafish. We were able to identify rotenone as a compound that was neurotoxic to dopamine neurons in zebrafish using the transgenic line described in Xi *et al.* (2011b), and validated our observations with behavioral assays for locomotor dysfunction related to parkinsonism and pathology-focused assays for protein and RNA markers for neurological damage. Furthermore, since there is a low relative abundance of dopamine neurons when considering the total number of cells and cell types within a single vertebrate organism, we also sought to develop a method of enriching these dopamine neurons using techniques developed for fluorescent cell sorting. This allowed us to isolate these dopamine neurons in the context of a Parkinson's disease animal model, and gives us the potential to assess for changes to the molecular biology of these cells, answering questions about the neurotoxicity and physiologic changes that exogenous compounds could have on the dopamine neurons. Here we show that rotenone affects the dopaminergic system of the zebrafish through a dose-dependent ablation of dopaminergic neurons in the ventral diencephalon by oxidative stress-induced apoptotic activity. We were also able to show that rotenone damages the mitochondria of these

dopamine neurons using imaging and flow cytometry, and this mitochondrial dysfunction plays a central role to the death of dopamine neurons. Furthermore, we also demonstrate that rotenone-induced dopamine neuron death manifests as a motor phenotype consistent with other models of parkinsonism in zebrafish. Overall, we hoped to have demonstrated the utility of the zebrafish as a model system for investigating neurodegeneration, with particular emphasis on rotenone's neurotoxic effects through reactive oxygen species formation.

Materials and Methods

2.1 Fish care and husbandry

Zebrafish embryos were obtained from the natural spawning of adult zebrafish maintained on a 14-hour light/10-hour dark cycle and fed a diet of fish pellets and *Artemia*. After cleaning and sorting, embryos were raised at 28.5°C from birth until up to 15 days post-fertilization (dpf) in embryo media (13mM NaCl, 0.5mM KCl, 0.02mM Na_2HPO_4, 0.04mM KH_2PO_4, 1.3mM $CaCl_2$, 1.0mM $MgSO_4$, and 4.2mM $NaHCO_3$). Selected embryos were raised to adulthood after being bleached in a 6% sodium hypochlorite solution at 24 hours post-fertilization (hpf) and raised in static tanks on a diet of GEMMA Micro (Skretting USA). When necessary, to prevent the formation of pigmentation in our developing embryos, phenylthiourea (Sigma-Aldrich) was added to the embryo media at 24 hpf to a final concentration of 0.2mM. We used two transgenic zebrafish lines in these experiments in addition to store-bought wild type zebrafish. Tg(*dat:EGFP*) is a transgenic line that was published in Xi *et al.* (2011b), in which the green fluorescent protein (GFP) is expressed under the control of *cis*-regulatory elements of the dopamine transporter (*dat*) gene thus labeling the dopamine neurons in the zebrafish with green fluorescent protein. Tg(*dat:tom20 MLS-mCherry*) is a transgenic line that was published in Noble *et al.* (2015), in which the red fluorescent protein (mCherry) is expressed under the same *cis*-regulatory elements as previously described, but fused to a mitochondria localization signal peptide (MLS) harvested from the *tom20* mitochondrial outer membrane protein, thus labeling the mitochondria only in dopamine neurons with mCherry. The University of Ottawa Animal Care Committee approved all

animal care procedures, and all animals used were governed by protocols in accordance with the recommendations of the Canadian Council for Animal Care.

2.2 Environmental toxin exposure

We exposed zebrafish to seven small molecules to test their effects on dopamine neuron physiology. Two of these compounds have demonstrable effects on zebrafish (MPTP and MPP+), three have been tested but demonstrated no reproducible effects on zebrafish (rotenone, paraquat, and 6-OHDA), and two were untested in zebrafish ($MnCl_2$ and ziram). These compounds were administered using a regimen similar to one that would be used in a large-scale screen of a small molecules. Compounds were first serially diluted in water in a half-log series to final concentrations listed in table 2.1. Tg(*dat:EGFP*) embryos were allowed to develop for 24 hpf then split into multi-well plates, the compounds were added and the embryos were incubated for an additional 72 hours. Embryos were then assessed at 7 dpf for changes in dopamine neuron distribution using the GFP reporter. For examination of the embryos, a petri dish containing a bed of 2% agarose gel was prepared with 1 mm-deep troughs cut into the agarose using a standard glass microscopy slide. Embryos were then anesthetized with a 0.168 mg/ml solution of MS-222 (Sigma-Aldrich), gently placed into a trough in the agarose bed with the dorsal side up, then imaged on a Leica MZ6 epifluorescence stereomicroscope to examine for changes in green fluorescence patterning. Larvae were examined in a single-blind fashion. Images were then assembled into panels using Adobe Photoshop CS5.

Toxin	Exposure				
6-OHDA	1μM	3μM	10μM	30μM	100μM
MPTP	0.1mM	0.5mM	1mM	5mM	10mM
MPP+	0.1mM	0.5mM	1.5mM	5mM	15mM
Ziram	1μM	3μM	10μM	30μM	100μM
Paraquat	1mM	3mM	10mM	30mM	100mM
$MnCl_2$	1mM	3mM	10mM	30mM	100mM
Rotenone	3nM	10nM	30nM	100nM	300nM

Table 2.1: Environmental toxins used in exposure experiments.
The above environmental toxins were administered to the embryo media of 24 hpf zebrafish embryos for 6 days: oxidopamine (6-OHDA; co-administered with 1% ascorbic acid), MPTP, MPP+, ziram (dissolved in 0.5% acetone), paraquat, MnCl2, and rotenone (dissolved in 0.01% DMSO). Concentrations for these exposure experiments followed an increasing half log series. The above concentrations were examined for any gross morphological changes, behavioral changes, and changes to dopamine neuron patterning.

After exposure, all solutions were bleached and subsequently disposed as hazardous wastes.

2.3 Rotenone preparation and administration

Rotenone powder (Sigma-Aldrich) was freshly dissolved in DMSO (Fisher Scientific) at a concentration of 1mM, then serially diluted up to 1,000,000-fold in double distilled water to half-log working concentrations between 1nM and 1000nM. Rotenone solutions older than 4 h were never used. Embryonic zebrafish were collected and raised in 6-well, 12-well or 24-well plates (Corning) with no more than 20 embryos per well. Embryos were exposed to a single dose of rotenone at 24 hpf without water changes until 7 dpf to simulate the effect of a single exposure to an environmental agent. Controls were zebrafish embryos exposed to a solution 0.01% DMSO, the same DMSO concentration used for the highest dose of rotenone. Larvae were then imaged as described previously. Rotenone from a different source (Fisher Scientific) was also assessed, and also produced comparable changes in neuronal patterning (data not shown).

2.4 Immunohistochemistry on whole zebrafish larvae

Zebrafish were raised to the appropriate developmental stage, manually dechorionated and euthanized with an overdose of MS-222. They were then fixed in a 4% solution of fresh electron microscopy grade paraformaldehyde (ThermoFisher Scientific) dissolved in phosphate buffered saline (137mM NaCl, 2.7mM KCl, 4.3mM Na_2HPO_4, 1.47mM KH_2PO_4, PBS) overnight at 4°C, then rinsed thrice in PBS and permeabilized for 15

minutes in PBS with 0.1% Triton X-100 (PBSTx). Samples were then blocked overnight at 4°C in a 10% heat-inactivated goat serum solution (Ambion) in PBS, followed by an incubation overnight at 4°C in primary antibody solution [either anti-TH (AB152, Millipore), ZN-12 (DSHB), anti-GFP (AS-55887, Anaspec), anti-caspase 9 (AS-55377, Anaspec) or anti-caspase 3 (AS-55372, Anaspec)] diluted to a 1:200 concentration in 10% goat serum in PBSTx. Samples were then washed thrice for 15 minutes at room temperature in PBSTx, then incubated overnight at 4°C in secondary antibody solution [goat anti-mouse Alexa 488 conjugate (A-11001, ThermoFisher Scientific) or goat anti-rabbit antibody Alexa 594 conjugate (A-11012, ThermoFisher Scientific)] diluted to a 1:200 concentration in 10% goat serum in PBSTx. Samples were again washed thrice for 15 minutes at room temperature in PBSTx following secondary antibody incubation, and imaged on a Leica MZ6 epifluorescence stereomicroscope as described above.

2.5 Immunohistochemistry on zebrafish cryosections

For immunohistochemistry, Tg(*dat:EGFP*) or wild type embryos/larvae were reared to the desired developmental stage, euthanized, manually dechorionated and fixed in 4% paraformaldehyde as previously described and equilibrated in a 30% sucrose/PBS solution overnight at 4°C. For immunohistochemistry on adult zebrafish brain, rotenone-exposed Tg(*dat:EGFP*) zebrafish were raised to 60 dpf, euthanized and fixed in 4% paraformadehyde overnight before being equilibrated in 30% sucrose/PBS. All samples were then flash frozen in Tissue-tek OCT media (VWR Canada) and sectioned onto Leica CM 1850 (Leica Microsystems, Weltzar, Germany) at a thickness of 14 µm on to

Superfrost class slides and stored at -20°C until use. Prior to incubating in anti-GAD antibody only, slides were incubated in a sodium citrate antigen retrieval buffer (10mM sodium citrate, 0.1% tween-20, pH 6.0) for 15 minutes at 85ºC before being allowed to cool back to room temperature and washed thrice in PBS. For the rest of the slides, after a short rehydration period for 10 minutes in PBS containing 0.1% tween-20 (PBSTw), sections were blocked in 10% goat serum in PBSTw at room temperature for 3 hours. Sections were then incubated overnight at 4°C with a 1:1000 dilution of primary antibody [either anti-TH (AB152, Millipore), ZN-12 (DSHB), anti-GFP (AS-55887, Anaspec), anti-caspase 9 (AS-55377, Anaspec), anti-caspase 3 (AS-55372, Anaspec), an alternative anti-caspase 3 (559565, BD Pharmingen), anti-mCherry (AB167453, Abcam), anti-GAD (AB11070, Abcam), anti-serotonin (S5545, Sigma-Aldrich), ZN-1 (DSHB), or ZNP-1 (DSHB)]. After three washes in PBSTw, sections were incubated for three hours at room temperature with a 1:1000 dilution of either goat anti-mouse antibody Alexa 488 conjugate (A-11001, ThermoFisher Scientific) or a 1:1000 dilution of goat anti-rabbit antibody Alexa 594 conjugate (A-11012, ThermoFisher Scientific), then washed three times in PBSTw. Sections were then incubated in NucBlue® Fixed Cell ReadyProbes® Reagent (R37606, ThermoFisher) for 10 minutes before being rinsed thrice in distilled water and mounted in Aqua-Poly/Mount (18606, Polysciences Inc.) and viewed using a Zeiss Axiophot upright epifluorescence microscope. Images were assembled using ImagePro, FIJI and Adobe Photoshop CS5.

2.6 Immunohistochemistry on dat:tom20 MLS-mCherry embryos

Embryos were euthanized, manually dechorionated and fixed in 4% paraformaldehyde as previously described, washed thrice in PBS and stored in 70% ethanol before being embedded in paraffin and cut into 3µm sections and adhered onto glass slides. Slides were then deparaffinized with a toluene-ethanol series and washed in PBS before undergoing an antigen retrieval step with sodium citrate antigen retrieval buffer and allowed to cool to room temperature. Slides were then blocked in 10% goat serum overnight at 4ºC, then incubated with a 1:3000 dilution of anti-mCherry (AB167453, Abcam) overnight at 4ºC. They were washed thrice in PBSTw, incubated with NL557-conjugate anti-rabbit IgG (NL004, R&D Systems) overnight at 4ºC, washed thrice in PBSTw and counterstained with DAPI before being imaged under a 100x oil immersion lens on a Zeiss Axiophot upright epifluorescence microscope. All immunohistochemistry experiments were performed in biological quadruplicates at minimum and the most representative sample images were chosen for publication.

2.7 MitoSOX Red oxidative stress assay

To assess for oxidative stress, we used a whole animal reactive oxygen species detection method as outlined in Mugoni *et al.* (2014). Embryos exposed to rotenone were grown to 3 dpf, anesthetized with a 0.168 mg/ml solution of MS-222, collected and rinsed thrice in Hank's Balanced Salt Solution (Sigma-Aldrich, HBSS). Embryos were then incubated in the dark for 15 minutes at 28ºC in a 5µM solution of MitoSOX Red (ThermoFisher) dissolved in HBSS. Following exposure to MitoSOX Red, embryos were then washed

twice in HBSS then gently placed into a trough in an agarose bedded plate in a dorsal-ventral orientation, and imaged as described previously.

2.8 Larval behavior assessment

To assess larval locomotion, zebrafish embryos that were exposed to rotenone or DMSO were raised to 7 dpf and placed into the individual wells of a black bottom 24-well plate. Zebrafish larvae were allowed to acclimatize to their new environment for 30 minutes before being recorded for 15 minutes with a Nikon D3100. This video recording was then processed using Noldus Ethovision XT and GraphPad PRISM was used to visualize and analyze locomotion. We performed these experiments in 9 biological replicates per sample group.

To measure zebrafish touch response following rotenone exposure, embryos that received rotenone or DMSO were raised to 96 hpf and placed in a 40 ml petri dish alone in the centre of the field of view under the highest (10x) magnification of a Leica MZ6 upright dissection microscope with bright field illumination. Larvae were then gently probed along the mid-trunk with a pair of No. 5 fine forceps, and filmed with a Grasshopper high-speed camera (Point Grey) at 120 frames per second. Video recordings were then split into component frames and each frame was manually counted to measure the amount of time required to clear the field of view, or the number of mechanical stimuli needed to elicit a motor response. GraphPad PRISM was used to visualize the locomotion data. All behavior experiments were performed in quadruplicates.

2.9 Adult behavior assessment

Zebrafish embryos that were exposed to either 0.01% DMSO alone, or 10nM or 100nM rotenone were raised to adulthood. Adult zebrafish were placed into individual tanks in an isolated environment and allowed to acclimatize to their new environment for 30 minutes before being recorded for 5 minutes using a Nikon Coolpix A camera. For the line-crossing behavioral assay, each tank had the midline depth demarcated with a rubber band, and manual analysis of the video recordings allowed us to count the number of times each fish crossed the midline depth of the tank. For light-dark experiments, fish were placed in a tank which had one-half covered in aluminum foil to emulate dark conditions. The tank was back-lit illuminating the uncovered portion of the tank, providing a bright environment. A manual analysis of the video recordings allowed us to measure the proportion of time that the fish spent in the lit half of the tank. Locomotion was measured from overhead with the same equipment and video recordings were processed using Ethovision XT (Noldus) and GraphPad PRISM to visualize and analyze the data. All behavior experiments were performed in biological quintuplicates.

2.10 RNA extraction and cDNA synthesis

Wild type zebrafish embryos were sorted into groups of forty to sixty embryos, exposed to either 0.01% DMSO, 30nM or 100nM rotenone at 24 hpf. Zebrafish were raised to either 3, 5 or 7 dpf, and euthanized with an overdose of MS-222. Approximately 50 larvae from each treatment group were homogenized in TriZol (Ambion) using a mortar

and pestle, and RNA was extracted according to manufacturer protocol. RNA concentrations were then quantified using a NanoDrop 2000 spectrophotometer (Thermo Scientific). Synthesis of cDNA was then accomplished by reverse transcription of total RNA. Two micrograms of total RNA were first combined with 5ng/µl random hexamers (New England Biolabs cat# S1230S), 2.5 mM dNTP (Invitrogen), heated to 80ºC for 5 minutes then immediately placed on ice for 15 minutes to anneal random hexamers to the RNA. Four hundred units of M-MuLV Reverse Transcriptase (New England Biolabs), 40 units of RNaseOUT inhibitor (Invitrogen), and 10× RT buffer (final concentration of 50mM Tris-HCl pH 8.3, 75mM KCl, 3mM $MgCl_2$, 10 mM DTT) were added and the mixture was then incubated at 42ºC for 60 minutes. The reverse transcriptase reaction was then stopped by heating the mixture to 90ºC for 15 minutes and stored at -20ºC. The cDNA concentrations were then quantified using a NanoDrop 2000 spectrophotometer (Thermo).

We assayed gene expression using primer sets described in table 2.2 that were previously described in Barreto-Valer *et al*. (2012). To ensure that were were generating unique PCR products free of primer dimers or other contamination, a PCT-100 Peltier Thermal Cycler (Bio-Rad) was used to amplify these specific cDNAs using iQ™ Supermix (Bio-Rad) under the following conditions: 95ºC for 10 minutes, followed by 37 cycles of 95ºC for 20s, 55ºC for 20s, then 72ºC for 20s. All primer pairs produced amplicons of the expected size. Following optimization for melting temperatures and primer efficiencies, a Bio-Rad CFX96™ Real-Time PCR Detection System was then used to assay transcripts of the

Gene of interest	Forward primer	Reverse Primer
dat	AGACATCTGGGAAGGTGGTG	ACCTGAGCATCATACAGGCG
drd1	ACGCTGTCCATCCTTATCTC	TGTCCGATTAAGGCTGGAG
drd2a	TGGTACTCCGGAAAAGACG	ACTCGGGATGGGTGCATTTC
drd2b	AAATAACACAGCTACACGGGAT	GAACCACGTAAATCTGCACG
ef1a	GTACTTCTCAGGCTGACTGTG	ACGATCAGCTGTTTCACTCC
β-actin	ACCACGGCCGAAAGAGAA	ATACCCAGGAAGGAAGGCTG

Table 2.2: Forward and reverse PCR primers sequences
Forward and reverse PCR primer pairs against *dopamine transporter* (dat), *dopamine receptor D1* (drd1), *dopamine receptor D2a* (drd2a), *dopamine receptor D2b* (drd2b), *elongation factor 1a* (ef1a), and *β-actin* are listed as above. Primer sequences were previously described in Barreto-Valer *et al.* (2012). Primers were diluted in ddH_2O to a 20µM stock concentration and kept at -20ºC until selected for use.

genes of interest by qPCR using SsoFast EvaGreen Supermix (Bio-Rad) under the following conditions: 95ºC for 30s, followed by 40 cycles of 95ºC for 5s and 60ºC for 5s, then a melt curve progressing from 65ºC to 95ºC, at 2s per 0.5ºC increase. *β-actin* and *ef1a* were used as reference genes. Data were analyzed using CFXManager (Bio-Rad), a paired Student's t-test and compiled using GraphPad PRISM.

2.11 Mitochondrial fractionation and Western blotting

For whole embryo homogenates, zebrafish were raised to 48 hpf, euthanized with an overdose of MS-222 and immediately homogenized in TriZol with a mortar and pestle as described previously. To separate the mitochondria from the cytosol, zebrafish were raised to 48 hpf, euthanized, and homogenized using a Douncer with solutions from a Mitochondria Isolation Kit for Tissue (Pierce). Following the manufacturer's instructions resulted in a mitochondrial pellet, that was immediately resuspended in TriZol, and a cytosolic fraction that was mixed 1:1 with TriZol. The proteinaceous fraction from each sample was then separated from the TriZol homogenate by phenol-chloroform and isopropanol precipitation, in accordance with the manufacturer's instructions. Pellets were then isolated, allowed to dry, resuspended, and quantified using a bicinchoninic acid (BCA) kit (Bio-Rad) on a NanoDrop 2000 spectrophotometer (Thermo).

Following quantification, protein samples were dissolved in 2× Laemmli buffer (4% SDS, 20% glycerol, 0.004% bromphenol blue and 125 mM Tris-HCl, pH 6.8, Sigma-Aldrich) in the presence of 10% 2-mercaptoethanol to simulate reducing conditions.

Samples (50µg each) were then loaded onto a 4–20% Mini-PROTEAN® TGX™ Precast Protein Gel (Bio-Rad) and run for 30 minutes at 200V to separate the protein fractions by molecular weight, then blotted to a methanol-hydrated chilled polyvinylene difluoride (PVDF) membrane for 120 minutes with a constant 200mA current. Membranes were blocked in 10% skim milk powder in PBSTw overnight at 4ºC, then incubated overnight in a 1:3000 solution of primary antibody [either anti-TH (AB152, Millipore), anti-Bad (AS-55478, Anaspec), anti-Bax-a (AS-55469, Anaspec), anti-Bax-b (AS-55498, Anaspec), anti-Bcl (AS-55396, Anaspec), anti-β-actin (sc-47778, Santa Cruz Biotechnologies), anti-Vdac1 (AB15895, Abcam) or anti-Gapdh (AB8245, Abcam)]. Membranes were washed thrice for 15 minutes in PBSTw and then incubated with a 1:1000 solution of either anti-mouse-horseradish peroxidase conjugate (A4416, Sigma-Aldrich) or anti-rabbit horseradish peroxidase conjugate (A8275, Sigma-Aldrich) secondary antibody overnight at 4ºC. Following the secondary antibody incubation, membranes were washed thrice with PBSTw before being visualized with an enhanced chemiluminescence (ECL) kit (Pierce). Membranes were then imaged onto an 8x10 in. CL-XPosure film (ThermoFisher), developed in a darkroom, scanned with an Epson V550 scanner and assembled in Adobe Photoshop CS5.

2.12 Zebrafish larva cell dissociation, flow cytometry and dopamine neuron enrichment

To prepare a single cell suspension of zebrafish embryos, Tg(*dat:EFGP*) zebrafish were raised to 48 hpf in 40 ml petri dishes, split into 400 embryos per treatment group, and then dechorionated with a 0.5 mg/ml pronase solution in embryo media. Zebrafish

embryos were euthanized with an overdose of MS-222, washed thrice in Ringers solution (116 mM NaCl, 2.9 mM KCl, 1.8 mM CaCl2, pH 7.2) and yolks were removed by vigorous trituration in deyolking buffer (55 mM NaCl, 1.8 mM KCl, 1.25 mM $NaHCO_3$). Freshly deyolked embryos were then transferred to a 100 micron cell strainer (VWR) and resuspended in FACSmax (Genlantis; PBS with 10mM EDTA can be substituted with varying success). We then used a plunger from a 0.5ml syringe to push the embryos through cell strainer, generating a mechanically dissociated cell suspension. This process was subsequently repeated twice using 40 micron strainers (VWR Canada) to generate a cell suspension of between 5 to 10 million cells/ml. Viability was assessed with trypan blue or propidium iodide to ensure low cellular necrosis.

After generating a single cell suspension, an aliquot of cells was then stained with MitoTracker Deep Red (M22426, ThermoFisher), a compound used to assess mitochondria viability. Cells were pelleted at 1200g for 5 minutes in a refrigerated centrifuge and the pellet resuspended in a 25nM solution of MitoTracker Deep Red followed by an incubation at 28.5ºC for 30 minutes to stain the cells. Cells were then washed three times for 10 minutes in chilled FACSmax before being read on a Gallios flow cytometer (Beckman-Coulter) for green fluorescence (GFP) or deep red fluorescence (MitoTracker Deep Red). Cells were kept from direct light to avoid photobleaching through the staining process. All flow cytometry reads were normalized to 100,000 events.

An aliquot of approximately 10 million unstained cells from zebrafish exposed to either 100nM rotenone or 0.01% DMSO were then sorted directly into TriZol using an MoFlo Astrios cell sorter (Beckman-Coulter). RNA was extracted from each sample as previously described in (2.10) followed by cDNA synthesis and qPCR. All cell dissociation experiments were done in biological and technical triplicates.

Results

3.1 Small scale screen of 7 compounds on zebrafish dopamine neuron patterning.

The initial central objective of this project was to develop the zebrafish as a platform for testing the *in vivo* biological effects of various environmental compounds, and assess the feasibility of using zebrafish in a large-scale chemical screen. Using live animals in a chemical screen presents an exciting opportunity to monitor and observe any environmentally-induced changes at the physiologic and organismal level. We therefore sought to optimize the conditions that would cause a reduction in dopamine neurons by performing a chemical screen for a small number of compounds linked to Parkinson's disease.

Embryos from the Tg(*dat:EGFP*) transgenic zebrafish line express the green fluorescent protein in most of their dopaminergic neurons (Xi *et al.*, 2011b). Exposing environmental compounds associated with Parkinson's disease to zebrafish embryos from the Tg(*dat:EGFP*) transgenic line has allowed us to identify if these compounds could cause gross changes to structures in the dopaminergic areas of the zebrafish brain. Embryos treated with these environmental agents were assessed for fluorescence loss in the telencephalon and ventral diencephalon (anterior to the midbrain-hindbrain boundary), suggesting for a dopamine neuron loss phenotype similar to previous observations of MPTP-treated embryos. We exposed our embryos to the following chemical compounds: ziram, paraquat, oxidopamine, $MnCl_2$, MPTP, MPP^+ and rotenone.

After administering these compounds to the fish water to test their biological effect on embryos, number of challenges became immediately obvious. Not all compounds were stable in solutions for extended periods of time. Oxidopamine (6-OHDA) is a dopamine analog with neurotoxic properties that has been used to induce dopamine neuron death in animal and cell culture models of Parkinson's disease. A solution of oxidopamine rapidly oxidizes (within minutes) when exposed to light, and must be co-administered with a high concentration of ascorbic acid (1%) in solution to protect its stability. Co-treatment of embryos exposed to oxidopamine with phenylthiourea, a pharmacological inhibitor of pigment development appears ineffective rendering microscopy impossibly challenging (figure 3.1A). Solutions of another compound, rotenone, have also been reported to have a half-life of 17h, requiring fresh dilutions made each day.

Additionally, some compounds changed the tonicity of the zebrafish growth media such as manganese chloride ($MnCl_2$). Manganese has been implicated in Parkinson's disease through a mechanism of toxicity where manganese ions accumulate and interfere with the function of dopamine neurons in the pallium of the brain (Olanow 2004, reviewed in Aschner *et al.*, 2009). Therefore, we sought to test the toxicity of manganese salts on zebrafish embryos with $MnCl_2$. We observed that embryos exposed to 30mM $MnCl_2$ demonstrated failure to hatch by 72 hpf and in some cases death by 96 hpf (figure 3.1C). There was also a marked increase in pigmentation and signs of developmental delay when compared to unexposed controls. Exposure of zebrafish to concentrations of $MnCl_2$

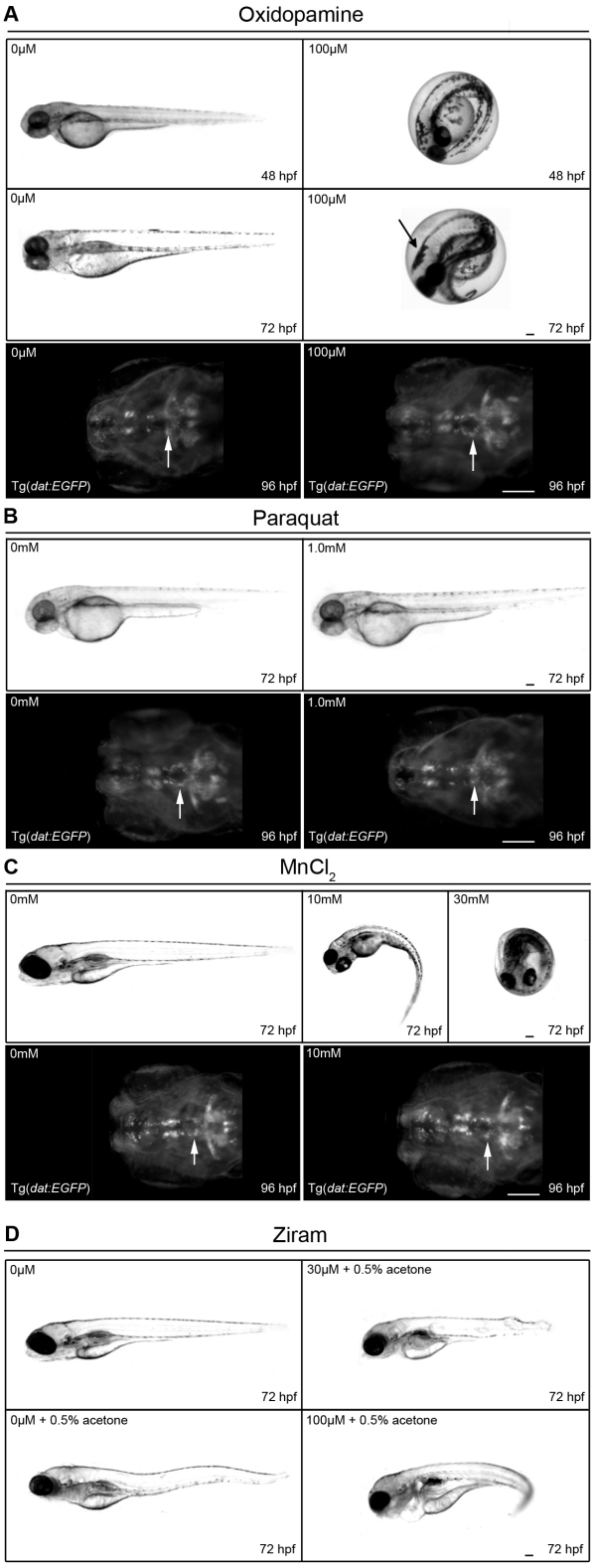
A
Oxidopamine
0μM
48 hpf
100μM
48 hpf
0μM
72 hpf
100μM
72 hpf
0μM
Tg(dat:EGFP)
96 hpf
100μM
Tg(dat:EGFP)
96 hpf
B
Paraquat
0mM
72 hpf
1.0mM
72 hpf
0mM
Tg(dat:EGFP)
96 hpf
1.0mM
Tg(dat:EGFP)
96 hpf
C
MnCl2
0mM
72 hpf
10mM
72 hpf
30mM
72 hpf
0mM
Tg(dat:EGFP)
96 hpf
10mM
Tg(dat:EGFP)
96 hpf
D
Ziram
0μM
72 hpf
30μM + 0.5% acetone
72 hpf
0μM + 0.5% acetone
72 hpf
100μM + 0.5% acetone
72 hpf

Figure 3.1: Small scale screen of oxidopamine, paraquat, $MnCl_2$ and ziram on the morphological and neurological development of dopamine neurons in zebrafish
Tg(*dat:EGFP*) zebrafish embryos were exposed to various concentrations of small molecule compounds linked to development of Parkinson's disease at 24 hpf and imaged with transmitted light microscopy and epifluorescence microscopy for changes to gross morphology or dopamine neuron distribution. Zebrafish exposed to 100µM oxidopamine (A) demonstrated persistent pigmentation (black arrow) in spite of PTU treatment (melanin synthesis inhibitor). These zebrafish also failed to hatch by 72 hpf. There was no apparent change in ventral diencephalic dopamine neuron patterning (white arrow). Embryos exposed to paraquat (B) did not demonstrate any developmental abnormalities by 72 hpf, and showed no apparent change in ventral diencephalic dopamine neuron patterning (white arrow). Zebrafish exposed to $MnCl_2$ (C) demonstrated axis curvature at 10nM or failed to hatch at 30mM exposures. However, there was no apparent change in ventral diencephalic dopamine neuron patterning (white arrow). Ziram exposure (D) appeared to induce lesion formation at 30µM, and developmental delay with axis curvature at 100µM exposures. However, these morphological abnormalities were also present when zebrafish were exposed exclusively to the solvent used to solubilize ziram. Scale bars: 50µm

required to affect dopamine neuron physiology may have created a hypertonic environment incompatible with the healthy development of zebrafish embryos.

Lastly, not all compounds exhibited solubility in water (an essential for scientific experiments with freshwater fish). Ziram is a commercially available fungicide used in the agriculture industry that has been linked to the development of Parkinson's disease. Recent work has demonstrated that ziram promotes the abnormal aggregation of alpha-synuclein *in vivo* in a manner seen in Parkinson's disease (Lulla *et al.*, 2016). However, when preparing zebrafish embryos for exposure to this fungicide, the path of administration or circumstances that would cause this compound to exhibit a biological effect were yet unpublished. We found that ziram was completely insoluble in water, and barely soluble in DMSO, a common solvent that demonstrates no effects to a concentration of 1% in water. Ziram was only soluble in acetone and chloroform, two compounds that are incompatible with life in zebrafish. For our experiments, ziram was dissolved in 0.5% acetone, which led to lesions forming along the trunk of the zebrafish embryos exposed to 30μM ziram, and yielded a very high mortality rate in acetone-only controls (figure 3.1D). Furthermore, at high concentrations, ziram gradually precipitated from solution over the course of the exposure yielding an inconsistent bioavailability. Rotenone was insoluble in water, and had to be dissolved to 1μM in DMSO before being serially diluted in water to physiologically active concentrations.

We then proceeded to assess for any gross changes in morphology and behavior on zebrafish larvae that have been incubated for 72 hours with these environmental agents. Paraquat is a potent herbicide that has been used commercially to kill grasses and weeds. It is an extremely water soluble compound that presents as a very bioavailable molecule with cytotoxic effects caused by its properties as an oxidizing agent. Embryos were exposed to concentrations of paraquat as high as 30mM with no changes to the development or behavior of these larvae. In fact, paraquat yielded no observable differences during the first 7 days of development (figure 3.1B). However, by 8 dpf, larvae exposed to concentrations of paraquat above 1mM all showed lethality clearly above that seen in control fish. Death after 7 days of exposure to paraquat was the only observable effect in zebrafish larvae. This is consistent with the lack of phenotype observed in by Bretaud *et al.* (2004).

MPTP (1-methyl-4-phenyl-1,2,3,6-tetrahydropyridine) is a neurotoxic compound that was initially synthesized as an inadvertent by-product of MPPP synthesis. MPTP acts as an analog to dopamine and binds readily to the dopamine receptor, becoming preferentially transported into dopamine neurons. Inside the brain, MPTP is converted to its active metabolite, 1-methyl-4-phenylpyridinium (MPP+), by monoamine oxidase B. MPP+ interferes with the function of mitochondrial complex I, leading to the accumulation of reactive oxygen species and subsequent death of the dopamine neurons. We observed that concentrations of 5mM MPTP and higher were lethal in 4 dpf larvae, consistent with previous studies of MPTP toxicity in zebrafish larva (McKinley *et al.*,

2005). At 1mM, we observed larvae demonstrating severe prognathism (rostralization of jaw and skull), a decrease in the intensity and structural distribution of dopamine neuron labeling (figure 3.2B), and an insensitivity to touch and other mechanical stimuli. We then manually assessed their behavior at 7 days post-fertilization (since larva show few non-spontaneous movements from rest until 5 days post-fertilization). The amount of locomotion as measured by total distance traveled, and number of spontaneous episodic movements was decreased in larvae exposed to MPTP and rotenone. These parameters have been validated in previous studies, with genetic or environmental models of PD in zebrafish demonstrating a significant reduction in average locomotion, touch response, and total distance traveled (Xi *et al.*, 2010; Sallinen *et al.*, 2009).

In summary, MPP+ and MPTP exhibited reproducible changes to the dopamine neuron physiology in the ventral diencephalon of developing larva (figure 3.2, arrows), consistent with previous studies, and rotenone appears to cause disruption in the dopamine neuron distribution in the ventral diencephalon (figure 3.2, arrows) and olfactory bulb (figure 3.2, arrowheads). Manganese, ziram and 6-OHDA interfered with the normal development of zebrafish larvae and did not appear to change dopamine neuron patterning. Paraquat had no observable effect on zebrafish survival or dopamine neuron physiology. Only rotenone demonstrated a reproducible dopamine neuron death phenotype at concentrations between 10nM to 100nM of rotenone (figure 3.2), as detailed in the following sections. Rotenone is a pesticide that is being presently used by governmental agencies as a commercial fish toxin in rivers and lakes to remove unwanted

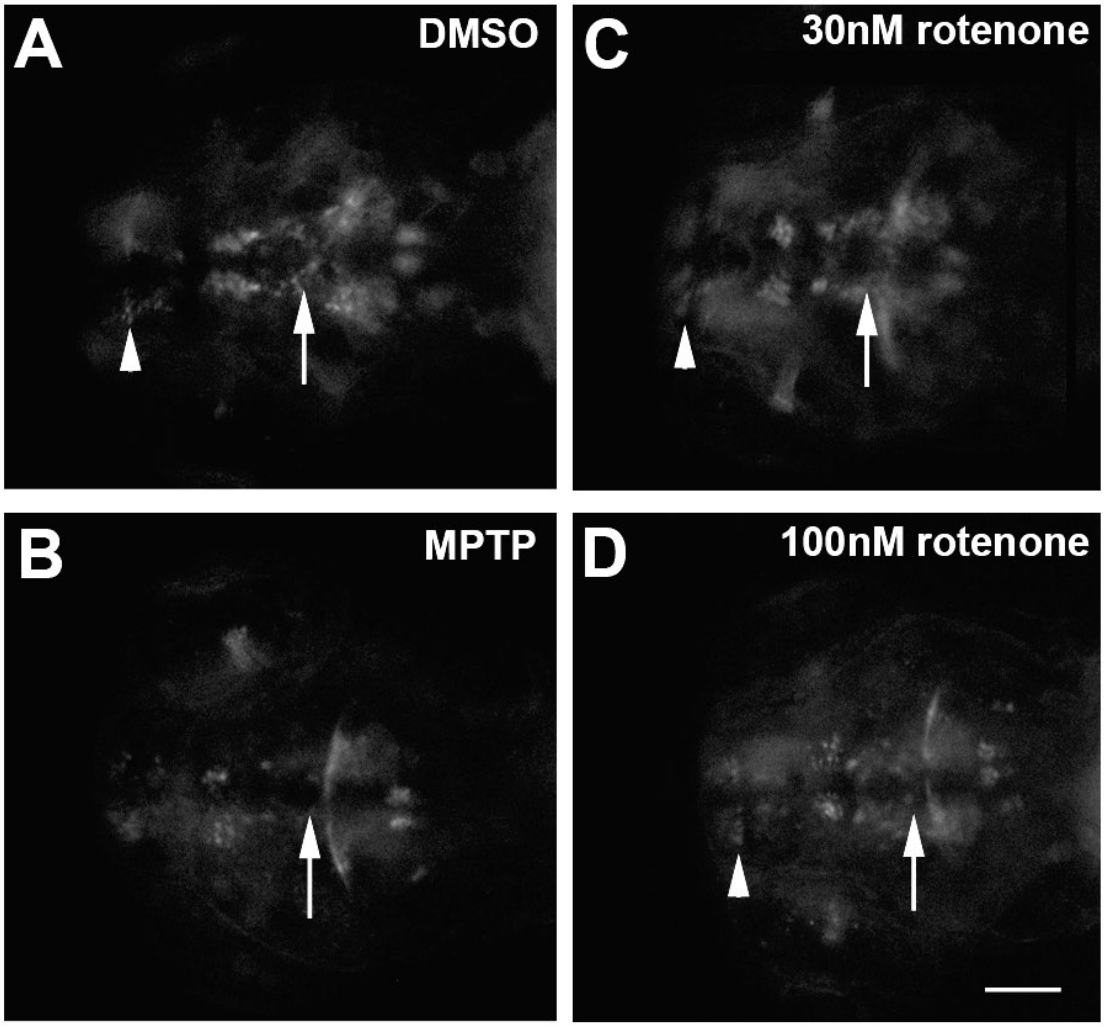

Figure 3.2: Results of a small-scale screen of chemicals that cause dopamine neuron loss in zebrafish

Live imaging under green fluorescence of 5 dpf Tg(*dat:EGFP*) larvae exposed to 0.01% DMSO (A), 1.0 mM MPTP (B), 30nM rotenone (C) or 100nM rotenone (D). Embryos were exposed at 24 hpf and demonstrated a decrease of GFP signal in ventral diencephalic clusters (arrows) as compared to controls. Embryos exposed to rotenone also demonstrate patterning defects in the telencephalon and olfactory bulb (arrowheads). Scale bar: 50μm

fish species. Rotenone is highly lipophilic and its MSDS mentions its exceptionally high toxicity to aquatic life. Initially, we observed that concentrations above 300nM are lethal within the first 24h of exposure to rotenone. Concentrations above 100nM show severe developmental defects by 48 hpf with some embryos demonstrating anterior-posterior axis malformation, massive pericardial effusion by 72 hpf (consistent with MPTP treatment in McKinley *et al.*, 2005), and gut malformations (figure 3.3).

To address the issues regarding environmental compound solubility, solution stability and animal toxicity, we have attempted to use serial dilutions and different solvents to limited success. However, these challenges will be abundantly present and multiplied many orders of magnitude in a large-scale chemical screen. These are inherent limitations of using a live animal system for high-throughput chemical screens. Exploration of alternatives must be done before we can scale our chemical screens to a large scale otherwise we risk ruling out many lead compounds as false negatives because of improper delivery methods or improper titration.

3.2 Rotenone is a potent fish toxin, and displays dopamine neuron neurotoxicity when fish are raised at 22ºC

As described in the previous section, we saw that rotenone had an observable effect on the development of zebrafish embryos. Initially, embryos were raised at 28.5ºC, as recommended per Westerfield 1995, however, these larvae demonstrated unrestrained mortality at rotenone concentrations above 30nM (figure 3.4). We observed 25% of

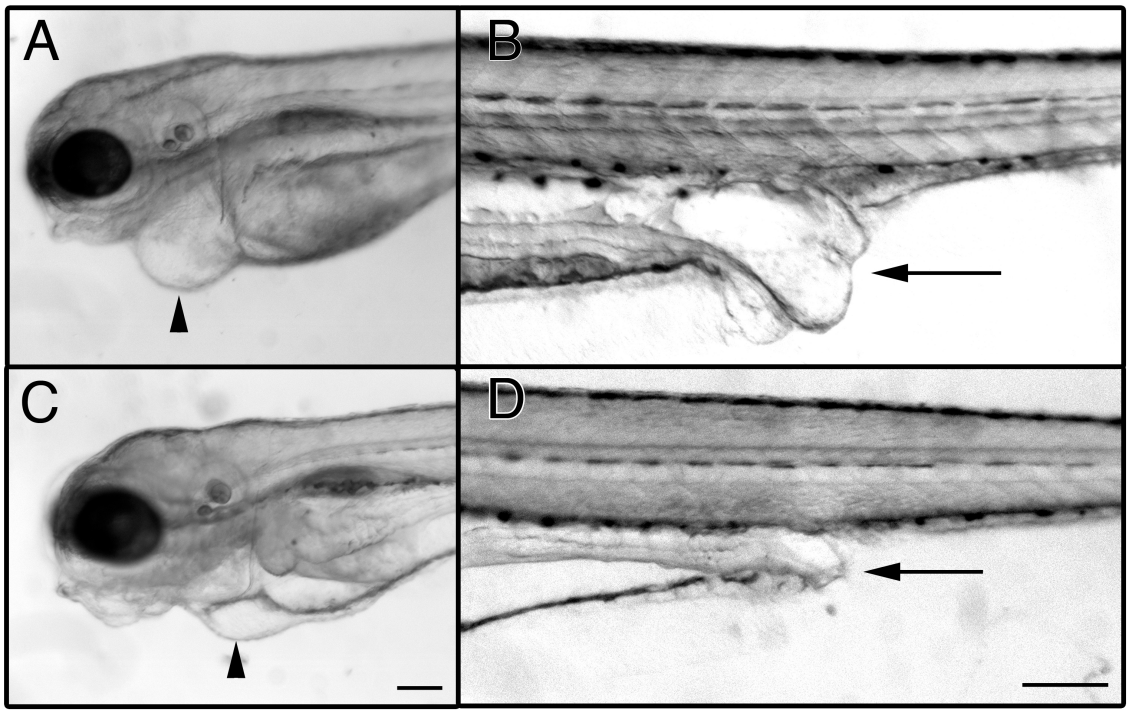

Figure 3.3: Rotenone-exposed zebrafish larva exhibit developmental abnormalities of the heart and gut

Zebrafish embryos exposed at 24 hours post-fertilization to 30nM rotenone (panels A, B) displayed non-specific developmental abnormalities such as pericardial edema (arrowheads) and gut malformations near the cloacal opening (arrows) by 7 dpf. These abnormalities were also observed in embryos treated with 100nM rotenone. Embryos treated with 0.01% DMSO exhibited no observable abnormalities (panels C, D). Scale bar: 50μm

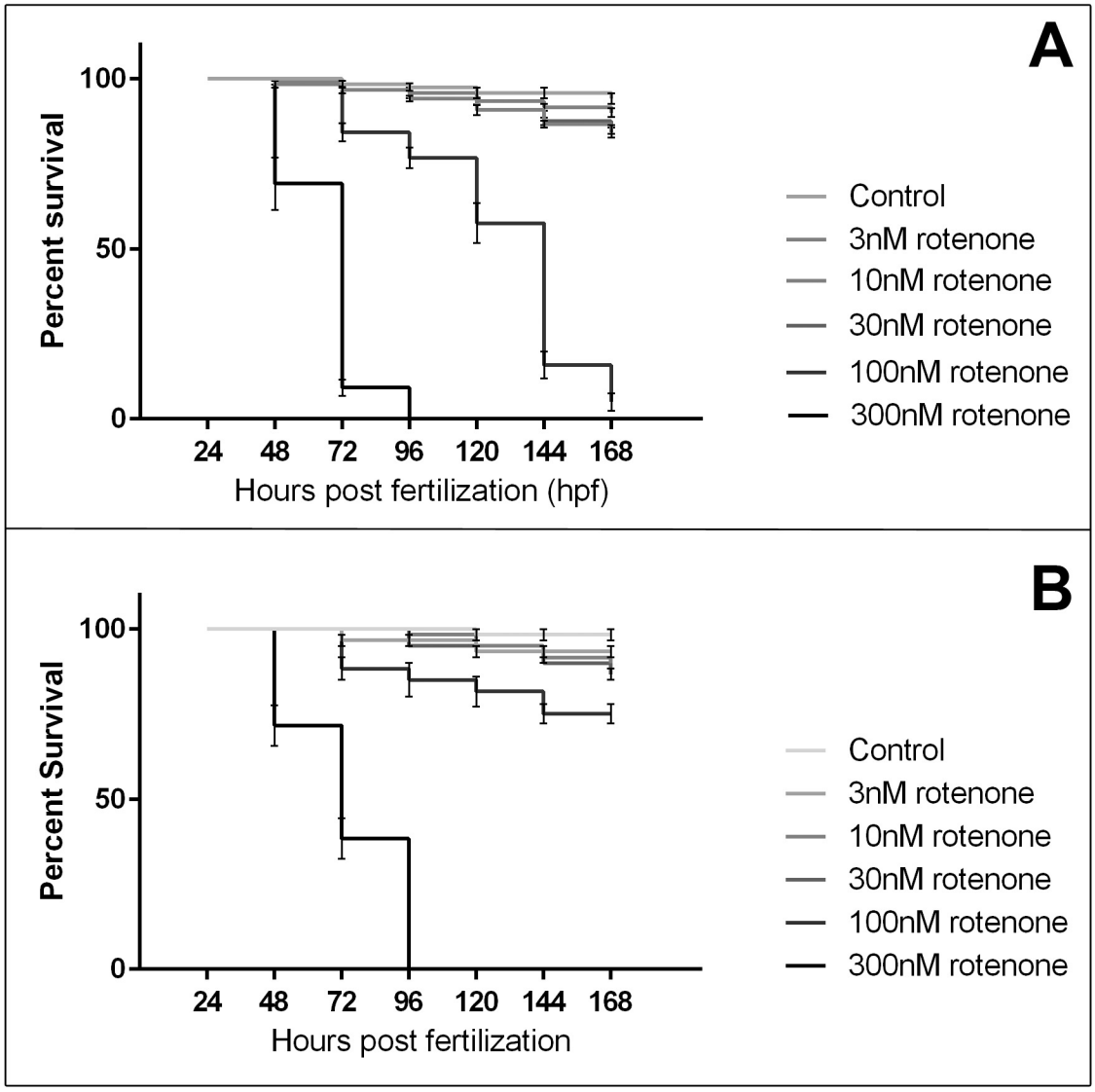

Figure 3.4: Survival of zebrafish larvae exposed to rotenone and raised at different temperatures

Embryos exposed to a half log increasing series of rotenone concentrations were raised at 28.5°C (A) and 22ºC (B). Increased mortality is seen in larvae exposed to 100nM rotenone that were raised at 28.5°C when compared to larvae raised at 22°C. Rotenone concentrations above 100nM were lethal to developing zebrafish at all temperatures.

larvae exposed to 100nM rotenone died by 96 hpf and 97% dead by 7 dpf, and 100% of larvae exposed to 300nM rotenone died by 96 hpf (figure 3.4A). We were able to keep larvae exposed to 100nM rotenone alive by raising them at room temperature (22.0ºC) instead of at 28.5ºC, increasing their survival at 7 dpf from 0% to 72% (figure 3.4B). Concentrations of rotenone above 100nM were lethal to developing larvae raised at any temperature, with no surviving larvae remaining by 96 hpf. Since zebrafish are poikilotherms, the observed difference in survival maybe dependent on their internal metabolic rate as regulated by their external temperature. As such, the cytotoxic effects of complex I inhibition will be less pronounced in animals with a lower basal metabolic rate, and the reactive oxygen species mediated damage to dopamine neurons will become more pronounced. Therefore, all of our experiments with rotenone were performed on embryos raised at 22.0°C after the first 24 hours of development.

3.3 Rotenone neurotoxicity displays a dose-dependent relationship with rotenone concentration

To validate the pharmacological disruption observed with rotenone, the Tg(*dat:EGFP*) transgenic zebrafish embryos were exposed to various concentrations of rotenone or to 0.01% DMSO vehicle control (figure 3.5A) and imaged at 7 dpf for changes in patterning of their dopaminergic neurons. Larvae exposed to low doses of rotenone (0.3 nM or 1nM respectively; figure 3.5, panels B, and C) demonstrated no appreciable changes in green fluorescence patterning compared to the DMSO controls. The first changes in neuronal patterning are first observed in the olfactory bulb (Ob) at a concentration of 1nM

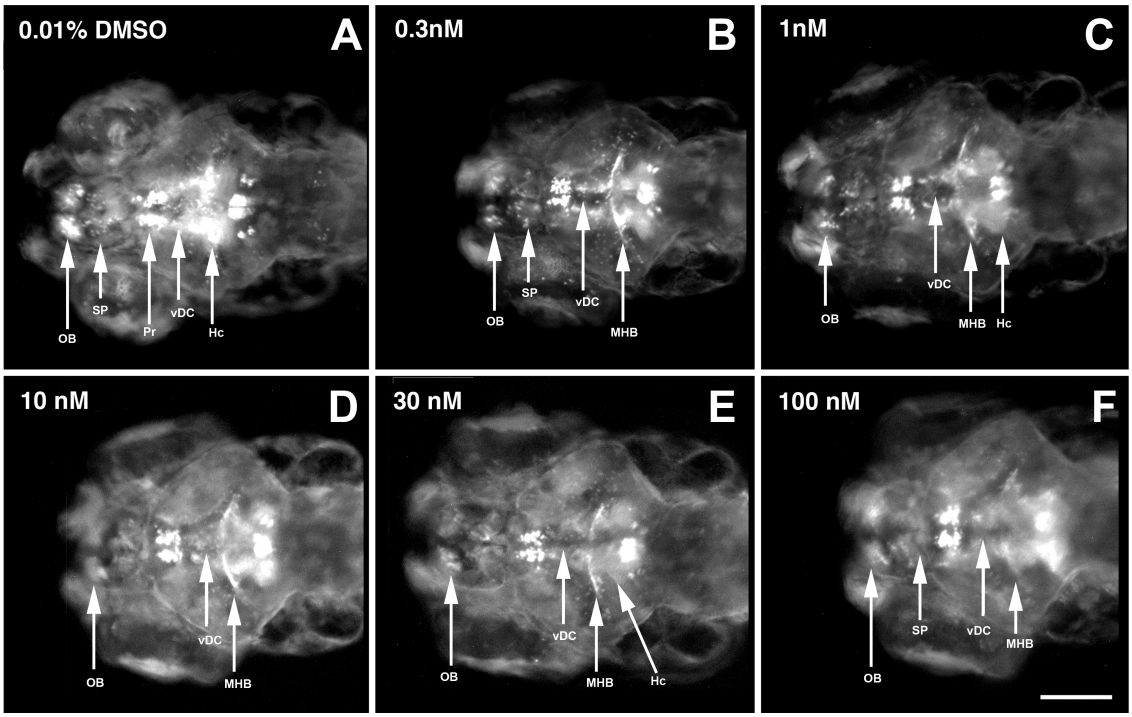

Figure 3.5: Morphology and distribution of dopaminergic neuron clusters in 7 dpf zebrafish embryos exposed to rotenone

Tg(*dat:EGFP*) zebrafish embryos were exposed at 24 hpf to either a 0.01% DMSO solution (A), or 1nM, 3nM, 10nM, 30nM or 100nM rotenone solutions (panels B-F respectively) then imaged at 7 dpf. GFP expression was examined in the olfactory bulb (Ob), pretectal area (Pr), ventral diencephalon (vDC), midbrain-hindbrain boundary (MHB), subpallium (SP) and hypothalamic clusters (Hc). All animals are shown in a dorsal view, anterior to the left. Scale bar: 50µm

rotenone (figure 3.5C), and labeling becomes completely absent at 10nM rotenone (figure 3.5D). Labeling of these neurons shows a decrease in fluorescence intensity in the ventral diencephalon (vDC) at a 30nM concentration (figure 3.5E), and labeling in both regions becomes almost entirely absent with exposure to 100nM rotenone (figure 3.5F). The midbrain-hindbrain boundary (MHB) and subpallium within the telencephalon (SP) also appears to become mildly disrupted at 100nM. Neuronal labeling in the pre-tectal (Pr) and hypothalamic (Hc) areas is unaffected even at the highest concentrations of rotenone. Larvae exposed to 300nM or 1000nM concentrations of rotenone did not survive past the third treatment day.

3.4 Rotenone causes developmental defects as early as 24h after exposure

Having seen the neurodegenerative changes at 7 dpf, we examined for rotenone-induced impairments over a developmental time course to determine the earliest onset of neurotoxic effects in Tg(*dat:EGFP*) embryos. At 48 hpf, these developing embryos express GFP in the developing MHB (figure 3.6A), Ob and nonspecifically in developing facial cartilage (Jc, figure 3.6A'). At this stage, and after 24h of exposure to 100nM rotenone, the green fluorescence signal appears slightly reduced in the developing MHB and Ob (figure 3.6, panels B and B'). At 4 dpf (figure 3.6, panels C and D) and 5 dpf (figure 3.6, panels E and F), the change in the pattern of fluorescence becomes more apparent, with rotenone-treated larvae displaying a marked reduction in Ob and MHB labeling (figure 3.6, panels D and F), and a conspicuous absence of neuronal labeling in the vDC at 5 dpf (figure 3.6, panel F) suggesting that the effect of rotenone neurotoxicity

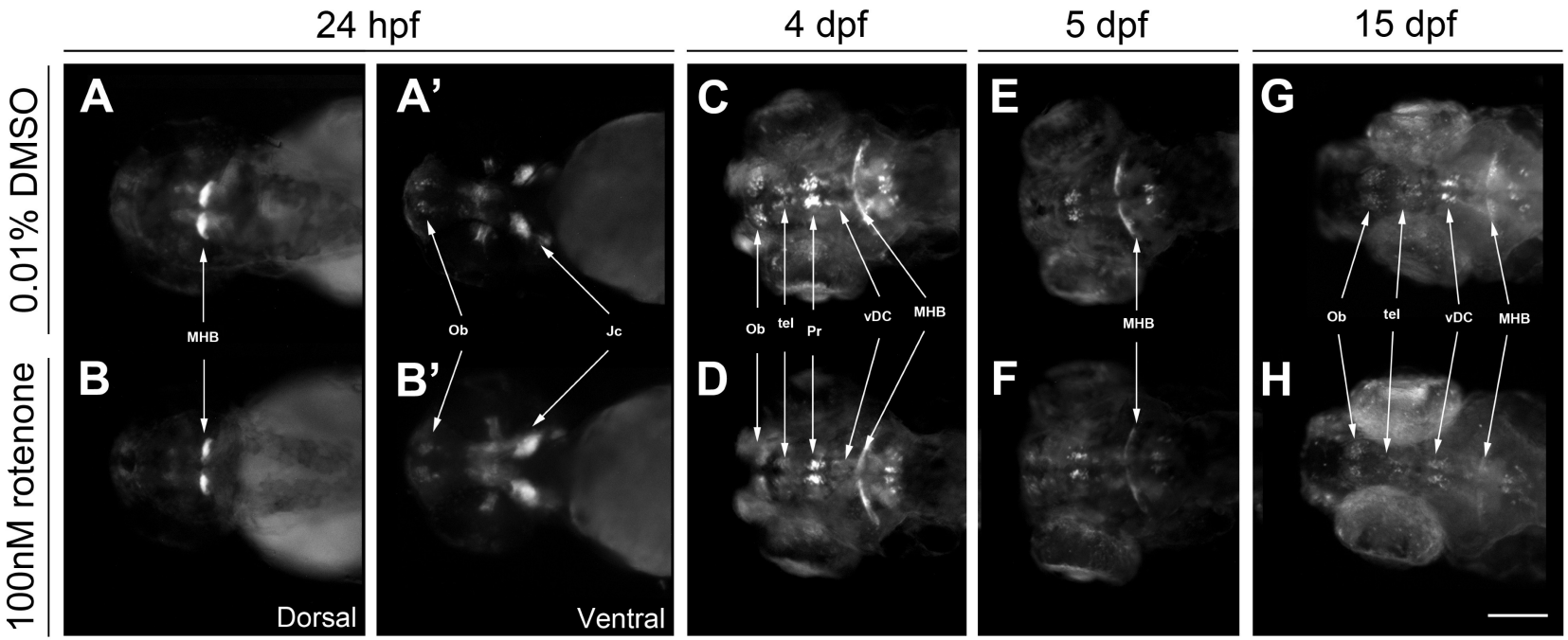

Figure 3.6: Developmental effects of rotenone on dopaminergic neuron clusters
Tg(*dat:EGFP*) zebrafish embryos were exposed at 24 hours post-fertilization to either a 0.01% DMSO solution (panels A, A', C, E and G), or a 100nM rotenone solution (panels B, B', D, F and H). Changes in GFP expression were assessed at the midbrain-hindbrain boundary (MHB), olfactory bulb (Ob), telencephalon (tel), pretectal area (Pr), and ventral diencephalon (vDC). Nonspecific expression was also observed in the jaw cartilages (Jc). Embryos were imaged at at 24 hpf (panels A, A', B and B'), 4 dpf (panels C and D), 5 dpf (panels E and F) and at 15 dpf (panels G and H). All animals are shown in a dorsal view (except for panels A' and B' which are ventral views), anterior to the left. Scale bar: 50µm

begins when these structures first develop. These changes appear permanent: when rotenone-treated larvae were imaged at 15 dpf (figure 3.6, panel G and H), rotenone-treated larvae show a reduction in labeling intensity in the MHB, an absence of labeling in the vDC and telencephalon (tel), and a smaller Ob fluorescent neuron cluster (figure 3.6, panel H). There was no evidence of recovery apparent by 15 dpf. Tg(*dat:EGFP*) larvae exposed to 1.0mM MPTP also demonstrated similar deficits to the olfactory bulb with the most salient findings in the ventral diencephalic area (figure 3.7), thus confirming our observations that rotenone was neurotoxic to dopamine neurons.

3.5 MPP+ and rotenone reduce number and intensity of tyrosine hydroxylase positive neurons

We performed immunolabeling with antibodies against proteins that are involved in the dopamine metabolism pathway. The effect of MPTP was previously documented in Xi *et al*. (2011b), so to validate the neurotoxic effect of rotenone and MPP+ (the active metabolite of the neurotoxin MPTP) on dopamine neurons, we used antibodies against tyrosine hydroxylase (TH), an enzyme that catalyzes the rate-limiting step in *de novo* dopamine synthesis to assess differences between the patterning of dopamine neurons in embryos that have been either treated with these environmental agents or left untreated. Wild type embryos were exposed to 1.5mM MPP+ or rotenone, and then immunolabeled to determine the number and distribution of TH-positive neurons. Embryos exposed to MPP+ demonstrated a decrease in TH-positive neurons in the vDC when imaged at 3 dpf (data not shown), and the difference became more pronounced

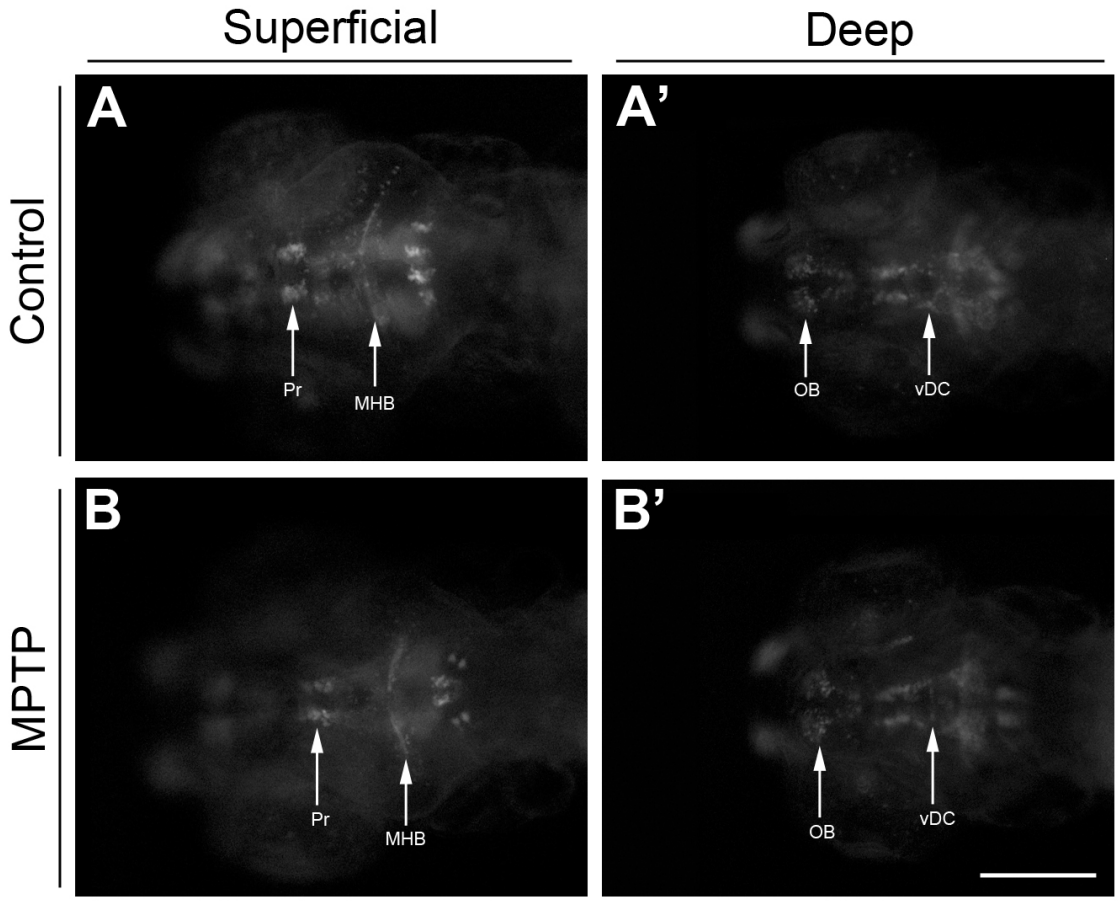

Figure 3.7: Morphology and distribution of dopaminergic neuron clusters in 7 dpf zebrafish embryos exposed to MPTP

7 dpf Tg(*dat:EGFP*) embryos exposed to 0.5mM MPTP at 24 hpf (panels B, B') demonstrate a number of changes in neuronal patterning when compared to untreated controls (panels A, A'). Changes were observed in superficial dopamine neuron populations such as the pretectum (Pr), and the number of neurons in the midbrain-hindbrain boundary (MHB). Changes were also observed to deep dopamine neuron populations, such as a disruption in the patterning and reduction in number of neurons in the ventral diencephalon (vDC). There appears to be no change in the size or number of neurons in the olfactory bulb (OB) of larva exposed to 0.5mM MPTP. Scale bar: 50µm

when larva were observed at 7 dpf (figure 3.8, arrows). We were also able to visualize a decreased dopaminergic neuron labeling with immunohistochemistry for TH on 3 dpf embryos that had been exposed to concentrations of rotenone greater than 10mM. This rotenone exposure resulted in a decrease in labeling of TH+ neurons in the ventral diencephalon (figure 3.9, arrows), comparable to the changes seen with MPP+ exposed embryos. However, immunolabeling on 7 dpf larvae were technically very difficult because of diminished tissue permeability to antibodies. With 3 dpf tissue, we observed successful staining in approximately only 20% of specimens per sample, yielding low reliability, high variability and certainly lacking the reproducibility needed for a large-scale *in vivo* chemical screen. To confirm our observations of decreased dopaminergic neuron labeling in our rotenone-exposed transgenic embryos, immunolabeling on cryosections 3 dpf embryos exposed rotenone were compared to immunolabeling on cryosections 3 dpf embryos exposed to MPP+. We performed immunolabeling on 14μm frozen sections from Tg(*dat:EGFP*) embryos and larvae at 3, 5 and 14 dpf, using anti-GFP and anti-tyrosine hydroxylase antibodies. We observed that larva exposed to rotenone displayed a reduction in the number of cells in the pretectum, olfactory bulb, locus coeruleus and ventral diencephalon at 5 dpf (figure 3.10). Reductions in the pretectum, olfactory bulb and ventral diencephalon are particularly interesting because of the high density of dopamine neurons in these locations, and reductions in the locus coeruleus are seen likely since dopamine is a precursor to norepinephrine catabolism. We observed 29.4% decrease in the pretectum (figure 3.10A), a 31.3% decrease in the olfactory bulb (figure 3.10B), and 57.1% decrease in neurons in the locus coeruleus

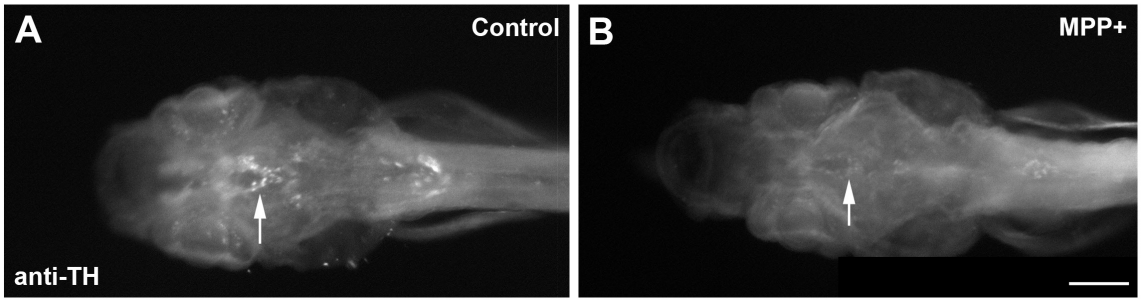

Figure 3.8: Immunohistochemistry for tyrosine hydroxylase in 7 dpf wild type zebrafish larvae exposed to MPP+

Anti-tyrosine hydroxylase immunostain of 7 dpf larva treated with 1.5mM MPP+ (B) demonstrates a decrease in intensity and number of TH-positive neurons in the ventral diencephalon (arrow) when compared to wild type controls (A). Scale bar: 50µm

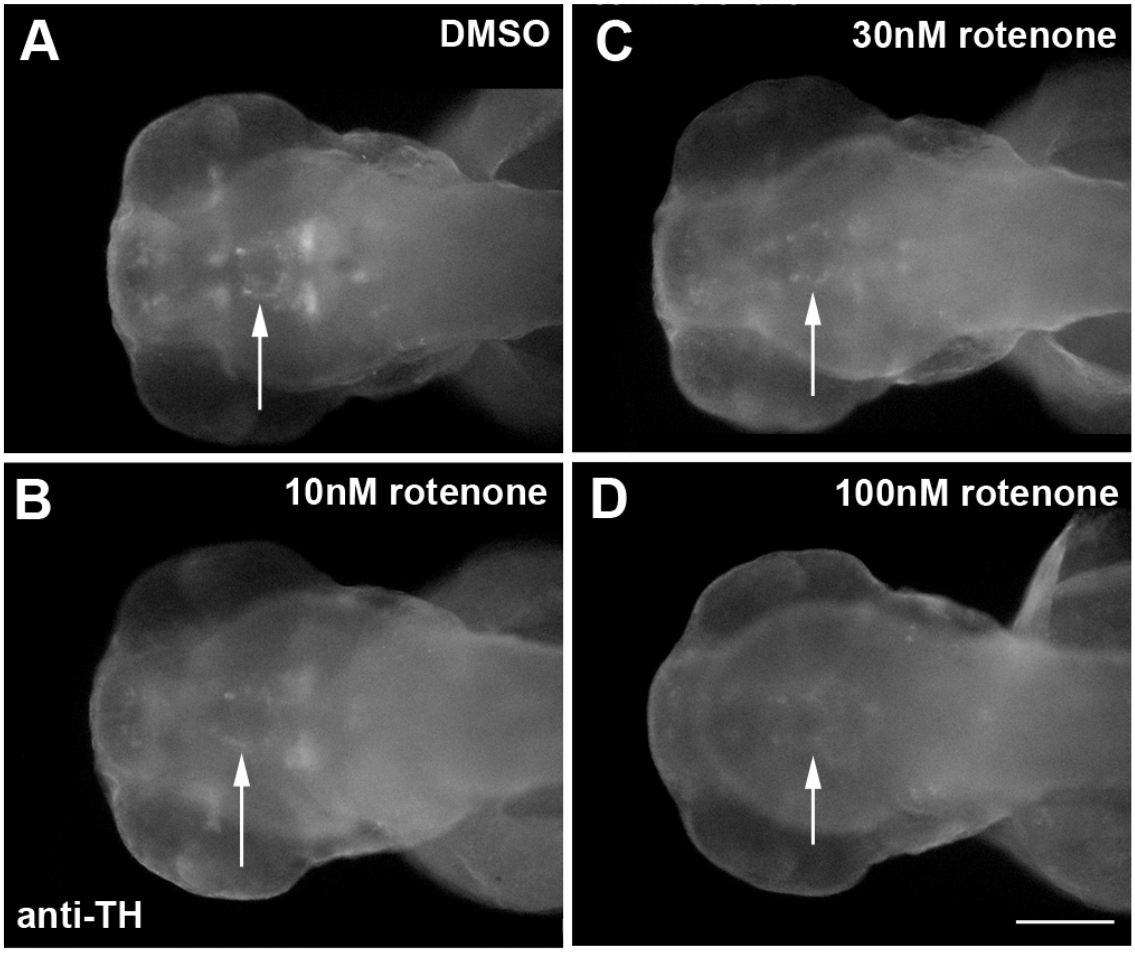

Figure 3.9: Immunohistochemistry for tyrosine hydroxylase in 3 dpf wild type zebrafish embryos exposed to rotenone
Anti-tyrosine hydroxylase (anti-TH) immunostains of 3 dpf larva treated with 10nM (B), 30nM (C) or 100nM (D) rotenone at 24 hpf demonstrates a graduated reduction in the intensity and number of TH-positive neurons in the ventral diencephalon (arrows) when compared to wild type controls (A). Scale bar: 50µm

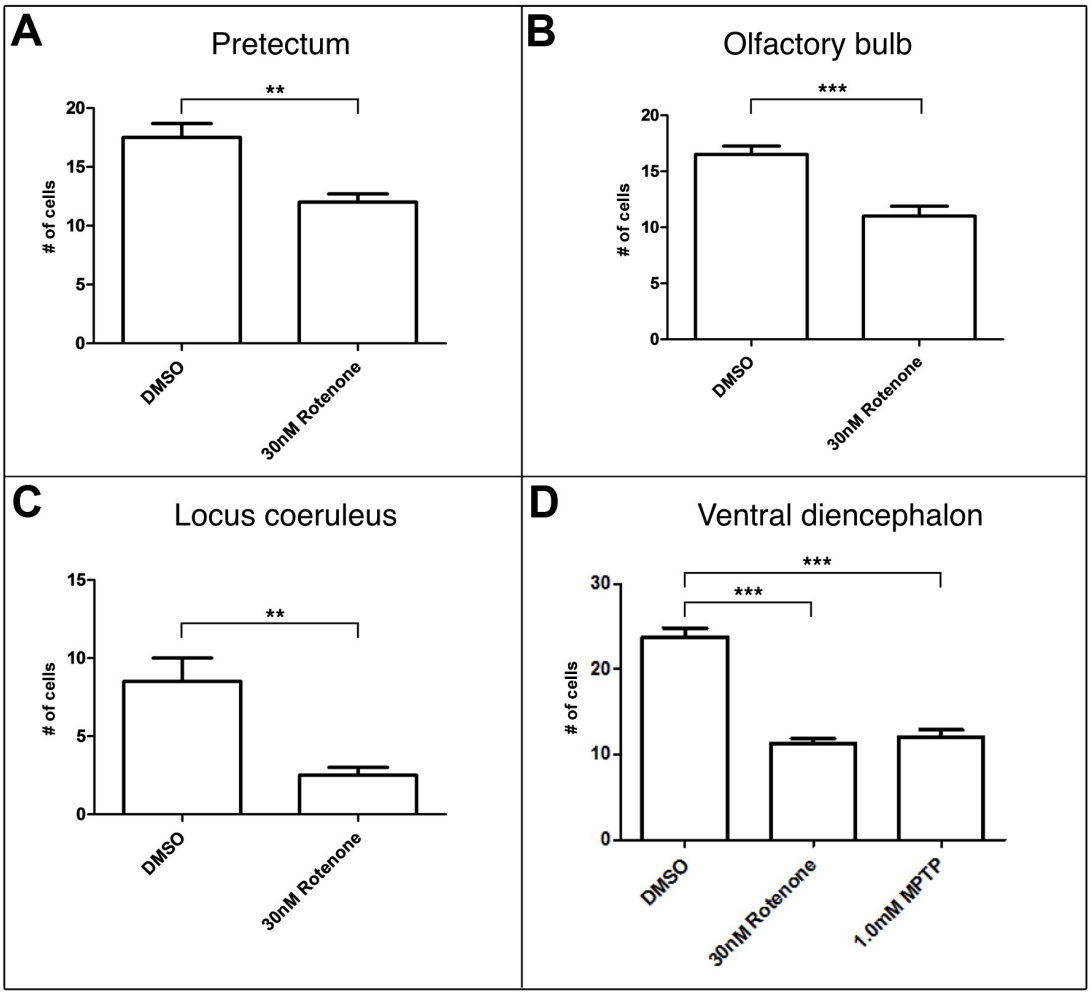

Figure 3.10: Numbers of dopamine neurons in various brain regions are reduced in 5 dpf embryos exposed to rotenone.
Tg(*dat:EGFP*) zebrafish embryos were exposed at 24 hours post-fertilization to either a 30nM rotenone or 1.0mM MPTP solution, or a 0.01% DMSO control, then raised to 5 dpf for quantification of dopamine neurons. Embryos were then cryosectioned to count the number of fluorescent cells in a single hemisphere of the pretectum, olfactory bulb, locus coeruleus and ventral diencephalon following exposure.. Changes in the number of neurons were observed with the pretectum (A, 17.50 ± 1.19 vs 12.00 ± 0.71, n=6, $p<0.01$), olfactory bulb (B, 16.50 ± 0.76 vs 11.00 ± 0.89, n=6, $p<0.001$), locus coeruleus (C, 9 ± 0.71 vs 4 ± 0.89, n=5, $p<0.01$) and ventral diencephalon (D, 24.06 ± 1.1 vs 11.52 ± 0.86, n=14, $p<0.001$). Changes to the ventral diencephalon (12.54 ± 1.2 decrease) were comparable to the proportion of neurons lost in embryos exposed to MPTP (12.56 ± 1.7 decrease), a known dopamine neuron neurotoxin.

(figure 3.10C). The dopamine neurons in these regions also appeared to have an abnormal distribution. We also observed a 52.1% reduction in dopamine neurons in the ventral diencephalon (figure 3.10D), which is consistent with the reduction in neuronal counts in the ventral diencephalon seen with MPTP (52.1% vs 47.8% decrease), and with the proportion of dopamine neurons lost in the *substantia nigra* in patients with Parkinson's disease (reviewed in Cheng *et al.*, 2010). These changes appeared most prominent at 5 dpf, likely because zebrafish larvae have developed an extensive network of dopamine neurons by this point. However, by 15 dpf, the changes to these dopamine neuron clusters appeared to be attenuated, and the differences between cell populations were decreased (figure 3.11).

3.6 MitoSOX Red shows that larva exposed to rotenone experience elevated oxidative stress

In order to explore the mechanism of action of rotenone, we used the mitochondrial superoxide indicator MitoSOX Red for live detection of reactive oxygen species damage. Dopamine neurons undergo a heavy oxidative stress load due to the high oxidative potential of dopamine itself during dopamine synthesis *de novo* (reviewed in Miyazaki and Asanuma, 2008). Furthermore, mitochondrial damage secondary to rotenone-induced inhibition of mitochondrial complex I will increase the oxidative load within a cell. As a result, we expected an increase in the number of foci of oxidative stress within the developing larva. MitoSOX Red is a chemical marker of oxidative stress, and previous studies have used MitoSOX Red *in vivo* as a label of oxidative stress foci. Embryos

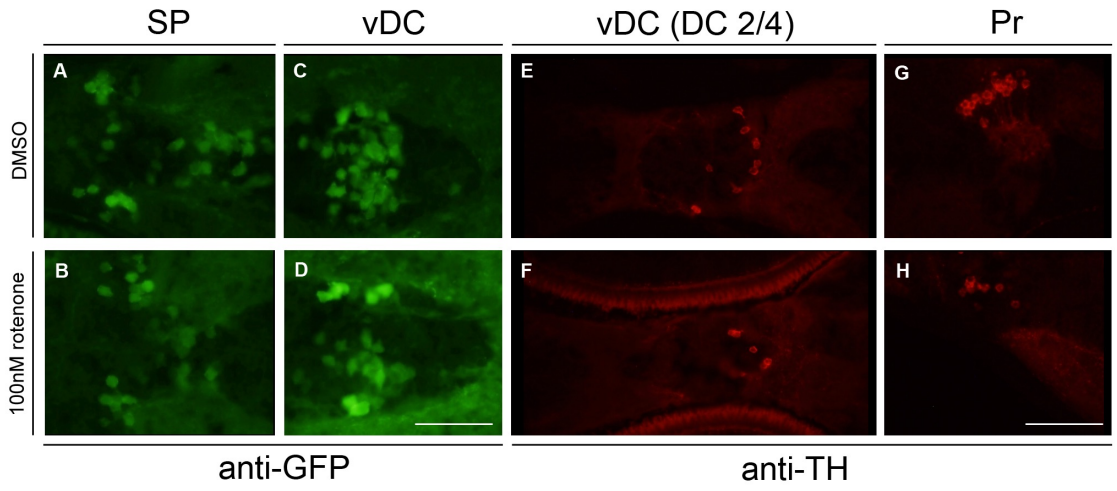

Figure 3.11: Rotenone-induced changes to the subpallium and ventral diencephalon appear attenuated by 15 dpf

Tg(*dat:EGFP*) embryos exposed to 100nM rotenone (panels B, D, F and H) or 0.1% DMSO (panels A, C, E and G) at 24 hpf were grown to 15 dpf. Frozen sections (14µm thickness) were immunolabeled with anti-GFP (panels A-D) and anti-tyrosine hydroxylase (panels E-H). Neurons were observed in the subpallium (SP), ventral diencephalic clusters (vDC), diencephalic clusters 2 and 4 (DC 2/4)and pretectum (Pr) to assess for changes to neuronal patterning and distribution. Changes appeared less pronounced than with embryos grown to 5 dpf after rotenone exposure. Scale bar: 50µm

exposed to rotenone were grown to 4 dpf, anesthetized, rinsed and incubated for 15 minutes in a solution of MitoSOX Red. Following exposure to MitoSOX Red, larvae were washed rigorously and imaged for fluorescence. We were able to count the number of foci of oxidative stress, and we saw an increase in number of these foci in larvae exposed to rotenone compared to unexposed larvae. The 15 minute incubation time in MitoSOX Red was insufficient to yield reagent penetration and fluorescent foci formation in deep brain structures within the head of the larva (figure 3.12A). Longer incubation times yielded embryonic toxicity and nonspecific superficial staining. Although no fluorescent foci were observable in the brain of both the control and the exposed fish, there appeared to be a correlation between the total number of red fluorescent foci along the trunk of the zebrafish larva, and concentration of rotenone (figure 3.12B). Embryos exposed to higher concentrations of rotenone showed more red fluorescent foci than the control larvae, demonstrating that rotenone is associated with dose-dependent oxidative stress. However, larvae exposed to 200μM of ascorbic acid (a powerful anti-oxidant) in a co-treatment with rotenone demonstrated an attenuation in the number of oxidative foci when compared to larvae exposed to rotenone alone (figure 3.12C). These data suggest that rotenone impairs the larva's ability to manage oxidative damage and that this impairment is fundamental to the pathogenesis of rotenone-induced neurotoxicity. Therefore, we decided to test if this oxidative damage could induce programmed cell death in dopamine neurons from larvae exposed to rotenone.

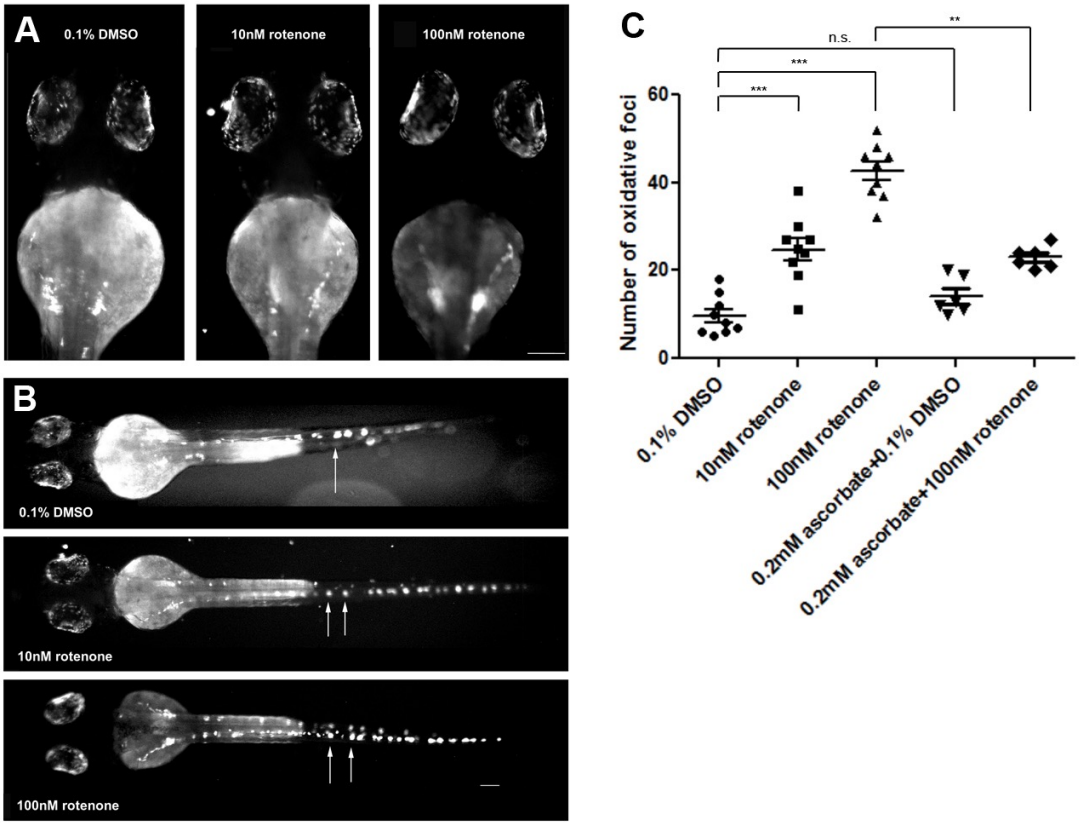

Figure 3.12: Assessment of reactive oxygen species-mediated damage in larvae exposed to rotenone

Embryos exposed to either 10nM rotenone, 100nM rotenone or 0.1% DMSO were raised to 4 dpf and were assessed for foci of oxidative stress along the head (A) and trunk (B, arrows). The number of MitoSOX Red foci in the trunk of zebrafish larvae (arrows) was manually quantified for each treatment group (C) as a marker of oxidative stress. Larvae exposed to 10nM rotenone (24.78 ± 2.5, n=9, $p<0.001$) or 100nM rotenone (42.56 ± 2.1, n=9, $p<0.001$) demonstrated an increase in the number of oxidative foci when compared to controls (9.667 ± 1.5, n=9). Larvae co-treated with 200µM ascorbic acid demonstrated reduced levels of oxidative stress in comparison to embryos exposed to rotenone only (19.56 ± 2.7 decrease, n=6, $p<0.01$). Ascorbic acid co-treatment did not significantly change the number of oxidative foci (14.17 ± 1.7, n=6). All animals are shown in a dorsal view; larvae were oriented anterior to the top in panel A, and anterior to the left in panel B. Scale bars:100µm.

3.7 Rotenone induces caspase-mediated cell death of dopamine neurons

Rotenone is a compound with strong oxidative properties due to its ability to inhibit mitochondrial complex I and subsequently disrupt the electron transport chain. As demonstrated previously, rotenone causes neuronal mis-patterning and decreases the number of dopaminergic neurons. To assess whether rotenone neurotoxicity was dependent on apoptosis secondary to reactive oxidative species damage, wild type embryos exposed to rotenone at 24 hpf were assessed at 3 dpf by immunolabeling with an anti-active caspase 3 antibody. Caspase 3 is a protein that is activated when exposed to extra-mitochondrial cytochrome *c*, acting as a marker for apoptosis caused by mitochondrial damage. Caspase 3 activity was seen in the olfactory bulb, telencephalon, and anterior hypothalamus/ventral diencephalon of these larval fish (figure 3.13 panels A-C). Similar clusters are also labeled with anti-active caspase 3 in larva exposed to MPTP (figure 3.13D and E). These clusters give rise to the areas seen at 7 dpf that are absent or severely mis-patterned when exposed to rotenone. These data show that when zebrafish embryos are exposed to high concentration of rotenone, the caspase protein is localized to the structures within 48 hours of exposure, therefore suggesting that rotenone can induce programmed cell death in these neurons. We then took cryosections of Tg(*dat:EGFP*) embryos and larva at various stages and exposures to different concentrations of rotenone, and immunolabeled them for active caspase 3 and caspase 9. Better optical clarity was achieved by performing immunolabeling on cryosections than with whole mount immunolabeling since the thinner sections allowed for better penetration of the large immunoglobulins used to label our neuroanatomical structures. We were then able

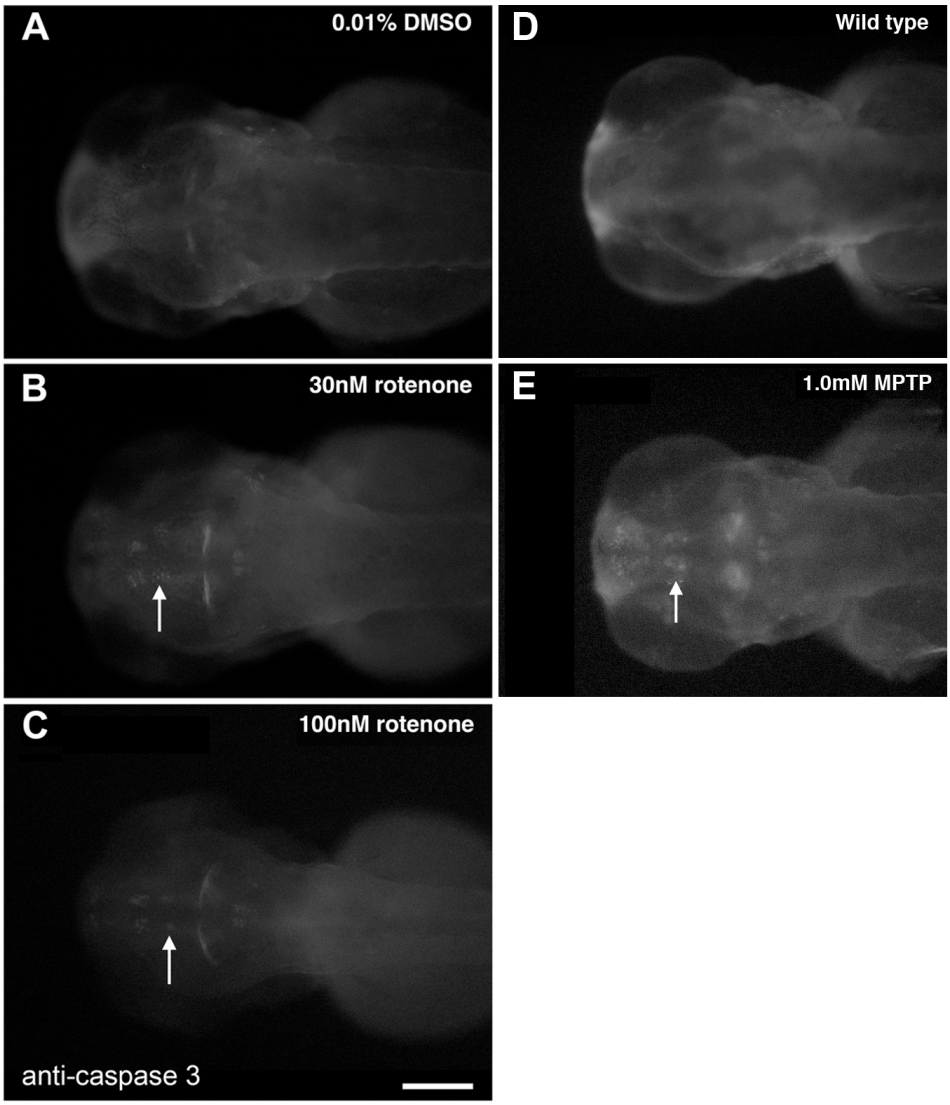

Figure 3.13: Immunohistochemistry against active caspase 3 in 3 dpf wild type zebrafish embryos exposed to rotenone or MPTP

Immunohistochemistry of anti-Caspase 3 in 3 dpf embryos treated with rotenone (panels B, C) or MPTP (E) demonstrates the presence of active caspase 3 in the ventral diencephalon (arrows). Labeling was also observed in the pretectum and locus coeruleus of 3 dpf embryos exposed to 30nM (B) at 24 hpf. Active caspase 3 was also observed in the olfactory bulb, telencephalon, pretectum and locus coeruleus of 3 dpf embryos exposed to 100nM rotenone (C) at 24 hpf. All treatment groups, including DMSO controls (A) show non-specific fluorescence in the midbrain-hindbrain boundary likely caused by antibody sequestration. 3 dpf embryos treated with 1.0mM MPTP (E) demonstrate the presence of caspase 3 in the olfactory bulb, ventral diencephalon (arrow) and anterior hypothalamus of 3 dpf embryos treated with 1.0mM MPTP, when compared to 3 dpf wild type embryos (D). Scale bar: 50μm

to co-localize GFP expression with both caspase 3 (figures 14 and 15) and caspase 9 expression (figure 3.16), suggesting that dopamine neurons were undergoing apoptosis. There was occasional caspase labeling in the subpallium of the embryonic zebrafish brain as well (figure 3.14B, arrowhead). Caspase labeling also did not overlap completely with GFP labeling, such as the pretectum (figure 3.14D, arrowhead), suggesting that some dopaminergic areas were spared from apoptosis (figure 3.15D'). Using confocal microscopy to image some of the rotenone-exposed samples, we were able to visualize the sub-cellular localization of the caspase signal (figure 3.17). Caspase 3 (red) appeared to localize in the cytoplasm of the dopamine neuron cell bodies, alongside the green fluorescent protein (figure 3.16B, arrows; figure 3.17, arrows), and distinct from the nucleus of the cell body (DAPI; blue). In many examples, the GFP signal appeared to be relatively weak, and the cell morphology different from regularly shaped healthy neurons (figure 3.18, arrowhead), but caspase signaling was most salient in the region of the developing ventral diencephalon near dopamine clusters 2 and 4 (figure 3.15D'', arrowheads; figure 3.16C' arrow; figure 3.17, arrowheads; figure 3.18C, arrowhead), and around the anterior hypothalamic regions (figure 3.18 panels C and D, arrows). The cell bodies also appeared to undergo a morphological shift, transforming from their usual stellate structure (figure 3.18 panels A and B) into an elliptical structure, in addition to displaying an increased nucleus-to-cytoplasm ratio (figure 3.17, arrowheads). These changes were also further quantified, averaging between 16.5 and 18.2 co-localizing foci in rotenone-exposed embryos versus 3.0 foci in vehicle controls (figure 3.19). The caspase signaling in rotenone-exposed larva was weak or below the limit of clear

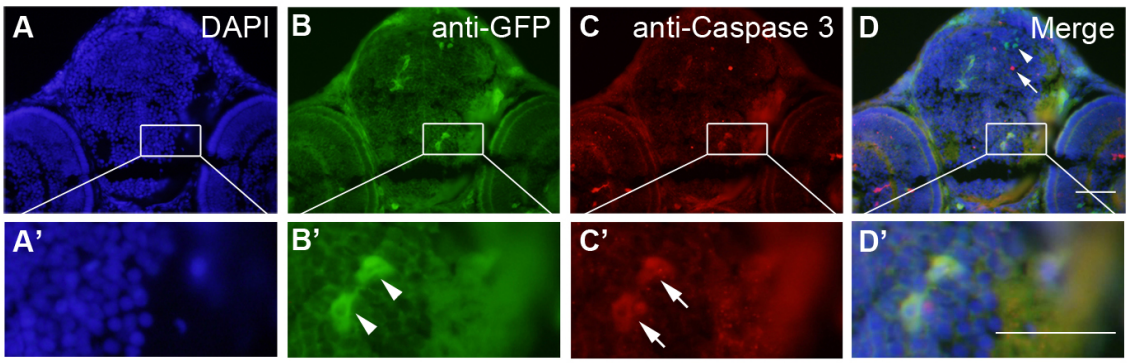

Figure 3.14: Rotenone induces caspase 3-mediated apoptosis in dopamine neurons
Frozen sections (14µm) of 3 dpf Tg(*dat:EGFP*) zebrafish embryos exposed to 30nM rotenone were immunolabeled with nuclear stain DAPI (A, A'), anti-GFP (B, B'), and anti-caspase 3 (C, C'). GFP labeling was observed in the dopamine neurons of the pretectum and ventral diencephalic clusters (B', arrowheads). Caspase 3 activity also observed in ventral diencephalic neurons (C', arrows) but not in pretectal neurons. A merge of the different channels (D) demonstrates co-localization of the caspase and GFP signals in the dopamine neurons of the ventral diencephalon (D'), in addition to foci of independent caspase 3 labeling (arrow) and pretectal neurons that do not co-localize with caspase 3 (arrowhead). Marked areas of interest are magnified in prime panels. Scale bars: 50µm

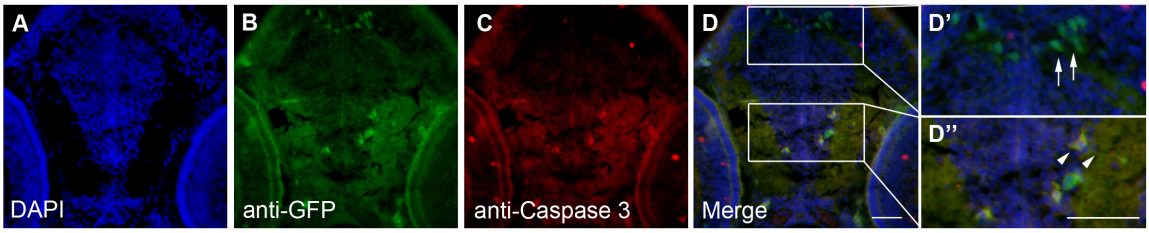

Figure 3.15: Caspase 3-mediated apoptosis is localized to ventral diencephalic dopamine neurons

Frozen sections (14µm) of 3 dpf Tg(*dat:EGFP*) zebrafish embryos exposed to 30nM rotenone were immunolabeled with nuclear stain DAPI (A), anti-GFP (B), and anti-caspase 3 (C). A merge of the different channels (D) demonstrates labeling in the pretectum that does not co-localize with caspase 3 (D', arrows), and co-localization of the caspase and GFP signals in the dopamine neurons of the ventral diencephalon (D'', arrowheads). Marked areas of interest are magnified in prime panels. Scale bar: 50µm

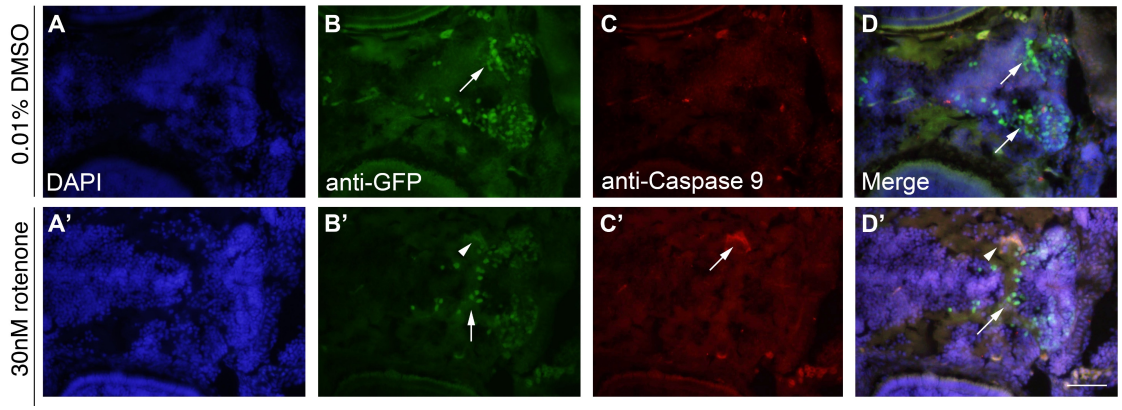

Figure 3.16: Immunohistochemistry for caspase 9 (red) and GFP (green) of 14µm transverse sections of 3 dpf Tg(*dat:EGFP*) zebrafish larvae exposed to rotenone
Frozen sections (14µm) of 3 dpf Tg(*dat:EGFP*) zebrafish embryos exposed to 0.1% DMSO (panels A-D) or 30nM rotenone (prime panels) were immunolabeled with anti-GFP (B, B'), anti-caspase 9 (C, C') and nuclear dye DAPI (C, C'). GFP labeling was observed in the dopamine neurons of the ventral diencephalic clusters (B, B', arrows), with some neurons undergoing a morphological change (B', arrowhead). Caspase 9 activity was observed in embryos exposed to 30nM rotenone (C', arrow). The caspase 9 signal co-localizes with the green GFP signal (arrowhead), suggesting dopamine neurons are undergoing cell death by apoptosis. Scale bar: 50µm

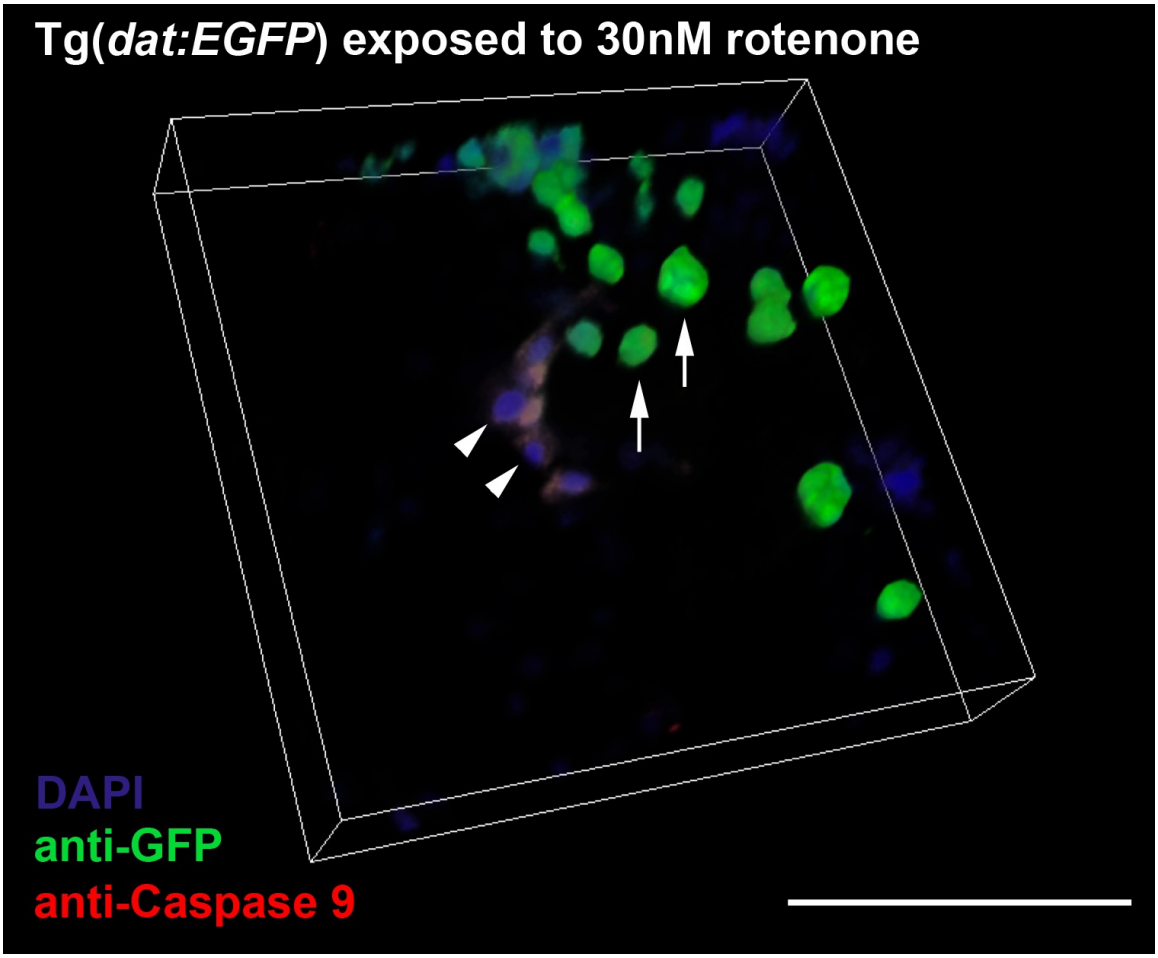

Figure 3.17: Confocal microscopy shows caspase 9 in dopamine neurons
Confocal microscopy of the sections from figure 3.16 show that GFP (green) co-localizes with caspase 9 suggesting that dopamine neurons are undergoing apoptosis. Neurons also appear to change morphology while undergoing apoptosis, transitioning from punctate (arrows) to elliptical shapes. DAPI (blue) staining also shows nuclear enlargement (arrowheads) against controls (data not shown), a late stage of apoptosis. Scale bar: 50µm

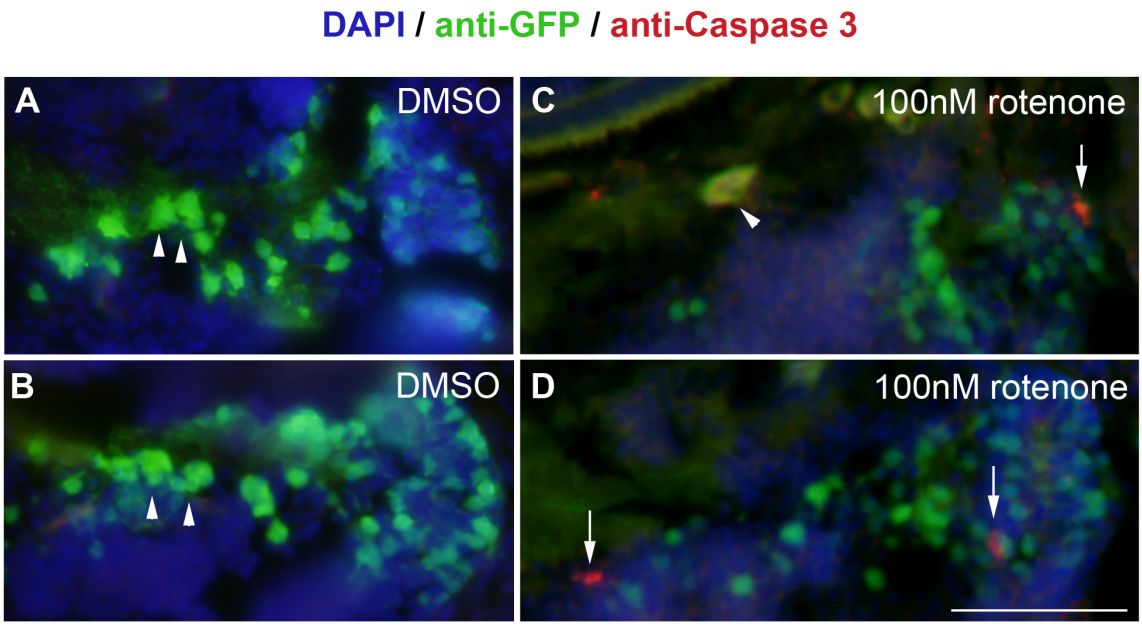

Figure 3.18: Co-localization of the caspase 3 signal with GFP-positive dopamine neurons in the ventral diencephalon of 3 dpf Tg(*dat:EGFP*) zebrafish
Frozen sections (14µm) from Tg(*dat:EGFP*) zebrafish embryos exposed to either 0.01% DMSO (panels A, B) or 100nM rotenone (panels C, D) at 24 hpf were immunolabeled with anti-caspase 3 (red) and anti-GFP (green). Embryos exposed to DMSO showed a rich population of dopamine neurons (A, B, arrowheads) and few foci of caspase 3 activity. Embryos exposed to 100nM rotenone demonstrated many foci of caspase activity either co-localizing with dopamine neurons (C, arrowheads) or adjacent to a GFP-positive dopamine neuron (C, D, arrows). Cells also appeared to change morphology when demonstrating caspase activity. Scale bar: 50µm

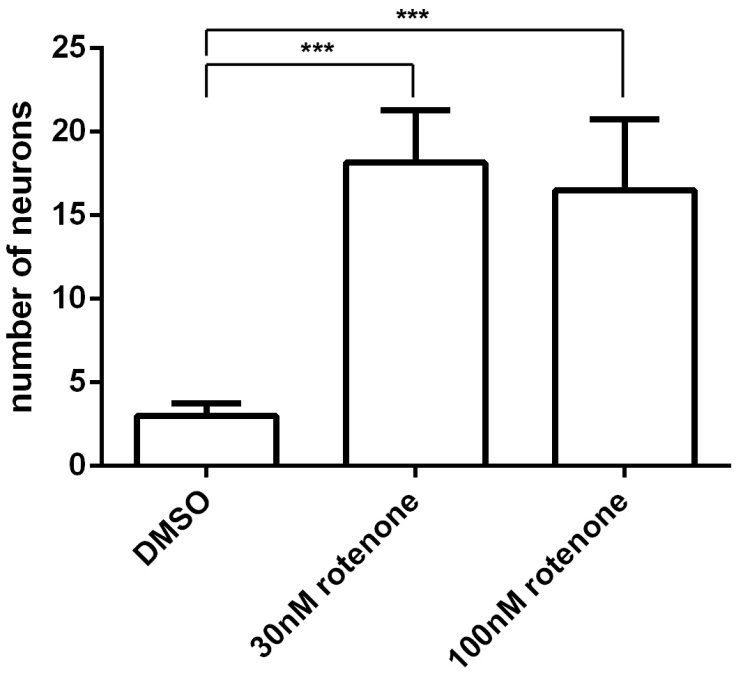

Figure 3.19: Rotenone increases co-localization between caspase 3 and dopamine neurons in developing zebrafish.
The number of co-localizing foci from the dataset used to assemble figure 3.18 were quantified, demonstrating 18.2 (± 3.1, n=12) co-localizing foci in 30nM rotenone-exposed embryos and 16.5 (± 4.3, n=12) co-localizing foci in 100nM rotenone-exposed embryos, versus 3.0 (± 0.73, n=12) foci in vehicle controls ($p<0.001$).

detection in 5 dpf and 7 dpf larva (data not shown), suggesting that caspase-mediated cell death occurs within the first 24-48h of rotenone exposure, and has little active neuronal cytotoxicity after this period. In summary, the caspase signal appears to co-localize with the dopamine neurons in embryos exposed to rotenone, peaking at 3 dpf then waning by 5 dpf and onwards. This supports our hypothesis that rotenone can induce programmed cell death of dopamine neurons secondary to mitochondrial toxicity within these cells.

3.8 Mitochondrial fractionation to look at mitochondria specific proteins in the context of rotenone exposure

Since rotenone is a potent inhibitor of mitochondrial complex I, we sought to demonstrate that the mitochondria will be directly affected in our animals exposed to rotenone neurotoxicity. Certain pro-apoptotic Bcl-family proteins will translocate to the mitochondria from the cytosol in situations that cause mitochondrial damage, so we sought to isolate these translocated proteins from the mitochondrial fraction of exposed embryos. We were able to examine proteins on a Western blot from lysates made from zebrafish embryos exposed to rotenone, and were able to observe that apoptosis-related regulator proteins translocate to the mitochondrial fraction of these lysates. Zebrafish have two paralogs of the pro-apoptotic protein Bax, Bax-a and Bax-b. We were able to visualize Bax-a proteins in zebrafish lysates (figure 3.20A). We also observed that in non-reducing conditions, Bax-a forms a high molecular weight complex at 150 kD in DMSO-exposed zebrafish that disappears when zebrafish are exposed to rotenone. We were able to demonstrate that Bax-a translocates to the mitochondria in rotenone-exposed zebrafish

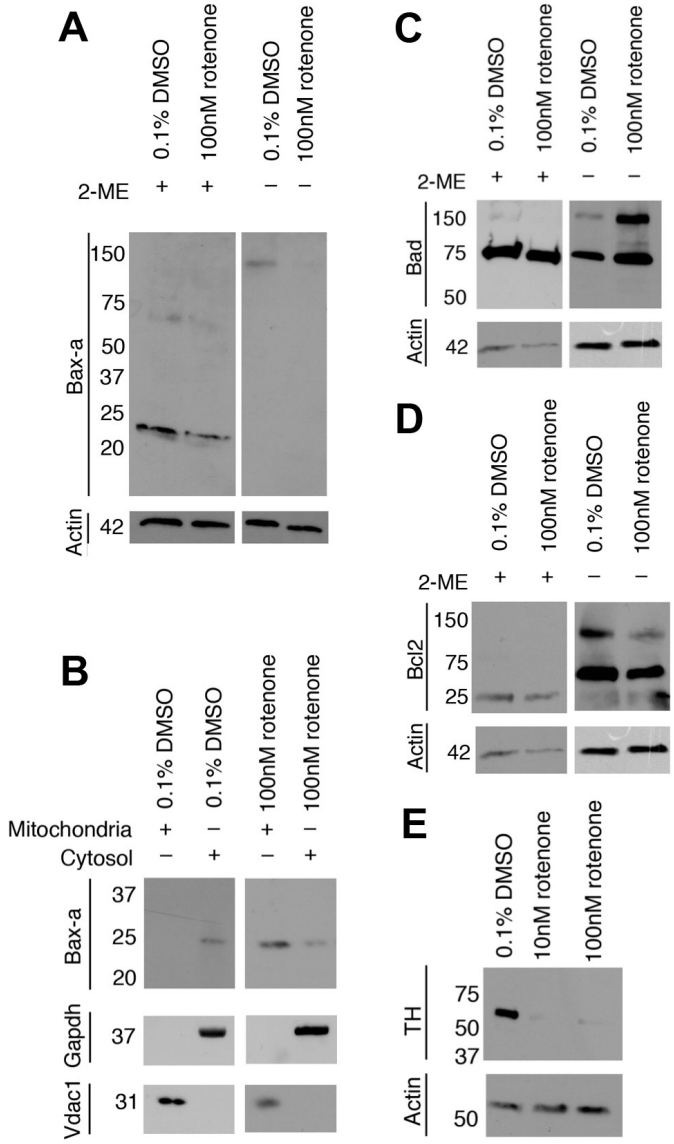

Figure 3.20: Western blots of Bax-a, tyrosine hydroxylase, Bad and Bcl2 on 48 hpf zebrafish homogenates

The pro-apoptotic protein Bax-a can be detected from 48 hpf zebrafish lysates, and appears to form a high molecular weight complex in non-reducing conditions which decreases with intensity when embryos are exposed to 100nM rotenone (A). Bax-a localizes to the cytosol in DMSO controls, and translocates to the mitochondria following rotenone exposure (B). High molecular weight complexes are found in non-reducing conditions for pro-apoptotic protein Bad (C) and anti-apoptotic protein Bcl2 (D). The complexes decrease in intensity when embryos are exposed to 100nM rotenone. Tyrosine hydroxylase levels are decreased when embryos are exposed to rotenone (E). Vdac1 is a mitochondrial marker, and Gapdh is a cytosolic marker. Actin was used as a loading control.

embryos (figure 3.20B) by the presence of a 24 kD band appearing in the fraction positive for porin (Vdac1), a mitochondrial membrane protein. This band was weaker in intensity in the fraction positive for glyceraldehyde-3-phosphate dehydrogenase (Gapdh), a glycolysis protein found exclusively in the cytoplasm. We were not able to visualize the migration of Bax-b (data not shown). This data shows that the pro-apoptotic protein Bax-a appears to translocate to the mitochondria in rotenone treated animals to activate an apoptosis cascade, and this is consistent with our model of rotenone-induced reactive oxygen species-mediated programmed cell death.

We were also able to identify both Bad (figure 3.20C) and Bcl2 proteins (figure 3.20D) from zebrafish lysates. Under non-reducing conditions, we observed that the pro-apoptotic Bad forms a 150kD high molecular weight complex in lysates from zebrafish exposed to 100nM rotenone. The anti-apoptotic Bcl2 also displayed a 100kD high molecular weight complex present only in non-reducing conditions which ameliorated with intensity in lysates from zebrafish exposed to 100nM rotenone. Bad and Bcl2 are both known to interact with other members of the Bcl-like protein family to initiate their pro- or anti-apoptotic activity. This may suggest that the intensification of the Bad high molecular weight band in lysates from rotenone-exposed zebrafish is associated with the sequestration of anti-apoptotic proteins by Bad, whereas the amelioration of the Bcl2 high molecular weight band in lysates from rotenone-exposed zebrafish may be associated with the dissociation of anti-apoptotic Bcl2 protein complexes.

We also observed that tyrosine hydroxylase (TH) levels were decreased in lysates from 48 hpf zebrafish embryos exposed to rotenone (figure 3.20 panel E), which was consistent with our morphological findings of TH-positive neuron loss. These changes were only apparent until 48 hpf. We saw little to no change in protein translocation at later stages (5 dpf, 7 dpf) (data not shown). Overall, these data strongly suggest that programmed cell death is induced by exposure of zebrafish embryos to rotenone.

3.9 Rotenone causes mitochondrial damage and a loss in mitochondrial membrane potential

To reinforce our previous Western blot observations showing that rotenone causes damage to the mitochondria, we sought to visualize the damage to mitochondria using transgenic Tg(*dat:tom20 MLS-mCherry*) embryos. These embryos express an mCherry fluorescent marker in the mitochondria of dopamine neurons only. We compared the morphology of mitochondria from rotenone-exposed embryos to mitochondria from embryos exposed to DMSO only. We sought to visualize the damaged mitochondria by immunolabeling for mitochondrial mCherry on 14µm frozen sections, but we were not able to visualize clear changes to the zebrafish mitochondria (figure 3.21, arrowheads) within these dopamine neurons because the thickness of the frozen sections greatly exceeded the size of the zebrafish mitochondria that we were trying to visualize. We were only able to visualize a loss in the overall number and density of dopamine neurons (figure 3.21 panels C and D, arrows) consistent with our previous findings. Instead, we

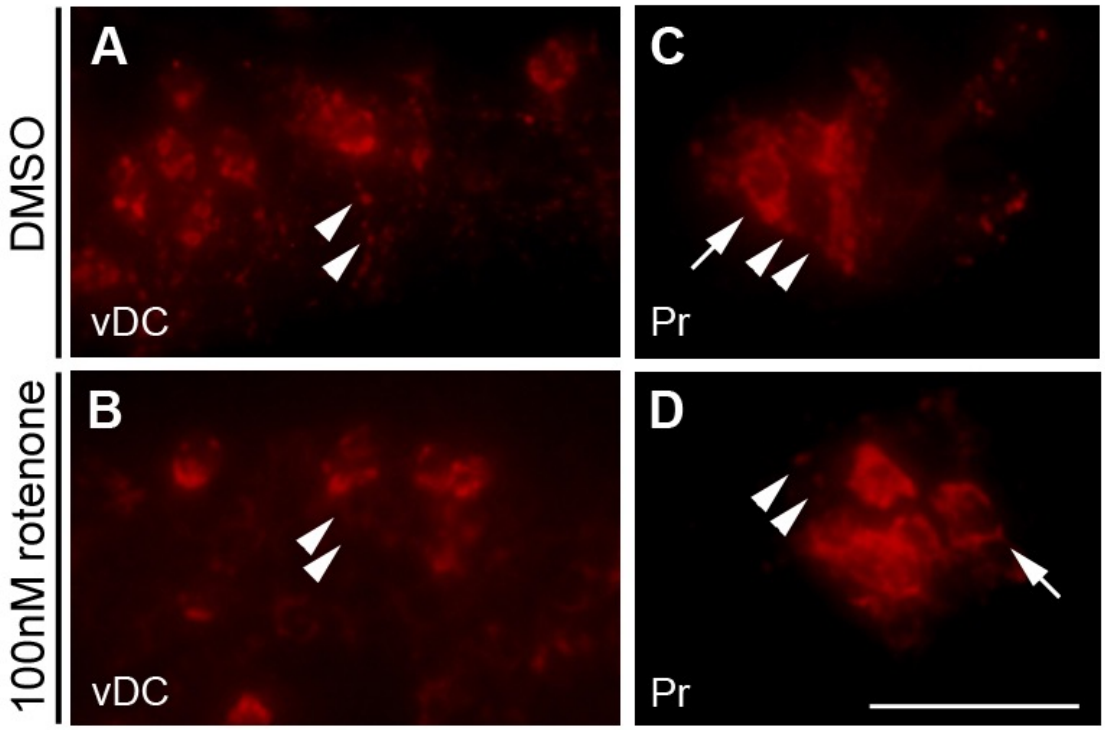

Figure 3.21: Rotenone exposure decreases the number of dopamine neurons in frozen sections from 3 dpf Tg(*dat:tom20 MLS-mCherry*) zebrafish
Frozen sections (14µm thickness) of 3 dpf Tg(*dat:tom20 MLS-mCherry*) zebrafish embryos exposed to 0.01% DMSO (panels A, C) or 100nM rotenone (panels B, D) were immunolabeled with anti-mCherry (red) to visualize the mitochondria of dopamine neurons in the ventral diencephalon (panels A, B) and pretectum (panels C, D). The number of mitochondria appears to decrease in the axonal projections of rotenone-exposed embryos (arrowheads), and the morphology of the cell body also appears to change in rotenone-exposed embryos (arrows). The number of dopamine neurons in embryos exposed to 100nM rotenone also appears to decrease when compared to DMSO controls. Scale bar: 50µm

turned to immunohistochemistry on 3µm paraffin sections of 48 hpf transgenic Tg(*dat:tom20 MLS-mCherry*) embryos. We were able to visualize the cell body from individual dopamine neurons (figure 3.22E, arrows) in the pretectum (figure 3.22 panels A and B, arrowheads) and ventral diencephalon (figure 3.22 panels A and B, arrows), and we observed that there was a decrease in intensity and number of mitochondrial foci in rotenone-exposed embryos when compared to DMSO-exposed controls (figure 3.22 panels E and F, arrowheads).

Using cell dissociation and FACS procedures we had developed in (2.12), we were able to use a mitochondrial stain to visualize damage to the mitochondrial membrane. Mitotracker Deep Red is a flow cytometry stain that binds to mitochondrial outer membrane that has lost proton-motive potential. We were able to visualize an increase in the number of events positive for both Mitotracker and GFP relative to the total percentage of GFP-positive events from samples exposed to 100nM rotenone (1.09% out of 1.49%) when compared to DMSO-exposed controls (1.25% out of 3.03%), suggesting that the remaining GFP-positive dopamine neurons from the rotenone-exposed samples displayed a greater proportion of mitochondrial damage (figure 3.23A). Furthermore, we were able to observe that the number of GFP-positive dopamine neurons decreased by half (figure 3.23B) in samples exposed to 100nM rotenone (1.49 ± 0.10%) when compared to DMSO-exposed controls (3.03 ± 0.04%). This is consistent with the decrease in the number of GFP-positive cells that we visualized by immunohistochemistry in figure 3.10. We were able to show that there was an increase in

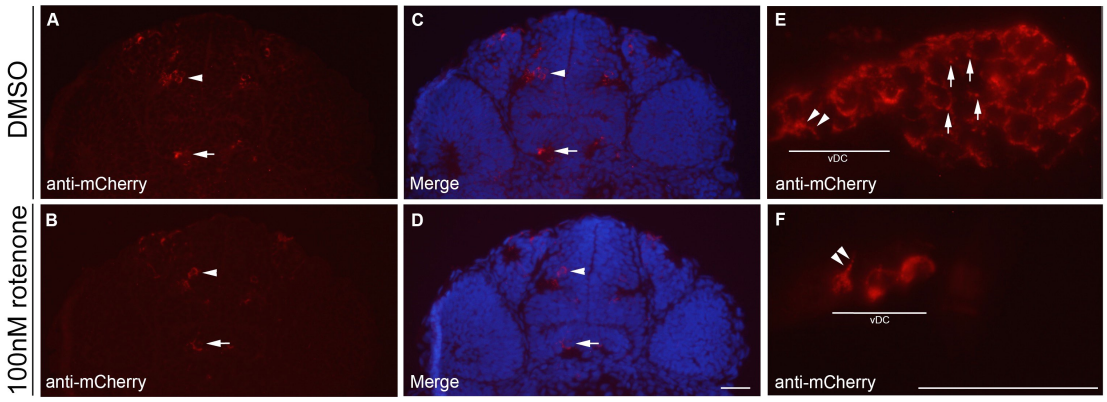

Figure 3.22: Rotenone decreases the number of mitochondria within dopamine neurons from 48 hpf Tg(*dat:tom20 MLS-mCherry*) zebrafish
Paraffin sections (3µm thickness) of Tg(*dat:tom20 MLS-mCherry*) zebrafish embryos exposed to 0.01% DMSO (panels A, C, E) or 100nM rotenone (panels B, D, F) were immunolabeled with anti-mCherry (red) and counterstained with DAPI (blue) to visualize the mitochondria of dopamine neuron populations in coronal sections of zebrafish embryo heads (panels A-D). The intensity and number of neurons in the ventral diencephalon (arrows) appears to decrease in rotenone-exposed zebrafish, whereas the pretectum appears unaffected (arrowheads). Neuronal clusters were resolved at sub-cellular resolutions using a 100x oil immersion lens (panels E, F). The number of dopamine neuron cell bodies (arrows) appears to decrease, with a further decrease in the number and number of mitochondrial foci (arrowheads) within the ventral diencephalic (vDC) axonal projections in rotenone-exposed embryos when compared to DMSO-exposed controls. Scale bar: 50µm

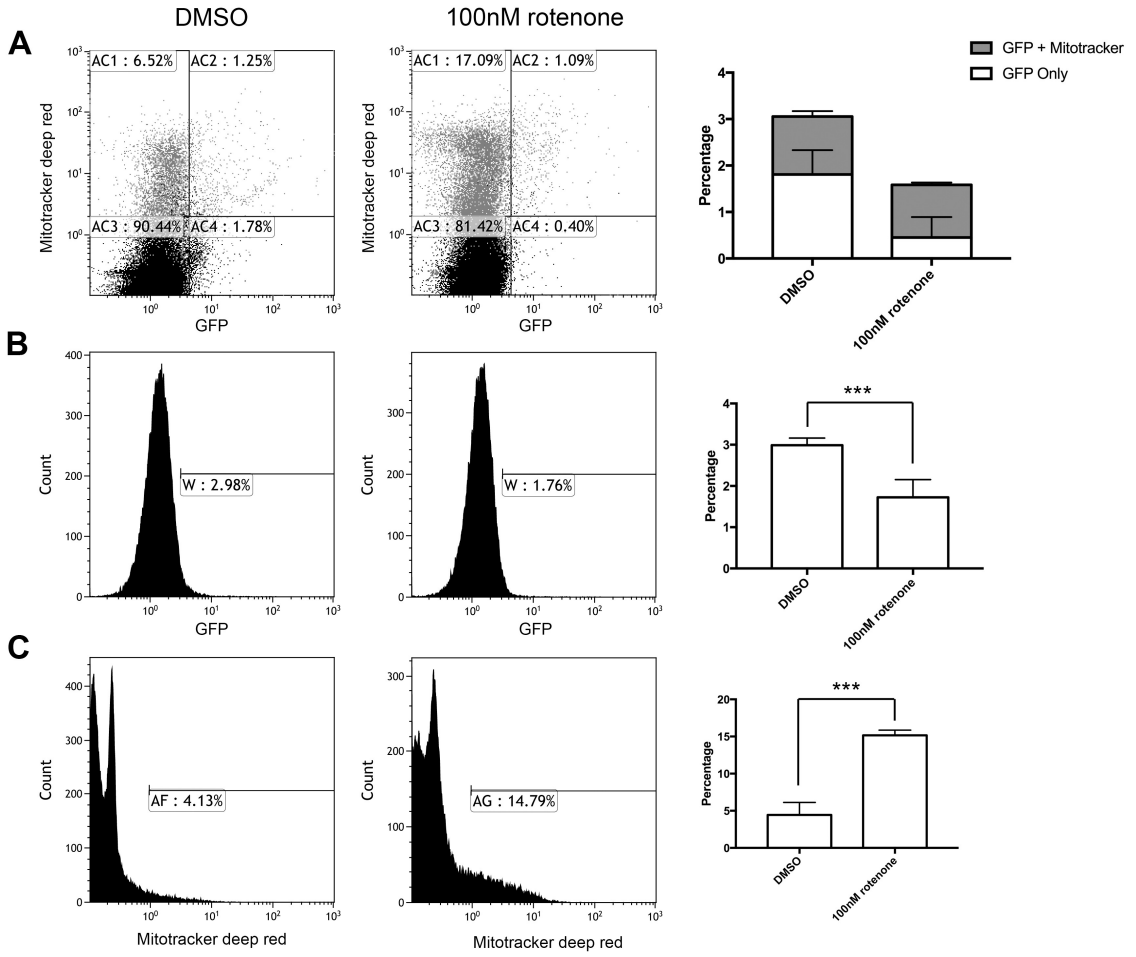

Figure 3.23: Flow cytometry on rotenone-exposed Tg(*dat:EGFP*) cells stained with MitoTracker Deep Red

Tg(*dat:EGFP*) zebrafish embryos were exposed to 0.01% DMSO or 100nM rotenone and raised to 48 hpf. Embryos were then dissociated into a cell suspension and exposed to MitoTracker Deep Red to visualize damage to mitochondrial membranes. Scatter plots (A) show a decrease in GFP-only events in embryos exposed to rotenone when compared to embryos exposed to DMSO alone (0.40% vs 1.78%), as well as an increase in the number of these events that were double positive for Mitotracker stain and GFP (AC2) relative to the total percentage of GFP-positive events (1.09% out of 1.49% vs 1.25% out of 3.03%). There was a decrease in the number of GFP-positive dopamine neurons (B) in samples exposed to rotenone when compared to controls (1.49 ± 0.10% vs 3.03 ± 0.04%; $p<0.001$). Furthermore, there was a corresponding increase in the number of events positive for Mitotracker Deep Red stain (C) in embryos exposed to rotenone when compared to controls (14.79 ± 0.70% vs 4.13 ± 0.39%; $p<0.001$).

the number of events positive for Mitotracker Deep Red stain (figure 3.23C) in cells from embryos exposed to 100nM rotenone when compared to DMSO-exposed controls (14.79 ± 0.70% vs 4.13 ± 0.39%) suggesting that rotenone exposure induces and elevates mitochondrial damage by approximately 10.50% above baseline (figure 3.24).

Together, these data suggest that rotenone is damaging mitochondria, likely a property of its ability to inhibit the activity of mitochondrial complex I. Dissociated cells exposed to 5μM rotenone for 15 minutes was used as a positive control, and unstained controls were also performed (figure 3.24). All flow cytometry readouts were performed in biological and technical triplicates, and normalized to 100,000 events.

3.10 Embryos exposed to rotenone display locomotor impairments

Total locomotion was assessed at 7 dpf in larvae exposed to rotenone. Embryos were placed in a 24-well plate and recorded for 5 minutes. Behavior was then assessed using the Noldus Ethovision XT software in the Behavior Core laboratory (University of Ottawa) to assess parameters of zebrafish kinematics and animal behavior. Larvae exposed to rotenone demonstrated an obvious motor phenotype when compared to unexposed siblings at the same developmental stage. This motor phenotype was quantified with three separate metrics to assess motor capacity (touch response, locomotive episodes and distance travelled). Larvae exposed to rotenone concentrations above 10nM demonstrated decrease in total distance travelled (figure 3.25A). Episodes of locomotion were decreased in larvae exposed to 10nM and 100nM of rotenone (from 123

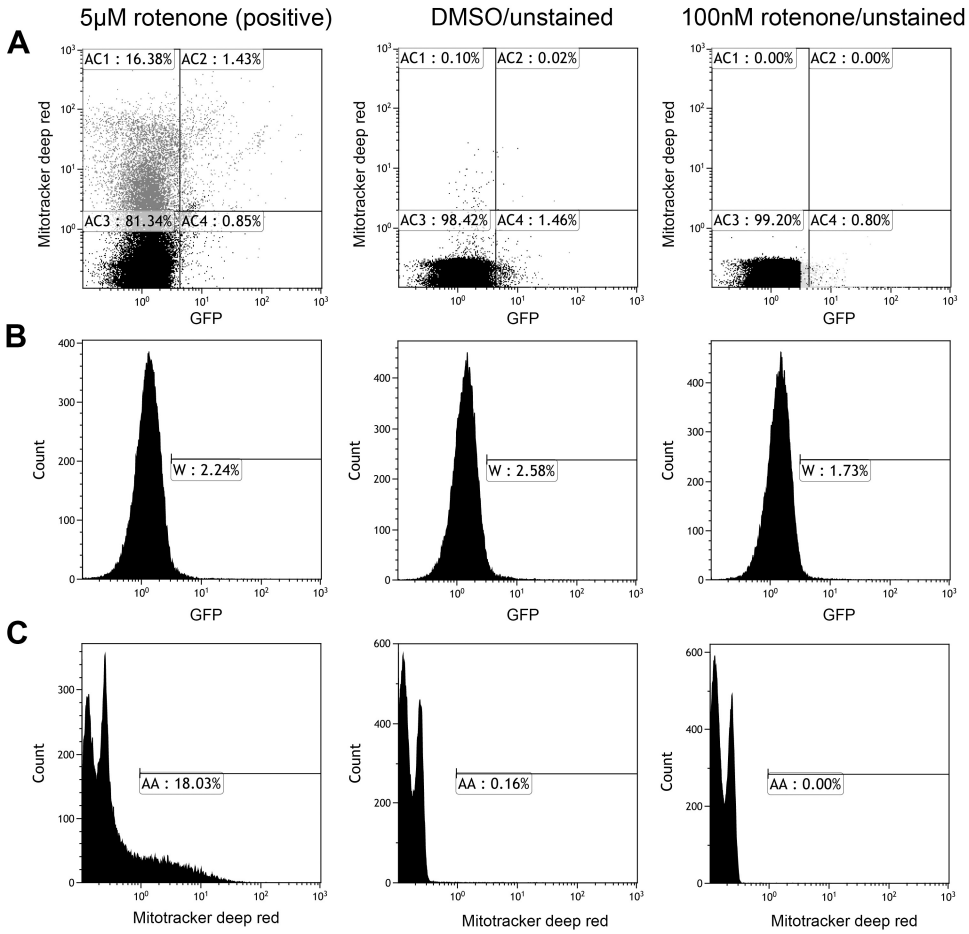

Figure 3.24: Flow cytometry controls

A 15 minute exposure of the cell suspension to 5µM rotenone was used as a positive control, alongside unstained DMSO and rotenone-exposed cell suspensions as negative controls. Scatter plots (A) show that the baseline number of events that were double positive (AC2) for Mitotracker stain and GFP is undetectable in negative controls. In cell suspensions exposed to 5µM rotenone, the frequency of double positive events (1.43%) exceeded the frequencies seen in samples illustrated in figure 3.23. GFP signal (B) also appeared to decrease in lysates exposed to 100nM rotenone when compared to both the DMSO-exposed lysates and the lysates exposed to rotenone for only 15 minutes. Unstained controls show that baseline MitoTracker Deep Red fluorescence produces a strong increase in far red fluorescence after a 15 minute exposure of the cell suspension to 5µM rotenone, but is undetectable in unstained DMSO-exposed embryos and unstained rotenone-exposed controls (C).

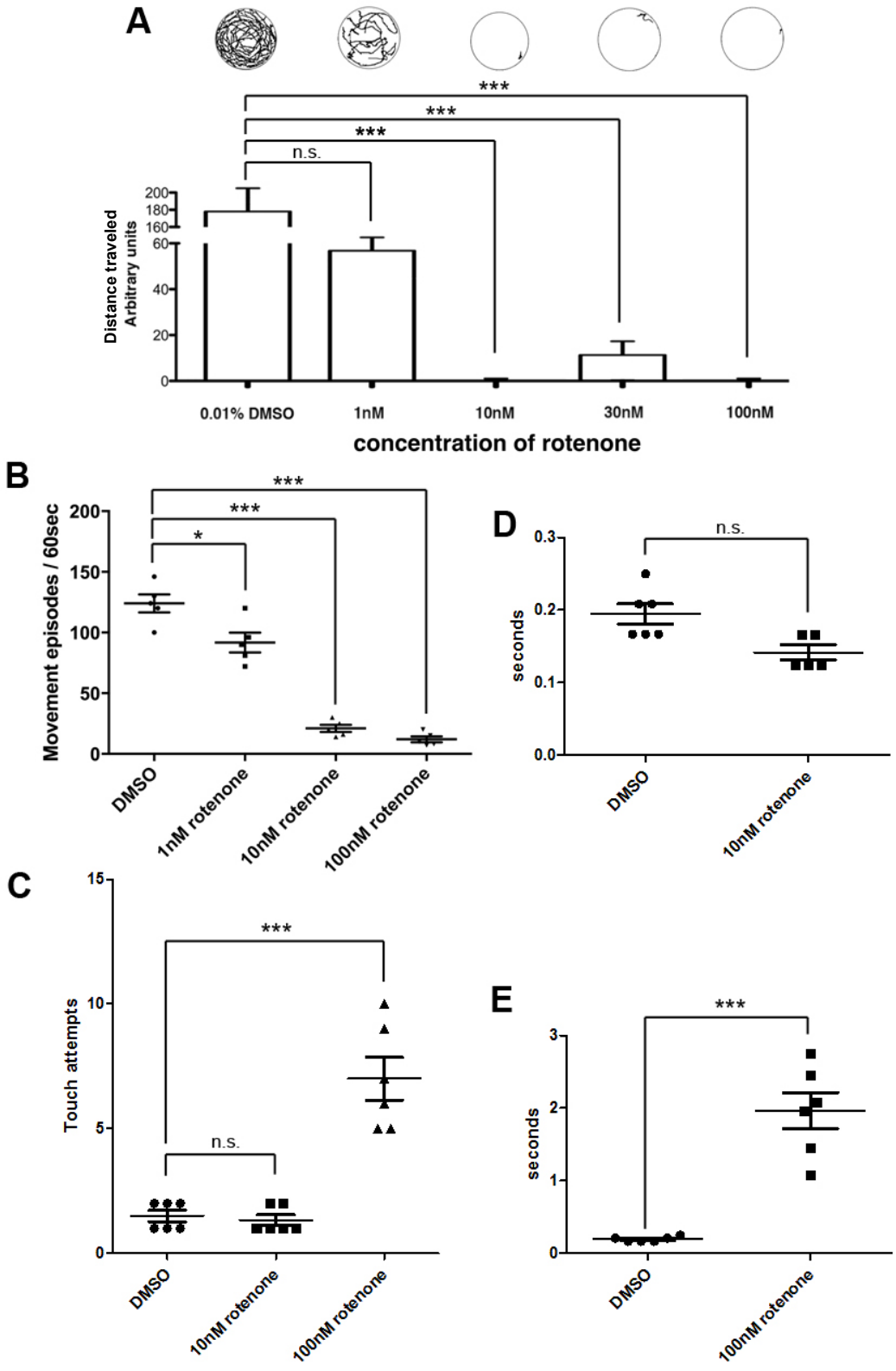
A
***
***
***
n.s.
Distance traveled
Arbitrary units
200
180
160
60
40
20
0
0.01% DMSO
1nM
10nM
30nM
100nM
concentration of rotenone
B
***
***
*
Movement episodes / 60sec
200
150
100
50
0
DMSO
1nM rotenone
10nM rotenone
100nM rotenone
D
n.s.
seconds
0.3
0.2
0.1
0.0
DMSO
10nM rotenone
C
***
n.s.
Touch attempts
15
10
5
0
DMSO
10nM rotenone
100nM rotenone
E
***
seconds
3
2
1
0
DMSO
100nM rotenone

Figure 3.25: Behavioral phenotype in rotenone-exposed embryos
Locomotion was assessed by manual tracking of 7 dpf larvae exposed to increasing concentrations of rotenone or of controls over 10 minutes (A). Larvae exposed to concentrations greater than 10nM rotenone show a decrease in total distance travelled, suggesting a bradykinetic phenotype ($n=5$, $p<0.001$). Representative traces of larval locomotion are shown above each sample. Larvae were then assessed for number of movement episodes per 60 seconds using Ethovision XT (B). Larvae exposed to 30nM or 100nM rotenone demonstrated a dose-dependent decrease in spontaneous movement frequency when compared to unexposed controls ($n=5$, $p<0.001$). Larvae exposed to 100nM rotenone also demonstrate insensitivity to touch (C), requiring a greater number of touch attempts to stimulate an escape response when compared to DMSO controls ($n=6$, $p<0.001$). Although larvae exposed to 10nM rotenone do not demonstrate a significant delay in clearing the field of view with their escape response (D)($n=6$, $p=0.342$), larvae exposed to 100nM rotenone required 9.5 times longer to clear the field of view (E) when compared to DMSO controls ($n=6$, $p<0.001$).

movement episodes per minute to 10 and 7 movement episodes per minute respectively), suggesting that rotenone caused difficulty in initiating locomotion (figure 3.25B). The touch response assay revealed that larvae exposed to 100nM rotenone required numerous mechanical stimuli before fleeing (figure 3.25C). Furthermore, rotenone impaired the larva's ability to generate a sustained motor response to the touch stimulus, and larva often took more than 2 seconds to clear the microscope's field of view (figure 3.25D), compared to 0.34 seconds for the DMSO-exposed larva (figure 3.25E).

To show that the motor phenotype was caused by dopamine neuron loss, we sought to demonstrate that were no gross changes in other neuronal populations. We immunolabeled for serotonin (5-HT) and glutamate decarboxylase (GAD), an enzyme involved in gamma-amino-butyric acid (GABA) synthesis. No gross differences were observed in these CNS neuron populations (figure 3.26). We observed the same number and distribution of serotonergic cells in the Raphe Nucleus (figure 3.26 panels A and B, RN), as well as a similar intensity and distribution in the deep anterolateral GAD-positive neuronal tracts of both rotenone-exposed and vehicle-exposed larvae (figure 3.26 panels C and D, arrows). We also immunolabeled for ZNP-1, ZN-1 and ZN-12, which are biological markers of peripheral motor and sensory neurons, and we saw no difference in the distribution and density of these sensory neurons or motor neurons (figure 3.27, arrowheads). We observed a similar number and distribution of peripheral sensory and motor fibers in the trunks of both rotenone-exposed and vehicle-exposed larva. Since there did not appear to be any gross morphological differences between neuronal

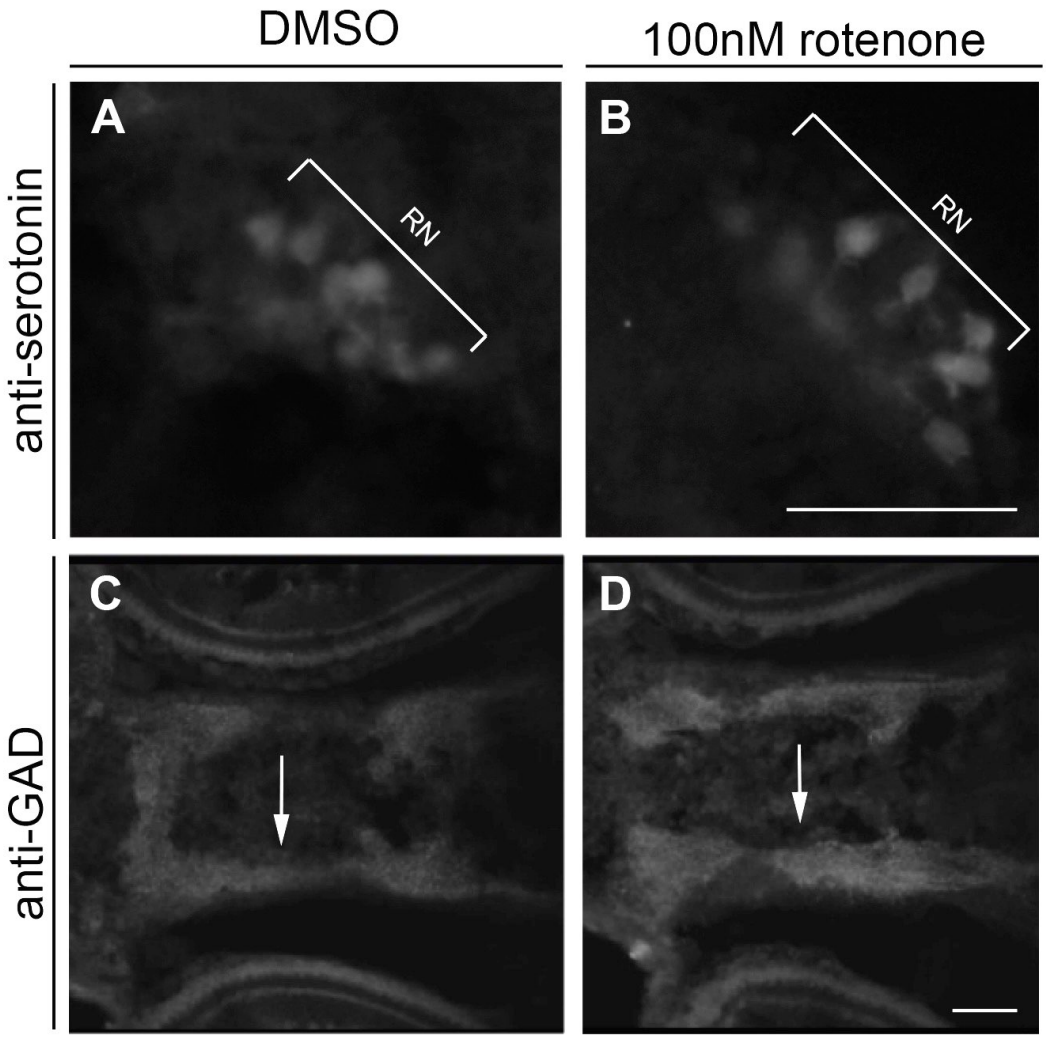

Figure 3.26: Rotenone does not affect serotonergic (anti-serotonin) nor GABA-ergic (anti-GAD) neurons

Frozen sections (14µm thickness) of 5 dpf larvae exposed to 0.01% DMSO (panels A, C) or 100nM rotenone (panels B, D) were immunolabeled with anti-serotonin and anti-GAD antibodies to visualize serotonergic and GABAergic neurons. Serotonergic neurons in the Raphe nucleus (RN) appear similar in number and distribution between DMSO-exposed (A) and rotenone-exposed (B) larvae. GABA neurons have similar interneuron tracts along the CNS (arrow) between DMSO-exposed (C) and rotenone-exposed (D) larvae. Scale bar: 50µm

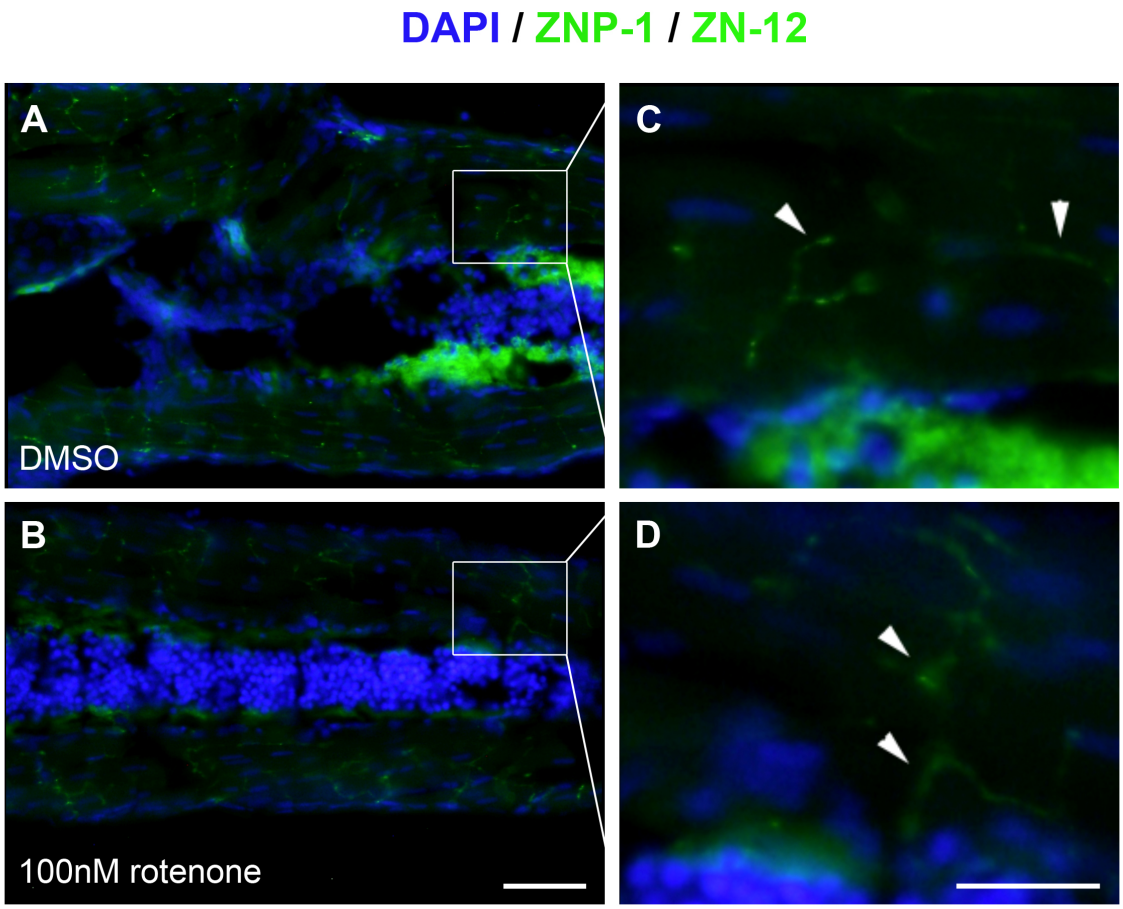

Figure 3.27: Rotenone exposure does not affect the primary motor and sensory neurons in zebrafish

Frozen sections (14µm thickness) of 5 dpf larvae exposed to 0.01% DMSO (panels A, C) or 100nM rotenone (panels B, D) were immunolabeled with a mixture of DAPI (blue) to label nuclei, and ZNP-1, ZN-12 and ZN-1 (green) to label primary sensory and motor neurons. Spinal nuclei and projections were then assessed in the trunk of the developing embryo to examine for any differences in peripheral neurons. Marked areas of interest are magnified (panels C, D) showing intact peripheral spinal projections (arrowheads) in both DMSO-exposed (C) and rotenone-exposed (D) larvae. Scale bars: 50µm.

populations, the locomotion phenotype was likely caused by dopamine neuron loss, and not caused by paralysis or decreased sensation to touch. Together, these data suggest that larvae exposed to rotenone clearly demonstrate a hypokinetic phenotype based on these findings when compared to controls, and this is consistent with both the known effect of MPTP on zebrafish, and the motor symptoms observed in patients with Parkinson's disease. This suggests that rotenone affects the kinematics of larval zebrafish and confers a bradykinetic phenotype, similar to the bradykinesia that is seen in patients with Parkinson's disease.

3.11 Quantitative PCR of genes involved in dopamine neuron physiology

Embryos exposed to rotenone demonstrate a number of neurophysiological deficits which are likely a result of, or result in, changes in expression of a number of genes. We were able to quantify *dopamine transporter* (*dat*) mRNA expression levels as an indicator of dopamine neuron health, as well as genes upstream or downstream from the dopamine signal cascade, such as *dopamine receptors D1* (*drd1*), *D2a* (*drd2a*), and *D2b* (*drd2b*). We examined the change in the pattern of expression of these transcripts in 3 dpf (figure 3.28A), 5 dpf (figure 3.28B) and 7 dpf (figure 3.28C) whole zebrafish lysates.

We saw a decrease in *dat* transcript levels at 3 dpf in embryos exposed to 30nM rotenone, decreasing by 21.2% compared to DMSO-exposed controls ($n=3$, $p<0.05$). A 73.1% decrease was observed following a 100nM rotenone exposure ($n=3$, $p<0.001$). This change was further magnified at 5 dpf, with larvae exposed to 30nM rotenone displaying

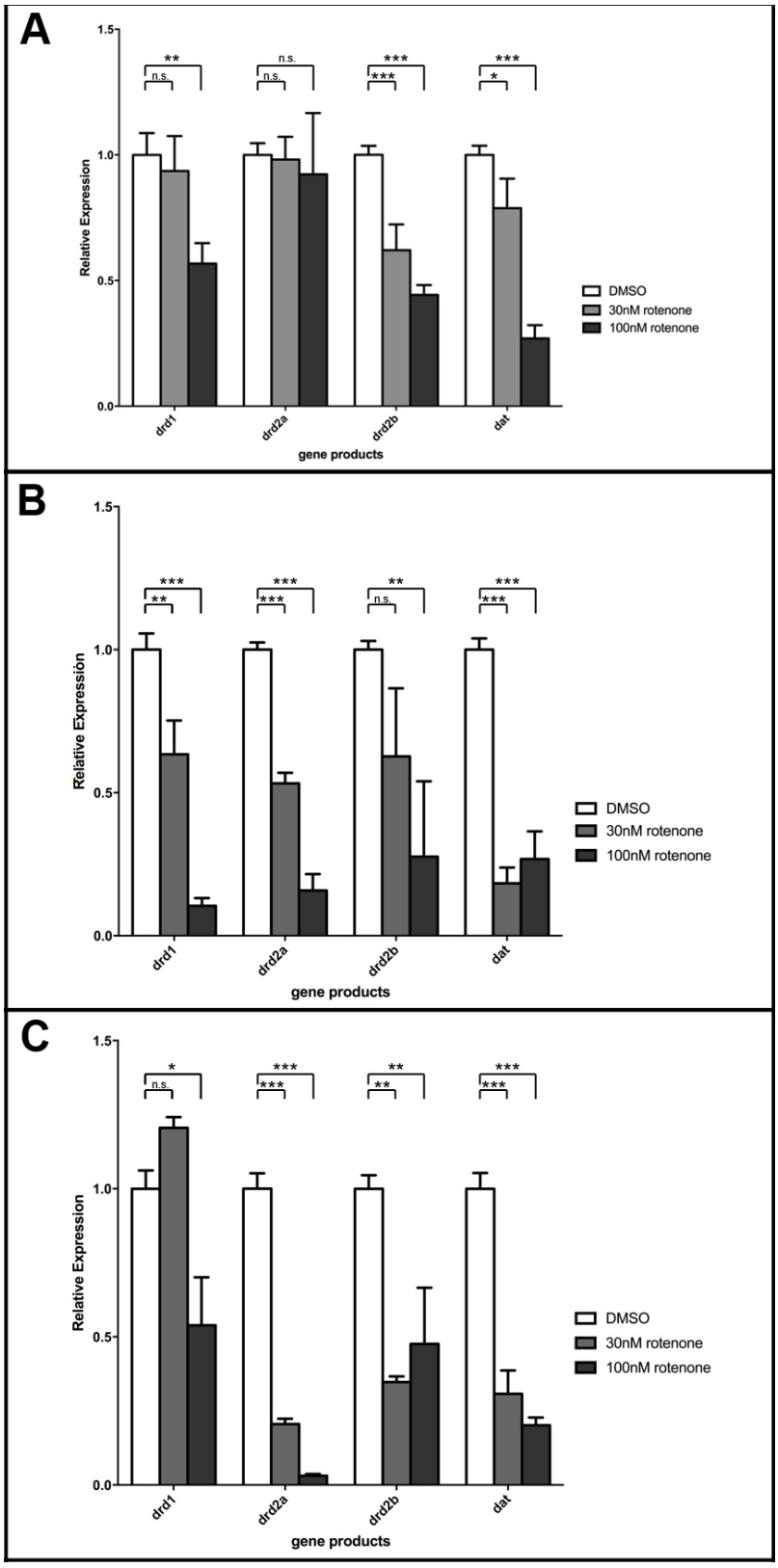
A
B
C
Relative Expression
1.5
1.0
0.5
0.0
n.s.
**
***
*
drd1
drd2a
drd2b
dat
gene products
DMSO
30nM rotenone
100nM rotenone

Figure 3.28: Effects of rotenone on mRNA levels of dopamine receptor genes and *dat* Zebrafish embryos were exposed to DMSO, 30nM or 100nM rotenone at 24 hpf and raised to either 3 dpf (A), 5 dpf (B) or 7 dpf (C) for quantification of mRNA levels. Levels of dopamine receptors *drd1*, *drd2b* and *dat* mRNA levels in rotenone-exposed 3 dpf zebrafish larvae show a dose-dependent decrease compared to DMSO controls (A). Changes in *drd2a* mRNA levels were not significant. Transcript levels for dopamine receptors *drd1*, *drd2a, drd2b* and *dat* mRNA in rotenone-exposed 5 dpf zebrafish larvae show a dose-dependent decrease compared to DMSO controls (B). Levels of dopamine receptors *drd1*, *drd2b* and *dat* mRNA levels in rotenone-exposed 7 dpf zebrafish larvae show a dose-dependent decrease compared to DMSO controls (C). However, rotenone exposure did not produce the same magnitude of change to *drd1* levels as seen in earlier stages. All mRNA levels were quantified in biological quintuplicates (n = 5 each) and technical triplicates, and normalized to *ef1a*.

a 81.7% decrease in *dat* expression (n=3, p<0.001) and larvae exposed to 100nM rotenone displaying a 73.2% decrease in *dat* expression (n=3, p<0.001). By 7 dpf, expression of *dat* in larvae exposed to 30nM rotenone appeared to begin to rebound, with only a 69.3% reduction in expression of *dat* (n=3, p<0.001) compared to DMSO-exposed controls. Expression of *dat* in 100nM rotenone exposed larvae remained decreased by 79.9% relative to DMSO-exposed controls (n=3, p<0.001). Expression levels at all stages were normalized to *ef1a* levels, using biological and technical triplicates.

There appeared to be no significant change in *drd1* expression in 3 dpf embryos exposed to 30nM rotenone (93.6%, p=0.699), however, *drd1* transcript levels decreased by 43.3% in embryos exposed to 100nM rotenone to controls (n=3, p<0.01). This change was also magnified at 5 dpf, with larvae exposed to 30nM rotenone displaying a 36.4% decrease in *drd1* expression levels (n=3, p<0.01), and larvae exposed to 100nM rotenone displaying a 89.5% decrease in *drd1* expression (n=3, p<0.001). By 7 dpf, expression of *drd1* in larvae exposed to 30nM rotenone appeared to begin to return comparable to controls (120.6%, p=0.096), and expression of *drd1* in 100nM rotenone exposed larvae recovered to a 46.1% decrease relative to controls (n=3, p<0.05).

With *drd2a*, we initially saw no significant changes in transcript levels at 3 dpf in embryos exposed to rotenone (98.1%, p=0.844; 92.3%, p=0.710), only demonstrating a change by 5 dpf, with larvae exposed to 30nM rotenone displaying a 46.7% decrease in *drd2a* expression levels (n=3, p<0.001), and larvae exposed to 100nM rotenone

displaying an even greater decrease in *drd2a* expression by 84.2% (n=3, $p<0.001$) relative to DMSO-exposed controls. By 7 dpf, *drd2a* expression in larvae exposed to rotenone appeared to decrease even further, with a 79.4% reduction in expression of *drd2a* in larvae exposed to 30nM rotenone compared to DMSO-exposed controls (n=3, $p<0.001$), and a 96.9% reduction in expression of *drd2a* in larvae exposed to 100nM rotenone (n=3, $p<0.001$) compared to DMSO-exposed controls.

We saw an immediate decrease in *drd2b* expression in 3 dpf embryos exposed to rotenone compared to DMSO-exposed controls with embryos exposed to 30nM rotenone displaying a 37.9% decrease in *drd2b* expression levels (n=3, $p<0.001$), and embryos exposed to 100nM rotenone displaying an even greater decrease in *drd2b* expression (n=3, $p<0.001$) by 55.7% relative to DMSO-exposed controls. These changes appeared to begin showing extensive biological variability but an overall trend in recovery by 5 dpf, with larvae exposed to 30nM rotenone displaying a non-significant 37.3% decrease in *drd2b* expression levels relative to DMSO-exposed controls ($p=0.077$), and larvae exposed to 100nM rotenone conversely displaying only a 72.4% decrease in *drd2b* expression (n=3, $p<0.01$) relative to DMSO-exposed controls. By 7 dpf, *drd2b* expression levels in larvae exposed to 30nM rotenone appeared to decrease to 65.3% relative to DMSO-exposed controls (n=3, $p<0.01$), whereas *drd2b* expression levels in larvae exposed to 100nM rotenone appeared to recover to only a 52.4% decrease relative to DMSO-exposed controls (n=3, $p<0.01$). Expression levels at all stages were normalized to *ef1a* levels, using biological and technical triplicates.

3.12 Dopamine neuron degeneration phenotype is partially rescued in embryos co-treated with rotenone and ascorbic acid

Since rotenone appears to cause dopamine neuron apoptosis through an oxidative-stress pathway, we sought to rescue the observed phenotype by the co-administering an anti-oxidant with rotenone. In order to partially restore locomotor activity and spare dopamine neurons from a cell-death fate, we attempted to alleviate the oxidative stress burden of these cells secondary to both rotenone and *de novo* dopamine synthesis. Ascorbic acid is a natural compound with potent antioxidant properties. We sought to use ascorbic acid to counteract the effects of oxidative stress damage on dopamine neurons induced by rotenone. We used the same methods as outlined in the previous sections to determine if the neuron losses, locomotive phenotype and caspase activity returned towards normal levels when zebrafish were exposed to both 30nM rotenone and 200µM ascorbic acid. We observed that 200µM ascorbic acid appeared to be neuroprotective against the rotenone-induced decreases in dopamine neurons using 5 dpf Tg(*dat:EGFP*) larvae that were exposed to 100nM rotenone (figure 3.29). There was a 51.9% reduction in the number of GFP-positive cells in in Tg(*dat:EGFP*) larvae exposed to 30nM rotenone compared to larva exposed to DMSO alone, whereas this reduction was only 23.6% in Tg(*dat:EGFP*) larvae exposed to both 30nM rotenone and 200µM ascorbic acid.

We then observed locomotion in larvae co-treated with ascorbic acid and rotenone. After co-administering 200µM ascorbic acid with 100nM rotenone at 24 hpf, we raised these

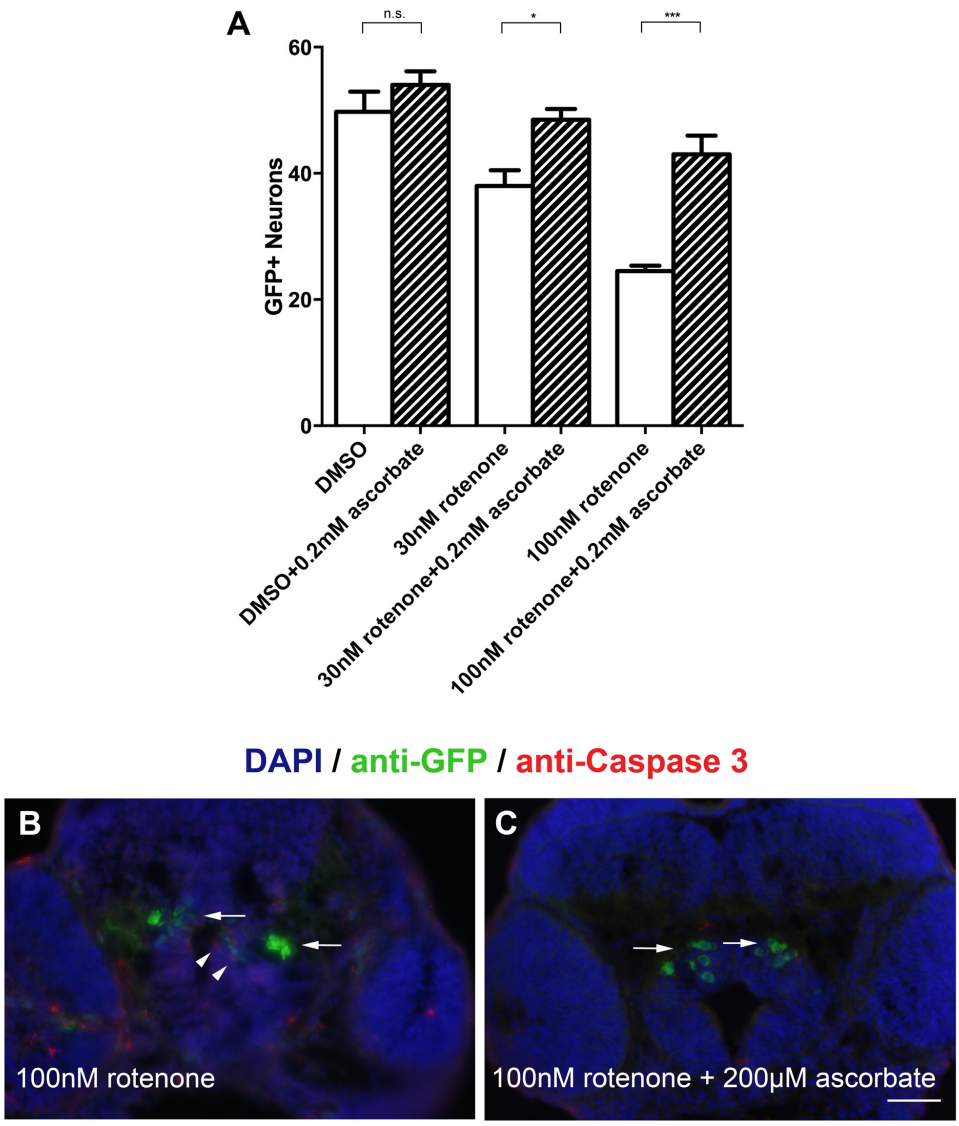

Figure 3.29: The dopamine neurodegeneration phenotype caused by rotenone can be partially rescued by ascorbic acid

Rotenone-exposed 5 dpf larvae co-treated with 200µM ascorbic acid demonstrate a partial rescue in the number of neurons when compared to rotenone-only larvae ($p<0.001$, $n=8$) with no significant change compared to the number of neurons in DMSO controls (A). Caspase activity (arrowheads) in rotenone-only larvae (B) appears less pronounced in larvae co-treated with 200µM ascorbic acid (C). Dopamine neuron clusters also appear better defined (arrows) in larvae co-treated with 200µM ascorbic acid. Nuclei are stained with DAPI (blue). Scale bar: 50µm

animals to 7 dpf and tracked their locomotion in 24-well plates. We observed a partial rescue in locomotion with ascorbic acid co-treatment (figure 3.30), with ascorbic acid-rescued larva displaying a 1.26 cm/minute average velocity when compared to the 0.72 cm/minute average velocity in rotenone-only exposed larvae.

We performed qPCR on 5 dpf larvae exposed to 100nM rotenone and 200µM ascorbic acid (figure 3.31). Co-treatment of larvae with ascorbic acid seems to partially return *dat* transcript levels towards control values, suggesting that ascorbic acid ameliorates the oxidative stress caused by rotenone. Together with the locomotion data and cell counts, these data suggest that the anti-oxidant properties of ascorbic acid can ameliorate the rotenone cytotoxicity phenotype.

3.13 Isolation and enrichment of dopaminergic neurons

Since dopamine neurons have a low relative abundance compared to the sheer number of other cells in the organism, transcriptional changes in dopamine neurons may often be masked by the transcriptional changes in other cells. Therefore, we developed a methodology relying on fluorescence-activated cell sorting (FACS) as a means to isolate and enrich the dopamine neuron subpopulation in zebrafish embryos and larvae. We were able to optimize this procedure in two ways, firstly by developing a methodology to dissociate whole zebrafish larvae into a viable single cell suspension, then by determining the enrichment of dopamine neurons relative to other cells. Our aim was to isolate enough genetic material from zebrafish dopamine neurons for assessment of

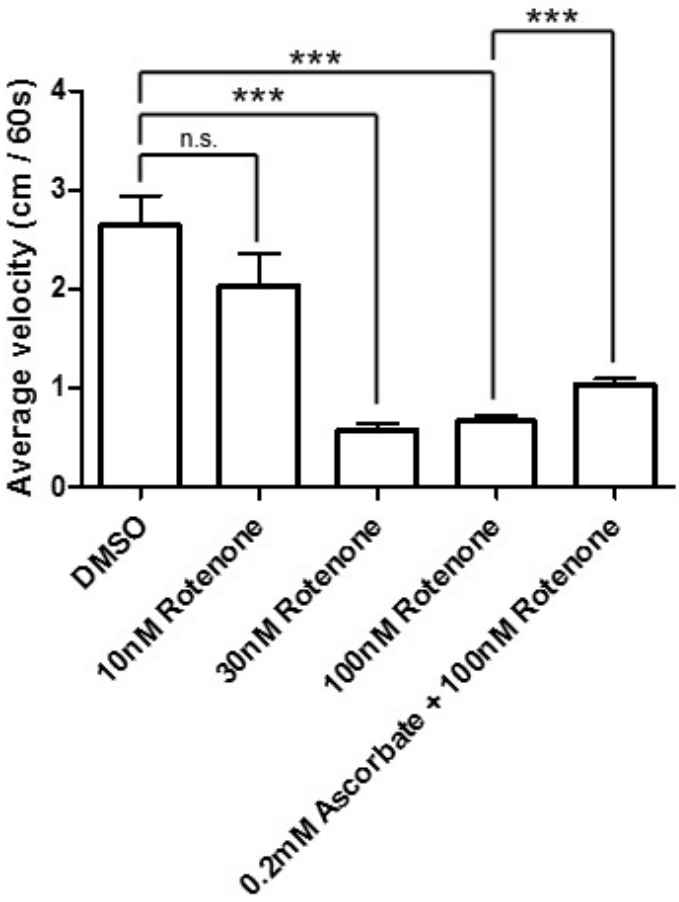

Figure 3.30: Locomotion of 7 dpf zebrafish larvae exposed to rotenone
Locomotion of 7 dpf larvae was recorded over 10 minutes and processed using Ethovision XT. Larvae exposed to rotenone show a dose-dependent decrease in average velocity beginning at 30nM rotenone exposure, suggesting a bradykinetic phenotype. However, embryos exposed to 100nM rotenone that were co-treated with 200µM ascorbic acid demonstrate a statistically significant ($p<0.001$, $n= 6$) recovery in velocity compared to rotenone-only exposed larvae, suggesting a partial rescue of the bradykinetic phenotype.

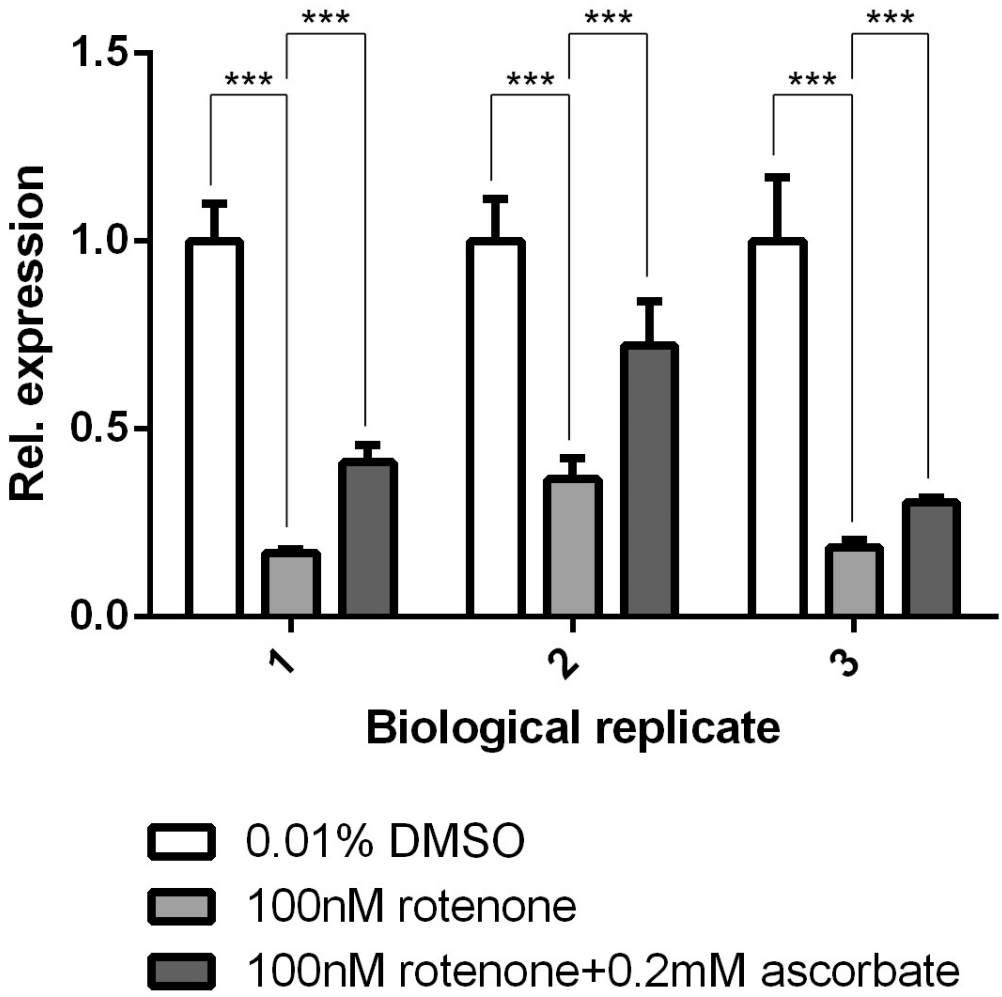

Figure 3.31: mRNA levels of *dopamine transporter* in 5 dpf larvae co-treated with ascorbic acid

Three biological replicates of mRNA levels for *dat* in 5 dpf zebrafish larvae co-treated with 200µM ascorbic acid show a partial rescue when compared to the mRNA levels in rotenone-only treated embryos ($p<0.001$, n=3 each). Levels were normalized to *ef1a.*

transcriptional changes by deep sequencing methods in neurons exposed to rotenone. We developed a protocol to create a single-cell suspension of primary cells from whole zebrafish embryos, generated by the mechanical dissociation of 48 hpf Tg(*dat:EGFP*) zebrafish embryos through a series of cell strainers (100µm and 40µm), and then transported to an Astrios cell sorter for enrichment (for details see Materials and Methods 2.12). We successfully sorted between 30,000 to 50,000 GFP-positive cells from a cell suspension made from 500 Tg(*dat:EGFP*) zebrafish embryos. The cell suspension was populated into 4 distinct subpopulations (two based on size, two based on relative fluorescence intensity). These cells were immediately harvested into TriZol for subsequent RNA isolation and reverse transcription. Once cDNA was made from these cells, we performed qPCR for *dopamine transporter* and *ef1a* levels. We were able to magnify the difference in *dopamine transporter* mRNA levels using digital droplet PCR and quantitative PCR on FACS-enriched dopamine neurons from control or rotenone-exposed embryos. Sorted cells from a cell suspension made from DMSO-exposed embryos showed a 172.4-fold enrichment of *dopamine transporter* transcript levels relative to *ef1a* when compared to ΔC_t values from qPCR on cDNA from embryonic tissue, over three biological replicates. This suggests that we are able to enrich dopamine neurons form a zebrafish cell suspension made from 48 hpf zebrafish embryos. In cell suspensions made from 48 hpf embryos exposed to 100nM rotenone at 24 hpf, sorted cells showed a 27.86-fold reduction in *dopamine transporter* levels relative to *ef1a* when compared to *dopamine transporter* levels relative to *ef1a* in DMSO-exposed controls (figure 3.32). This method therefore allows us to better visualize the magnitude of

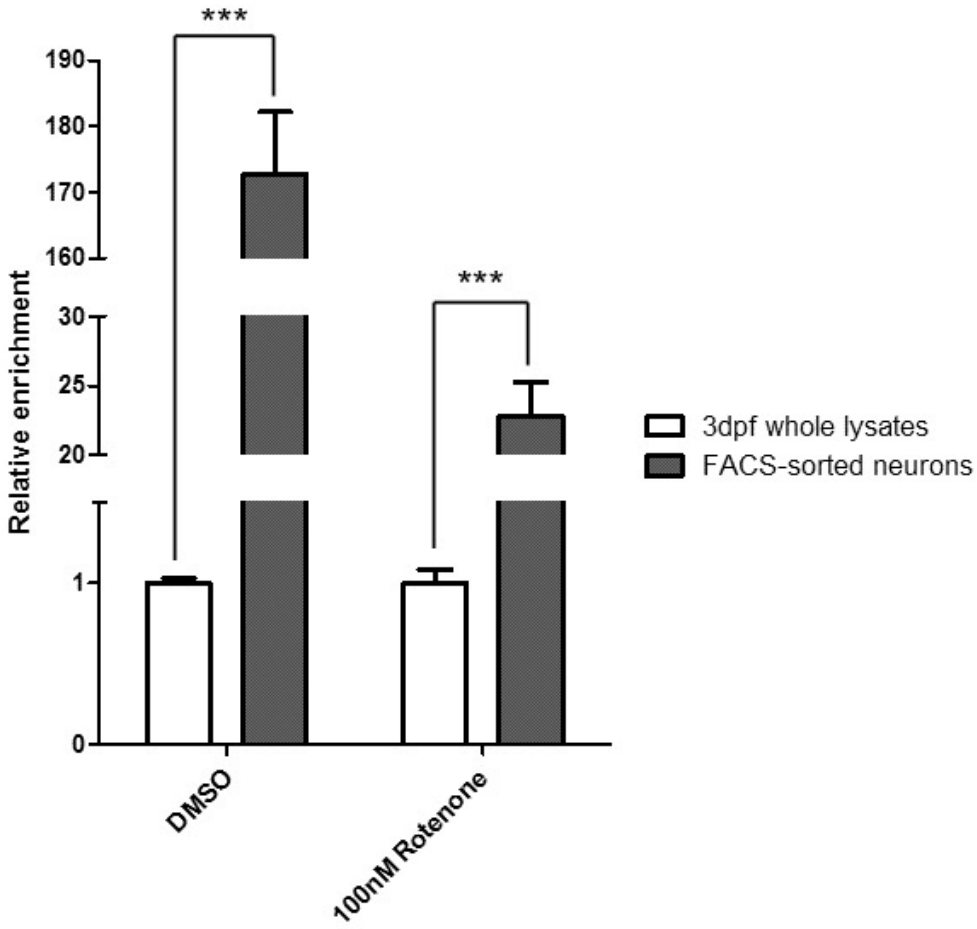

Figure 3.32: Enrichment of *dat* mRNA by FACS
Relative mRNA levels of *dat* from FACS-sorted 48 hpf zebrafish larval tissue were quantified using qPCR using *ef1a* as a reference gene, and compared to the relative mRNA levels in 3 dpf embryo lysates. Dopamine neurons were enriched 172.8-fold in untreated embryos by FACS, and 22.8-fold in rotenone—exposed embryos ($p<0.001$, $n=3$)

rotenone-induced decrease in *dat* expression, and validates our ability to use FACS to enrich dopamine neurons from other somatic cell types. In whole lysates from 3 dpf embryos, *dat* relative expression is decreased by 72.54%, whereas quantification from FACS enriched dopamine neurons by qPCR and ddPCR showed *dat* expression decreases by 96.38% and by 91.86% respectively (figure 3.33). Levels were normalized to *ef1a.* These results may suggest that GFP-positive dopamine neurons cease expressing *dopamine transporter* transcripts when exposed to rotenone, and may adopt a cytostatic or apoptotic phenotype in response to this oxidative stressor.

3.14 Behavioral examination of adult zebrafish - locomotion, line-crossing, light/dark test

Rotenone is frequently administered in higher concentrations than used in this project for its piscicidal and insecticidal properties, and long-term exposure has been associated with the development of Parkinson's disease. Because of this strong correlation between pesticide exposure and development of Parkinson's disease, we sought to examine whether rotenone exposure would cause any long-term impacts or lasting changes to these zebrafish larvae. We were able to raise several clutches of rotenone-exposed zebrafish larvae to adulthood and examine for a locomotion phenotype and dopamine neuron mispatterning using a series of behavioral tests and molecular methods on adult zebrafish grown from larvae exposed to rotenone.

To assess locomotion, adult fish were placed in a standard fish tank with a fixed depth of water and tracked for 10 minutes to measure their spontaneous motor activity.

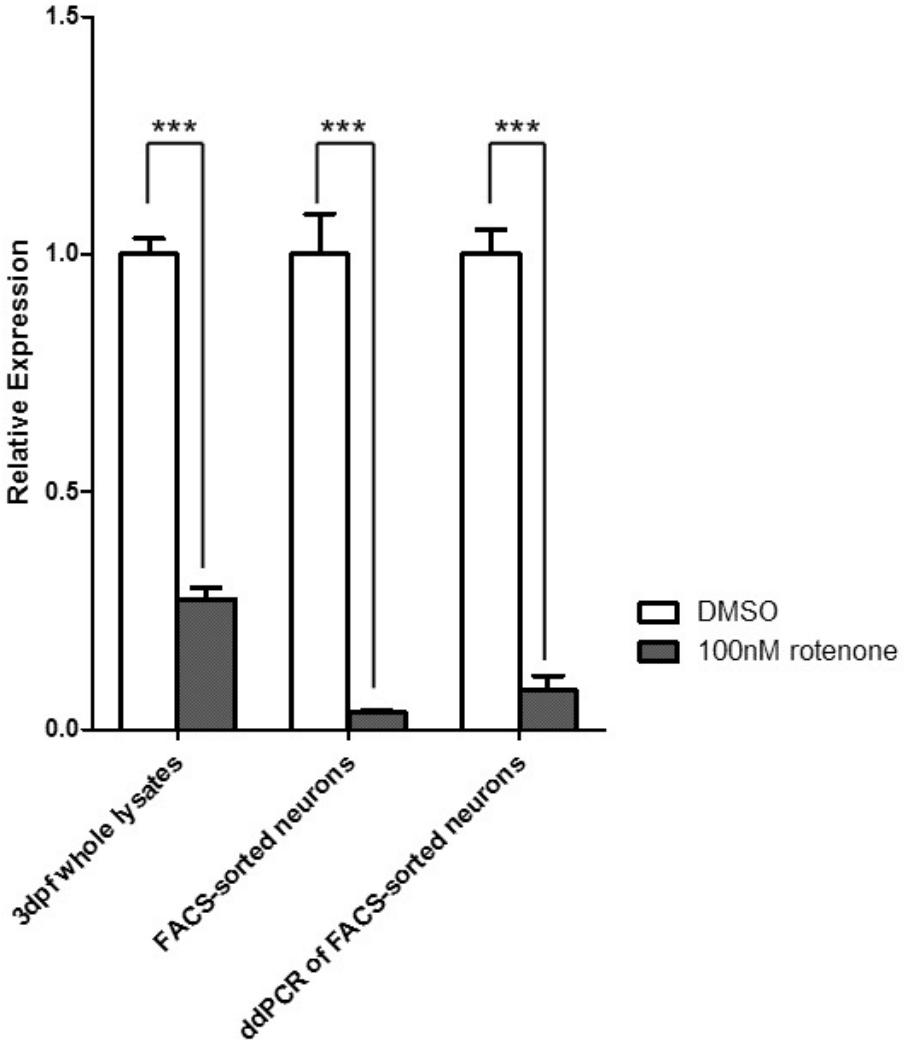

Figure 3.33: Comparison of relative *dat* expression between whole lysate and FACS-sorted neurons

In whole lysates from 3 dpf embryos, *dat* relative expression is decreased by 72.54% ($p<0.001$, n=3), whereas quantification by qPCR and ddPCR decreased *dat* expression by 96.38% ($p<0.001$, n=3) and by 91.86% ($p<0.001$, n=3) respectively. All mRNA levels were quantified in biological quintuplicates (n = 5 each) and technical triplicates, and normalized to *ef1a.*

Measurement of total locomotion in adult zebrafish showed no bradykinetic phenotype, demonstrated by an equivalent distance travelled by adult zebrafish grown from rotenone-treated and control larva (figure 3.34A).

We then assessed anxiety-like behavior by quantifying the proportion of time that an adult fish exposed to rotenone will spend in certain zones of the fish tank. We used both midline crossing analysis and a light/dark test to examine for anxiety-like behavior. We then sought to determine the propensity of the zebrafish to explore the entirety of the tank by examining the number of tank midline crossings by these zebrafish. Fish are placed in a tank with the midline depth demarcated with a solid line, and allowed 30 minutes to acclimatize to this new environment. Following acclimatization, fish tend to cross the midline abundantly while freely exploring this new tank. Anxiety-like behaviors can be elucidated by observing for fish that demonstrate a preference to the depths of the tank by crossing the midline at a lower frequency than control fish. We observed that the zebrafish exposed to 100nM rotenone as embryos were less likely to explore the tank and cross the midline of the tank compared to zebrafish exposed to 10nM rotenone as embryos or unexposed controls (figure 3.34B), suggesting that they are exhibiting anxiety-like behavior due to the perceived vulnerability especially at the surface of the tank (49 crossings vs 60 crossings vs 128 crossings, $n=5$, $p<0.001$).

The light/dark test is a complementary test to the midline-crossing test for anxiety-like behavior in zebrafish. In this test, fish were placed in a tank with half of this tank covered

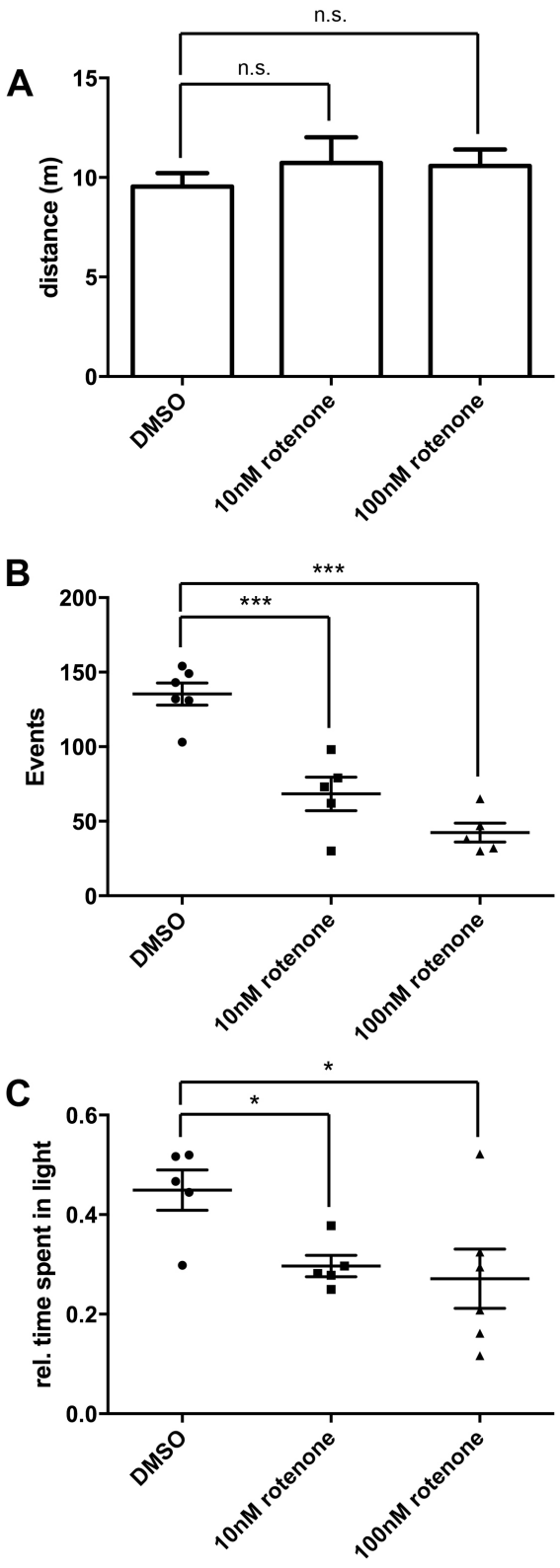
A
n.s.
n.s.
distance (m)
15
10
5
0
DMSO
10nM rotenone
100nM rotenone
B
***
***
Events
200
150
100
50
0
DMSO
10nM rotenone
100nM rotenone
C
*
*
rel. time spent in light
0.6
0.4
0.2
0.0
DMSO
10nM rotenone
100nM rotenone

Figure 3.34: Rotenone causes changes to adult zebrafish behavior
Zebrafish exposed to DMSO, 10nM or 100nM rotenone as embryos were raised to adulthood and assessed for changes in behavior. Adult zebrafish were placed in a standalone tank and monitored for five minutes for various behavioral changes. Zebrafish exposed to rotenone display no significant ($n=5$, $p=0.45$) locomotion deficits (A), but appear to demonstrate a distinct anxiety-like behavioral phenotype. Midline crossing events (number of times an individual fish crossed the midline depth of the tank) were quantified (B) showing that rotenone-exposed zebrafish cross the midline more sparingly ($n=6$, $p<0.001$) than DMSO controls. Light/dark studies quantified the amount of time an individual fish spent in the foil-covered zone of the tank (C), showing that adult zebrafish exposed to rotenone tend to favor the darkness ($n=6$, $p<0.05$) when compared to DMSO controls.

in aluminum foil. This covered area simulates a low light environment and serves as an area of shelter from a strong backlight behind this tank. Fish are allowed 30 minutes to acclimatize to this new environment, and anxiety-like behaviors can be elucidated by observing for fish that prefer to remain in the sheltered area rather than freely explore following acclimatization. The fish were analyzed for the proportion of time they spend in the well-lit area versus the dark area of the tank (figure 3.34C). We observed that fish exposed to 100nM rotenone will spend a decreased proportion of their time in the well-lit area when compared to fish exposed to 10nM rotenone or unexposed controls (29.7% vs 30.2% vs 45.1%, $n=5$, $p<0.05$).

These findings also suggest anxiety-like behavior in zebrafish exposed to rotenone perhaps due to the perceived vulnerability to predators in a well-lit environment. Together, these data show that although locomotion is no longer affected by the time zebrafish larvae exposed to rotenone have been raised to adulthood, these fish clearly exhibit a phenotype manifesting as anxiety-like behavior. These may show the behavioral effects of dopamine dysregulation, a phenomenon seen in late stage Parkinson's disease, where the disease begins having psychological and mood disturbances.

3.15 Adult zebrafish appear to regenerate their neurons

Since the embryos raised to adulthood descend from the Tg(*dat:EGFP*) transgenic line, dopamine neurons in the adult brains will be fluorescent. This property can then be used to quantify the number of surviving dopamine neurons from fish exposed to rotenone in

comparison to unexposed fish. Larvae that were exposed to rotenone during the embryonic stage showed significant changes to the patterning of their dopaminergic neurons, along with decreases in the number of dopamine neurons. However, the larvae had not been examined for losses past 14 days of development.

The zebrafish is a powerful platform for studying regeneration. Neural regeneration has also been extensively documented (Godoy *et al.*, in preparation; Reimer *et al*., 2013; Fleish *et al.*, 2011). Larvae exposed to rotenone were raised to adulthood to examine if the deficits seen in the larval zebrafish persist to adulthood. We collected the brains from adult zebrafish at 60 dpf and examined them for major changes in morphology and in the distribution and number of dopamine neurons. We then obtained cryosections of brains that were dissected from adult Tg(*dat:EGFP*) zebrafish (n=8), and performed immunolabeling for GFP and tyrosine hydroxylase to qualify the distribution of, and obtain an estimate of the number of GFP-positive neurons that are present in the adult brain. We expected to see a dose-dependent response between rotenone concentration and the number of surviving dopamine neurons, but instead there did not appear to be any changes on gross histology, and no changes in the dopamine neuron clusters (figure 3.35, arrows) or nuclei (figure 3.35, arrowheads). Since there were no changes to the number or pattern of dopamine neuron distribution in the anterior forebrain clusters, this would suggest that the fish brain has the regenerative capacity to replace lost dopamine neurons.

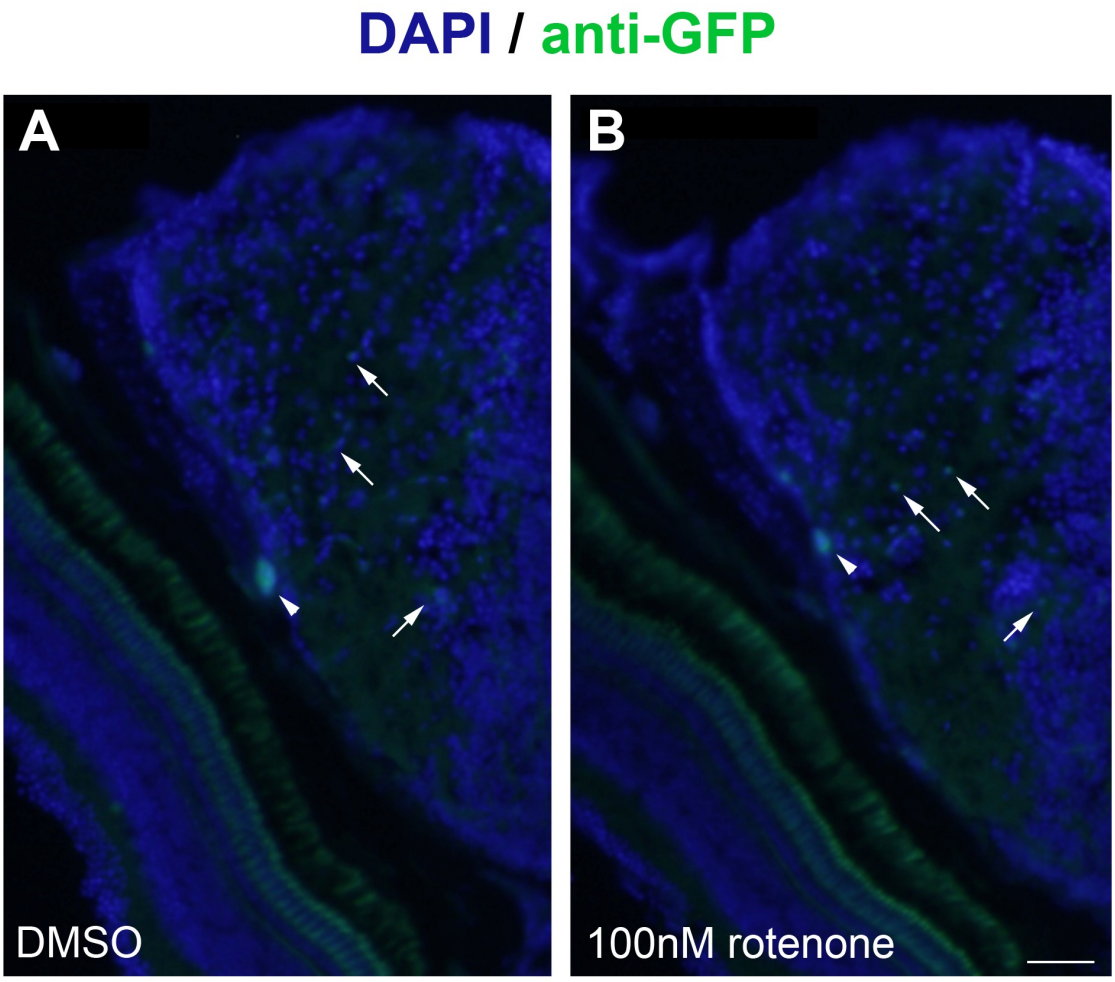

Figure 3.35: Adult zebrafish appear to regenerate their neurons
Frozen sections (14µm thickness) were taken from the posterior forebrain of 60 dpf Tg(*dat:EGFP*) zebrafish exposed to 100nM rotenone or 0.01% DMSO at 24 hpf. Immunohistochemistry for DAPI (blue) or GFP (green) shows no difference in either the axonal projections (arrows) or cell bodies (arrowheads) between DMSO-exposed (A) and rotenone-exposed (B) adults. Scale bar: 50µm

We sought to determine whether the anxiety-like behaviors documented in the previous section in the fish exposed to rotenone were linked to neurophysiological changes, leading us to examine for changes in the gross distribution of neurons in the locus coeruleus (LC). The locus coeruleus is a hindbrain structure responsible for stress and panic responses, and the main center for noradrenalin production in the central nervous system. We initially decided to reexamine the LC of 14 dpf zebrafish samples exposed to rotenone where we had initially seen a recovery of dopamine neurons. LC neurons are reliant on tyrosine hydroxylase to produce L-DOPA, a precursor to noradrenalin, and are, therefore, a population that would be affected by downstream effects from dopamine synthesis disruption. Initially, we observed a 47.4% decrease in the number of LC neurons in a single hemisphere of 5 dpf zebrafish larvae exposed to 30nM rotenone when compared to their untreated controls. However, although there was a gross increase in the number of locus coeruleus neurons in 14 dpf zebrafish larvae (22.67 vs. 9.83 at 5 dpf), there did not appear to be any statistically significant relative decrease in the number of locus coeruleus neurons in rotenone-exposed juveniles compared to untreated controls (figure 3.36A). The increase in the number of locus coeruleus neurons between 5 dpf and 14 dpf larvae can be attributed to the normal developmental process. However, the lack of a gross morphological difference in LC patterning between larvae exposed to rotenone and unexposed controls at 14 dpf detracts from our hypothesis that changes to the LC are responsible for these anxiety-like behaviors in rotenone-exposed fish. The LC appeared fully recovered in rotenone-exposed larvae by 14 dpf (figure 3.36 panels B and C) and we were not able to visualize appreciable changes to the adult brain of rotenone-exposed

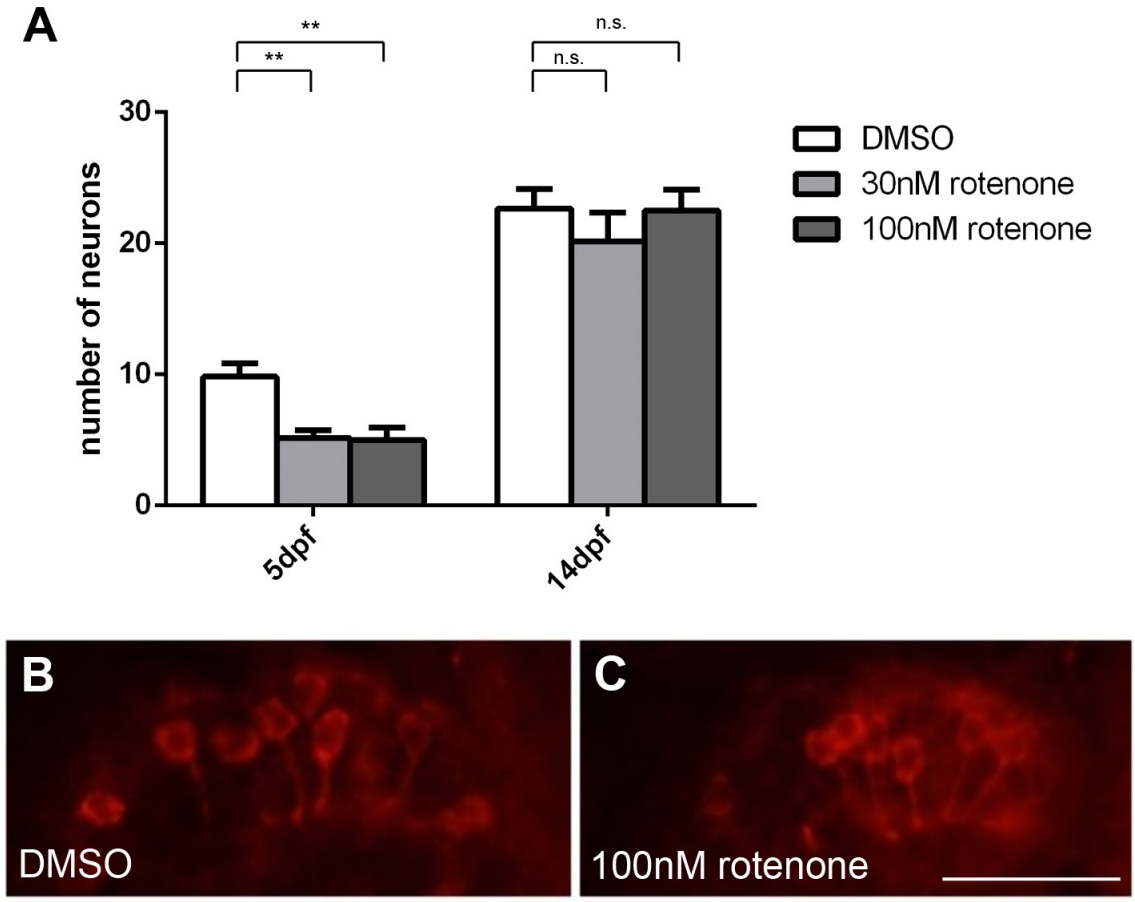

Figure 3.36: Rotenone does not affect the locus coeruleus in 14 dpf zebrafish larvae Frozen sections (14µm) of 5 dpf and 14 dpf larvae exposed to 100nM rotenone or 0.01% DMSO were immunolabeled with anti-tyrosine hydroxylase. The number of neurons in the locus coeruleus was then quantified (A) over 6 representative samples per experimental group. There appeared to be a difference in the locus coeruleus population of 5 dpf zebrafish larvae exposed to rotenone when compared to untreated controls ($p<0.01$, $n=6$) but this difference did not persist to 14 dpf. Furthermore, there did not appear to be any change in distribution or patterning of the locus coeruleus between 14 dpf zebrafish larvae exposed DMSO alone (B) and zebrafish exposed to 100nM rotenone (C). Scale bar: 50µm

fish, suggesting another mechanism was responsible for generating these anxiety-like behaviors.

3.16 Quantitative PCR on adult zebrafish brain

Although we saw no major neuronal patterning deficits in the brain of adult fish exposed to rotenone, we sought to explore potential causes for the observed anxiety-like behavior. We examined for differences in gene expression between rotenone-exposed adults and vehicle controls and performed qPCR for the same transcripts investigated in rotenone-exposed embryos (figure 3.37).

Brains from adult zebrafish treated with rotenone did not appear to demonstrate much significant change in *dat* transcript levels. We saw a non-significant 7.0% reduction in samples taken from adult zebrafish raised from embryos exposed to 30nM rotenone ($p=0.754$, $n= 3$) and a 30.5% reduction in brains taken from adult zebrafish raised from embryos exposed to 100nM rotenone. Although there was a significant decrease in *dat* expression in brains from adult zebrafish raised from embryos exposed to 100nM rotenone, its magnitude was not as dramatic as observed in the embryonic stages which suggests that the fish that are exposed to rotenone as embryos were able to recover to some extent from dopamine neuron decreases.

We did, however, observe that transcript levels for the various dopamine receptors were significantly disrupted in fish exposed to rotenone. We saw that *drd1* expression levels

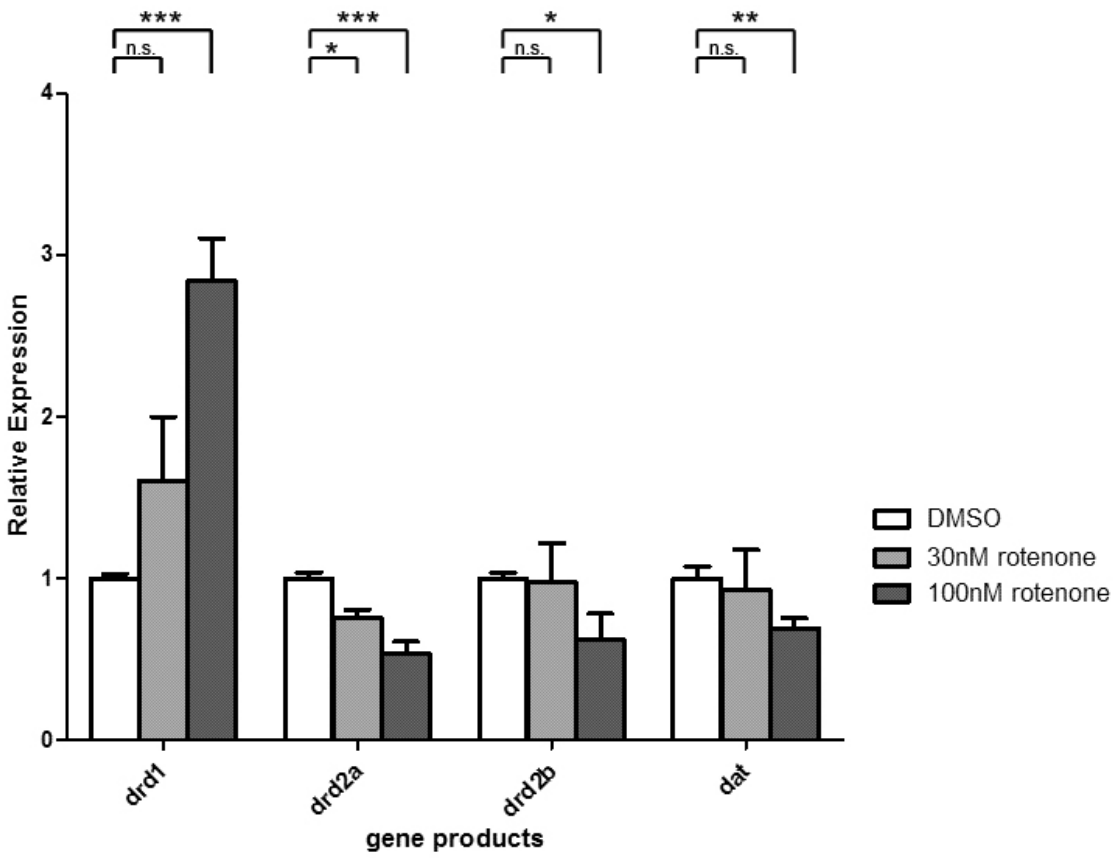

Figure 3.37: mRNA levels of dopamine receptors and *dat* in the adult zebrafish brain

Brains from adult zebrafish raised from embryos exposed to DMSO, 30nM or 100nM rotenone at 24 hpf were quantified for changes to *drd1*, *drd2a, drd2b* and *dat* mRNA levels. Levels of *drd1* mRNA were strongly increased in rotenone-exposed adults, whereas rotenone exposure appeared to cause a strong decrease in *drd2a* mRNA levels. There was a mild decrease in *drd2b* and *dat* transcript levels only observable in in adult zebrafish exposed to 100nM rotenone. Rotenone exposure did not produce the same magnitude of change to *drd2b* and *dat* mRNA levels as seen in Figure 3.28. All mRNA levels were quantified in biological quintuplicates (n=5 each) and technical triplicates, and normalized to *ef1a*.

were increased in brains taken from adult zebrafish raised from embryos exposed to 30nM rotenone, although this change was not significant (160.5%, p=0.144) due to high biological variability. Brains taken from adult zebrafish raised from embryos exposed to 100nM rotenone did however show a significant increase in expression of *drd1* by 283.9% compared to brains taken from DMSO-exposed control fish. Expression of *drd2a* transcripts appeared significantly decreased, with brains taken from adult zebrafish raised from embryos exposed to 30nM rotenone showing a 24.5% decrease, and those resulting from 100nM rotenone exposure showing a 46.3% decrease. There did not appear to be such changes in *drd2b* transcript levels with no significant differences in *drd2b* expression (98.1%, p=0.938) to the 30nM rotenone group, and only a 37.5% decrease in the 100nM rotenone group. These changes demonstrate that rotenone exposure results in lasting transcriptional changes to a variety of gene products liked to dopamine neuron physiology and homeostasis, although not to the same extent as observed in the embryonic and larval stages.

Discussion

Parkinson disease is a complex disease, originating from a combination of either genetic or environmental factors (reviewed in Kitada *et al.*, 2012). We have long since been able to demonstrate the involvement of a particular subset of genes related to dopamine neuron survival, but we have struggled to identify environmental factors that play a causative role in dopamine neuron death.

Though our experiments within this body of work, we were able to use zebrafish larvae in a small scale screen of 7 compounds associated with Parkinson's disease to identify compounds with dopamine neurotoxicity characteristics. Based on these criteria, we found that rotenone reduced the number, density and patterning of dopamine neurons in zebrafish larvae exposed to this compound. Furthermore, there were obvious locomotor deficiencies observed in larvae exposed to rotenone. These changes were also observed with zebrafish larvae exposed to MPTP and MPP+, which has been documented by other groups (Bretaud *et al.*, 2004, Sallinen *et al.*, 2009). These findings provide support for our hypothesis that rotenone causes dopaminergic neurotoxicity in a manner similar to MPTP and MPP+, and suggest that rotenone's mitochondrial complex I inhibitory effect disproportionally affects dopamine neurons more than other somatic cells. However, we did not observe any changes to the patterning of dopamine neurons in zebrafish larvae exposed to the paraquat, another pesticide compound that is thought to act in a similar mechanism of action to rotenone and MPTP (Smeyne and Jackson-Lewis, 2005). Neither manganese, oxidopamine, nor ziram showed any effects in changing the dopamine

neuron pattering of zebrafish larvae (figure 3.1). Although both manganese and ziram exposure have both been linked to dopamine neuron pathology (Aschner *et al.*, 2009; Lulla *et al.*, 2016), the bioavailability of simple free manganese ions or partially dissolved ziram appears unable to induce dopamine neuron loss in zebrafish larvae. Oxidopamine displayed many stability issues and pervasive degradation shortly after solubilization in water. Consequently, similar bioavailability issues appeared to diminish the neurotoxic effects of oxidopamine as observed with ziram or manganese, illustrating the complex pharmacokinetics that underscore a chemical screen on live animals.

Regardless, we were able to identify rotenone as a hit on our small scale screen and able to further characterize its mechanism of action and specificity to dopamine neuron death at nanomolar concentrations. We observed that rotenone demonstrated this neurotoxic effect only on zebrafish larvae raised at 22ºC, since larvae raised at 28.5ºC demonstrated unrestrained mortality (figure 3.4). These observations suggest that the decrease in metabolic rate from being raised at 22ºC is critical to striking a balance between the neurotoxic effects of mitochondrial complex I inhibition (figure 3.2) with the cytotoxic effects of mitochondrial complex I inhibition (figure 3.3). We observed that rotenone causes changes to dopamine neuron patterning as early as 48 hpf through 15 dpf (figure 3.6) although these changes are not as marked by 15 dpf (figure 3.11). The quantity of dopamine neuron decrease observed in rotenone-exposed larvae is comparable to both the number of neurons lost in larvae exposed to MPTP (figure 3.10) and we were able to confirm our observations using molecular techniques such as with qPCR of *dat* mRNA

levels (figure 3.27), and Western blots of TH protein levels (figure 3.20) demonstrating a clear decrease in these markers of dopamine neurons. Furthermore, we were able to establish this parkinsonism phenotype by showing that rotenone affected the locomotion of zebrafish larvae in a dose dependent manner (figure 3.25),

Rotenone's mechanism of action strongly suggests that it induces neurotoxicity in dopamine neurons by exacerbating a baseline oxidative stress within the dopamine neurons, creating ROSs that induce oxidative damage and programmed cell death. We were able to show that rotenone induces an oxidative stress in zebrafish larvae (figure 3.12) and subsequent damage to the mitochondria of dopamine neurons with our positive findings using MitoTracker stain (figure 3.23) and *dat:tom20 MLS-mCherry* larvae (figure 3.22), allowing us to visualize damage to the mitochondrial inner membrane as well as whole mitochondria within the body of these dopamine neurons. Furthermore, this rotenone-induced ROS damage could be rescued with an anti-oxidant (co-treatment with ascorbic acid), partially rescuing the dopamine neuron loss (figure 3.29) and locomotive phenotypes (figure 3.30), supporting an ROS-induced mechanism of action.

This rotenone-induced damage to dopamine neurons appears to engage a Bax-a-dependent apoptotic pathway. Our data showed that dopamine neurons in the ventral diencephalon of rotenone-exposed larvae were also positive for active caspase 3 (figure 3.14) and active caspase 9 (figure 3.16) staining, which was markedly absent in control larvae. These number of colocalizing dopamine neuron/caspase-positive foci was also

increased (figure 3.19), and Bax-a translocation to the mitochondria was also demonstrated with Western blotting (figure 3.20), which is the initial step to engaging an apoptotic cascade. However, the underlying between rotenone exposure and Bax-a recruitment is currently unclear.

We were able to visualize changes to dopamine receptors in zebrafish exposed to rotenone (figure 3.27). Downstream genes used in dopamine physiology saw strict downregulation (As seen in *drd2a* and *drd2b*) or compensatory upregulation following an initial decrease as with *drd1*. These findings suggest a complex dynamic in dopamine receptor autoregulation following changes to the density of dopamine neurons and amount of available dopamine. Furthermore, we were able to develop novel flow cytometry and FACS methods for zebrafish larvae, allowing us to enrich dopamine neurons from single cell suspensions made from zebrafish larvae exposed to rotenone (figure 3.32), magnifying the decrease in *dat* mRNA levels when compared to non-enriched controls (figure 3.33). These novel techniques have many downstream applications for cell sorting and *ex vivo* culture methods, as well as the potential for deep sequencing of dopamine neuron transcriptomes.

Unfortunately, we did not see any lasting dopamine neuron death phenotype in adult zebrafish raised from larvae exposed to rotenone. Dopamine neuron populations appeared unchanged (figure 3.35) and the amount of *dat*, *drd2a* and *drd2b* mRNA levels did not appear as markedly decreased as observed in larval populations (figure 3.37). However,

we did visualize a different behavioral phenotype in zebrafish adults raised from larvae exposed to rotenone, manifesting as an anxiety-like behaviors with apprehension of tank exploration (figure 3.34) and a significant concomitant increase in *drd1* mRNA levels following rotenone exposure.

Overall, these results have shown that zebrafish can be used as an *in vivo* screening system for phenotypes exerted by neurotoxic compounds. Furthermore, we have been able to characterize the biological effects of our hits and demonstrate the utility of zebrafish as an *in vivo* platform for modeling the effects of dopamine neuron loss.

4.1 Potential challenges of using zebrafish for large scale screens

The advent of automation and high-throughput screening has led many laboratories to develop and refine existing platforms for small molecule screening. The development of an *in vivo* platform of high-throughput small molecule screening is the initial goal in characterizing the biological effects of these small molecules. When using an *in vitro* screening platform on human cell cultures, relatively few of these active compounds translate to an identical biological effect in their respective *in vivo* animal models. Many laboratories have identified the utility of zebrafish tissue and its derivatives to identify small molecules that cause physiological effects, and compounds screened using cultured zebrafish cells can be easily validated with their respective zebrafish disease models (Xu *et al.*, 2013). Furthermore, a number of behavior-based screens have used live zebrafish

larvae to identify novel small molecule compounds with psychoactive properties (Kokel *et al.*, 2010).

This project has shown that we can use zebrafish to demonstrate the *in vivo* effects of chemical treatments manifest as observable phenotypes. We were able to distribute embryos into multi-well plates, maintain them for up to 7 days without feeding, and treat with minimal concentrations of small molecule compounds. We were able to use MPTP and MPP+ as positive controls in our small scale screen for chemicals that cause dopamine neuron loss. Since MPTP and MPP+ are established compounds that both obviate dopamine neurons in zebrafish and have been used to model Parkinson's disease in mammalian systems, we were able to provide a frame of reference for our expected parkinsonism phenotype by using these small molecules. We used three observable parameters in our transgenic fluorescent fish - morphology, fluorescence and behavior. We chose these parameters because we sought to identify small molecules that could cause dopamine neuron loss similar to MPTP without causing gross malformations to developing zebrafish embryos, since we needed to ensure that our compounds displayed preferential toxicity to dopamine neurons rather than simply exhibiting a cytotoxic effect to all neurons. The dopamine neuron loss was then qualified as a phenotype based on a compound's ability to alter larval behavior, and decrease the number and distribution of dopamine neurons in Tg(*dat:EFGP*) embryos. Since the pathophysiology of Parkinson's disease manifests as a movement disorder caused by an underlying loss of dopamine neurons, inclusion of behavior and fluorescence were fundamental parameters in our

screen. Once we conducted our small scale screen, we observed one “hit” (rotenone) out of 5 compounds tested. We were unable to visualize any dopamine neuron losses in zebrafish embryos exposed to paraquat at any concentration, or to manganese, ziram or oxidopamine before off-target cytotoxic effects manifested. As a result, this screen was able to identify rotenone as a compound that could preferentially eliminate dopamine neurons and change larval behavior, encouraging us to further characterize the neurotoxic effects of rotenone on dopamine neurons.

Development of an *in vivo* large-scale screen would demonstrate biologically relevant effects on phenotype, and allow further study of diseases that are determined by a clinical diagnosis, or phenotypic representation. However, numerous challenges must be overcome before a large-scale screen for neurodegenerative and neuroprotective agents can be performed. A number of major factors may pose a challenge to any experimental set-up, such as assay design, assay reliability, solubility of compounds, initial concentration of compounds or length of exposure to the treatment agents. For example, many small molecule libraries are often organic compounds that exhibit extremely low solubility in water, and must then be pre-dissolved in an organic solvent, such as DMSO, which in high concentrations begins to affect normal embryonic development, physiology and behavior (Chen *et al.*, 2011). Once dissolved and assuming that all of these agents are diluted to the same concentration, embryos are exposed for an arbitrary exposure window before being removed from the agent and allowed to recover. Phenotypes generated from these chemical exposures are dependent on time and concentration of the agent during the

exposure window, and can then be further explored with alternative exposure times and concentrations. These are challenges that can be addressed by undertaking a small-scale screen of neuroactive compounds linked to the development of dopaminergic cell death, and of compounds known or used in the treatment of Parkinson disease to establish the assay and protocols necessary to perform a large-scale screen. Being able to perform a large-scale screen would presuppose that all of our predicted observations have been rigorously examined in our established models of dopaminergic cell death, and that we would address these criteria in a high-throughput manner amenable to automation. A key component of high-throughput screening requires the automated selection of positive and negative results through the proper selection of "hits" from "misses."

Behavioral differences may be used to discriminate and select for hits using behavioral assays used in this project. These behavioral assays are fairly amenable to automation since most of these assays rely on quantification a certain physical parameter, such as average speed, distance travelled or number of movement episodes. However, these assays can also lead to a number of challenges (reviewed in Rihel and Schier, 2011). Currently, our equipment for the analysis of zebrafish behavior is limited to basic quantification of locomotor activity. We are currently limited to measuring touch response, locomotion episodes, distance and its derivatives in embryos. For adults, we are only able to measure distance and its derivatives, and simple improvisation has allowed us to examine for anxiety-like behaviors. However, we hope to acquire and develop more equipment to allow us to analyze different behaviors according to the zebrafish

behavioral atlas as described in Kalueff *et al.* (2013). Unfortunately, the utility of developing further specificity in our behavioral assays is limited. Dopamine deficiency is one of many causes for a locomotion-deficient phenotype (reviewed in Mathur and Guo, 2010). Other causes of behavioral changes could be from peripheral nervous system dysfunction (Villegas *et al.*, 2012) or cortical abnormalities (Teng *et al.*, 2010), thus reinforcing the need for validation of observable behavioral phenotypes with other parameters in parallel. We have sought to exclude these possibilities as much as possible through our characterization of other neuron populations in any observable phenotypes, and through histological examination of brains from zebrafish that display abnormal behavior. However, the low specificity of zebrafish behavioral profiles makes screening for behavioral abnormalities a poor selection criteria for the basis of the chemical screen.

The most specific metric for observing dopamine neuron loss is the use of fluorescence/ immunological detection. However, automated cell counting is not as amenable to automation as behavior tracking, since dopamine neuron loss can be characterized by a number of parameters. A dopamine neuron loss phenotype is not only characterized by an absolute decrease in the number of dopaminergic nuclei, but also with mispatterning of dopaminergic nuclei, or failed axonal projections from these neurons. Machine learning is necessary to detect these subtle changes, and for this project, we relied on extensive examination of various histological sections from larvae exposed to rotenone. Each larval specimen would require consistent anatomical orientation prior to examination, followed by observation at various depths of field per sample to visualize different neuronal

clusters at different depths while accounting for or excluding larvae that demonstrate abnormal morphology. These considerations require extensive data collection per sample, as well as intensive computational power to process and analyze these data. Transgenic larvae may also exhibit variability with fluorescence intensity, which may occur during the course of observation under fluorescence microscopy through the process of photobleaching. Furthermore, these algorithms would need to exclude signals due to non-specific fluorescence. Larvae in a large scale screen would ideally be assessed for changes in behavior corresponding to a bradykinetic phenotype, and for reductions in the number, morphology or patterning of diencephalic dopaminergic neurons. Developing a strategy of automating these parallel screening methods would be critical for minimizing the false positive rate for obtaining hits from a large scale screen.

Hits must also be validated for their efficacy by using a replicate dosing and exposure with the same chemical synthesized by a different company, and with a half-log dilution series by two orders of magnitude to ensure a true dose-response curve. Validation would ensure that any changes are directly caused by the chemical hit itself, as opposed to a contaminant introduced during synthesis, and ensure its reproducibility in inducing a reliable and reproducible phenotype. This would allow us to link individual chemical compounds to losses in dopaminergic neurons, and in changes of behavior correlating to a dopamine neuron loss parkinsonism phenotype. These linkages would therefore allow us to draw hypotheses and connections between potential chemical properties or compounds and the development of Parkinson's disease, thus allowing us to engage in

targeted searches for environmentally acquired compounds that could cause Parkinson's disease.

By developing this platform into an efficient assay of neurodegeneration, the zebrafish could be used in a variety of drug discovery and environmental toxicology studies in the future. An effective zebrafish model of Parkinson's disease has been created, and interventions and treatments to this model can be therefore investigated in a highly efficient manner through mass screening techniques that this project will develop. Drug discovery using live animal models provides biologically relevant answers that cannot yet be answered by using only *in vitro* tissue culture studies and pharmacokinetics, and the zebrafish model organism provides an excellent stepping stone towards the prospect of using *in vivo* systems for mass screening.

4.2 The mechanism of rotenone-induced dopamine neuron cell death

Rotenone has been previously explored for dopamine neuron toxicity in zebrafish, though no clear relationship between rotenone toxicity and dopamine neuron death was revealed due to rotenone's potent piscicidal properties (Bretaud *et al.*, 2004; Makhija and Jagtap, 2014). However, we were able to elicit an effect after careful titration of rotenone concentrations to nanomolar concentrations, lower than the concentrations used in Bretaud *et al.* (2004). We also found that zebrafish larvae mortality was decreased when we raised larvae at a temperature lower than is typically used to rear zebrafish in the lab. These factors allowed us to isolate a window of neurotoxicity independent of a window

of cytotoxicity. As a result, we were able to visualize the *in vivo* effects of rotenone-dependent neurotoxicity in zebrafish.

Rotenone reduced the number of dopamine neurons by 52.1% in the ventral diencephalon (figure 3.10D). Although Tay *et al.* (2011) suggests that the dopamine neurons in the posterior tuberculum of the ventral diencephalon map to the A11 nuclei based on a combination of transcription factor mapping and projection data, the A11 nuclei in mammals appears to be hypothalamic in nature, projects posteriorly and lacks *dopamine transporter* expression (Koblinger *et al.*, 2014). Instead, the efferent dopaminergic pathways from the posterior tuberculum appear to project to the subpallium (reviewed in Schweitzer *et al.*, 2012), a region which is thought to be homologous to the striatum (Rink and Wullimann, 2004). This suggests that the dopamine neurons in the posterior tuberculum of the ventral diencephalon are homologous to the nigrostriatal neurons that regulate the cortical motor signals in the subpallium. The magnitude of the decrease that we observed is consistent with the decreases in GFP-positive events seen with flow cytometry (figure 3.23B, 50.8%), and with the decreases seen in the *substantia nigra* of patients with Parkinson's disease (reviewed in Cheng *et al.*, 2010). Furthermore, larvae that have lost these neurons display a hypokinetic behavioral phenotype, demonstrate touch insensitivity, difficulty initiating movements and a decrease in total locomotion (figure 3.25). This combination of a hypokinetic behavioral phenotype in association with a decrease of ventral diencephalic dopamine neurons has also been characterized in a number of other models of dopamine neuron pathology or zebrafish models of

Parkinson's disease (table 4.1). This combined deficit in behavior and dopamine neuron distribution suggests that rotenone exposure is consistent with the mechanism of action of other mitochondrial complex I inhibitors, and also with genes that cause a loss of mitochondrial function in Parkinson's disease (Schapira *et al.*, 1990; reviewed in Sai *et al.*, 2012).

We were also able to visualize a decrease in other dopamine neuron populations aside from the ventral diencephalon. We observed a 31.4% decrease in dopamine neurons in the pretectum (figure 3.10A) of rotenone-exposed larvae. The pretectal nucleus is involved in the optokinetic response and pupillary light reflex, and oculomotor abnormalities have long been documented as a late stage clinical finding in patients with Parkinson's disease (Corin *et al.*, 1972). However, losses of dopamine neurons in the pretectum have not yet been definitively linked to the development of Parkinson's disease. We also observed a 33.3% decrease in dopamine neurons in the olfactory bulb of rotenone-exposed larvae. Anosmia (loss of olfaction) is not a cardinal finding of Parkinson's disease, but has been linked to the development and progression of Parkinson's disease (Haehner *et al.*, 2011; Cavaco *et al.*, 2015), and may even be an early manifestation of a subclinical stage (reviewed in Doty 2012). The olfactory bulb plays an important role in the Braak hypothesis (Braak *et al.*, 2003), whereby alpha-synuclein (SNCA) is thought to originate from a distal source such as the olfactory bulb (reviewed in Lim *et al.*, 2009), and spread rostrally to the *substantia nigra* via a prion-like mechanism of protein misfolding. The misfolded SNCA would then form aggregates and

Model of dopamine neuron loss	Mechanism of action	Dopamine neuron pathology	Locomotion phenotype	Citation
MPTP	Mitochondria complex I inhibition	Decreases in ventral diencephalon[1,2,3]	Bradykinesia[2,3], touch insensitivity[4]	[1]Lam *et al.*, 2005; [2]McKinley *et al.*, 2005; [3]Sallinen *et al.*, 2009; [4]Xi *et al.*, 2011b
Oxidopamine	Dopamine analogue, forms ROS	Loss of TH+ neurons	Decreased locomotion rescued with Vitamin E	Feng *et al.*, 2014
Lrrk2	Unknown	*Lrrk2* morphants lost dopamine neurons in the diencephalon[1,2]	Reduced locomotion, with shorter and less frequent episodes of movement[1]	[1]Sheng *et al.*, 2010; [2]Prabhudesai *et al.*, 2016
Parkin	Ubiquitin-E3 ligase, proteosome priming (cellular maintenance)	Decreases in the posterior tuberculum of the ventral diencephalon	No observable locomotor deficits	Flinn *et al.*, 2009
DJ-1	Responsible for the regulation of cellular oxidative stress	No decrease in the number of dopaminergic neurons. However, *DJ-1* morphants exposed to H_2O_2 and proteasome inhibitors demonstrated decreases in dopaminergic neurons.	Not assessed	Bretaud *et al.*, 2007
Pink1	Protein kinase critical to mitochondrial function. *Pink1* morphants demonstrate increased apoptosis[1]	Impaired neuronal patterning within DC2, 4 and 5 of ventral diencephalon with no apparent loss of neurons. Shortened or absent projections to the subpallium[2]	Tactile insensitivity[2]; decreased locomotion[2]	[1]Anichtchik *et al.*, 2008; [2]Xi *et al.*, 2010
Parl	Mitochondrial inner membrane protease that interacts with both *pink1* and *parkin*. Murine *parl* mutants demonstrate cristae remodeling and widespread apoptosis	Impaired neuronal patterning within DC2, 4 and 5 of ventral diencephalon	Not assessed	Noble *et al.*, 2012

Table 4.1: Comparison of various zebrafish models of dopamine neuron loss and Parkinson's disease.
A systematic literature review of the various models of Parkinson's disease shows that most environmental and genetic models act through mitochondrial inhibition, cause a reduction in the ventral diencephalic dopamine neuron population, and result in a locomotion phenotype.

tangles, the main form of Lewy bodies, and cause further misfolding of native SNCA and dopamine neuron dysfunction (reviewed in Visanji *et al.*, 2013). However, although this theory remains controversial and not universally accepted (reviewed in Burke *et al.*, 2008), the loss of dopamine neurons in the olfactory bulb of patients with Parkinson's disease remains a persistent yet oft overlooked finding of Parkinson's disease. Since zebrafish lack endogenous SNCA and do not form Lewy bodies in their dysfunctional dopamine neurons, the loss of dopamine neurons in the olfactory bulb of rotenone-exposed of zebrafish may demonstrate a mechanism of neurotoxicity independent of the Braak hypothesis.

Rotenone appears to precipitate ROS-mediated damage, inducing a cascade of Bax-a, caspase 3 and caspase 9 apoptosis signaling proteins to induce programmed cell death in dopamine neurons. Rotenone-exposed larvae demonstrated an increased number of foci of caspase activity in their dopaminergic clusters, particularly in the ventral diencephalon (figure 3.19). Our data show an increase in Bax-a translocation to the mitochondria in rotenone-exposed larvae (figure 3.20B) suggesting the engagement of an apoptotic cascade. Additionally, we also observed dissociation of high molecular weight Bax-a complexes (figure 3.20A), a decrease in high molecular weight Bcl complexes (figure 3.20C) and an increase high molecular weight Bad proteins (figure 3.20B). Anti-apoptotic Bcl proteins will complex with pro-apoptotic proteins such as Bax to sequester their activity, and their dissociation is necessary for the engagement of the apoptotic cascade. However, Bad is a pro-apoptotic protein that acts by sequestering anti-apoptotic proteins

like Bcl in a heterodimeric complex. Therefore, these observations suggest that rotenone exposure engages an apoptotic cascade. Our flow cytometry data from dissociated cells from rotenone-exposed larvae were able to show mitochondrial damage in GFP-positive events (figure 3.23). We infer that these GFP-positive events are individual dopamine neurons, and that their increased uptake of MitoTracker Deep Red stain suggests that rotenone is causing mitochondrial membrane depolarization in these rotenone-exposed neurons. We were also able to visualize foci of oxidative stress with our MitoSOX staining of live zebrafish larvae (figure 3.12), and although we were unable visualize these oxidative foci in the diencephalon of these rotenone-exposed larvae. However, the context provided by these data taken together suggest that rotenone generates superoxide radicals from mitochondrial damage, causing the initiation of an apoptotic pathway in these dopamine neurons. These data are supported by previous studies confirming that rotenone toxicity *in vivo* leads to oxidative damage to the mitochondria, and cell death in both *ex vivo* animal tissues and *in vivo* studies with rats (Scherer *et al.*, 2003; Cannon *et al.*, 2009) which is consistent with mitochondrial dysfunction seen in patients with Parkinson's disease (Penn *et al.*, 1995; Navarro *et al.*, 2009). Rotenone is a potent inhibitor of mitochondrial complex I (Li *et al.*, 2003). Rotenone can strongly bind to complex I and prevent the transfer of electrons along the electron transport chain in the process of oxidative phosphorylation. Inhibition of complex I causes an accumulation of electrons that cannot be shuttled onto complex III via coenzyme Q (reviewed in Sazanov, 2015). This accumulation of electrons in an oxygen-rich milieu along the mitochondrial

inner membrane provides an ideal environment for the conversion of oxygen molecules into superoxide free radicals, one of the main reactive oxygen species.

There was an overall decrease in *drd1* mRNA expression in 3 dpf embryos and 5 dpf larvae exposed to rotenone. Zebrafish express two homologues of dopamine receptor D2 known as *drd2a* and *drd2b*, and their mRNA expression is generally lowered after rotenone exposure, with *drd2a* decreasing dramatically in 5 dpf and 7 dpf larvae, and *drd2b* decreasing immediately following rotenone exposure in 3 dpf embryos, and remaining low through 7 days of development. These findings are particularly interesting because they shed light on dopamine regulation post-rotenone exposure. In mammals, the *substantia nigra* exerts regulatory control over different regions of the basal ganglia through its modulation of the GABAergic striatopallidal neurons. These GABAergic neurons that connect the striatum to the *globus pallidus* express dopamine receptors that modulate their activity. Secretion of dopamine acts on the direct pathway by decreasing the amount of GABA produced by the *globus pallidus interna* via D_1-like dopamine receptors, so inhibition of the suppressive signals from the *globus pallidus interna* neurons will therefore increase the acceptance of thalamic motor signals. The indirect pathway has the opposite effect, and secretion of dopamine acts to cause inhibition of the *globus pallidus externa* via D_2-like dopamine receptors, indirectly promoting the transmission of suppressive signals from the the *globus pallidus interna* neurons exclude thalamic motor signals. As mentioned previously, these pathways work in parallel to control the overall net signal transmission from the motor cortex (reviewed in Calabresi

et al., 2014). The decrease in *drd1* mRNA levels is observed at 3 dpf (48h after rotenone exposure), when embryos experience the greatest amount of caspase activity. A decrease in bioavailable dopamine due to an absence of neurons in the structures homologous to the nigrostriatal pathway would result in a relative decrease in the acceptance of motor signals. This imbalance may be corrected with a concomitant downregulation of *drd1* mRNA expression. If this imbalance is indeed linked to the posterior tuberculum's modulatory effect on subpallial neurons, the decrease in *drd2a* and *drd2b* mRNA expression may suggest a reduction in inhibitory subpallial activity secondary to dopamine neuron loss. A compensatory decrease in the expression of *drd1* mRNA expression may therefore act to restore the balance between direct and indirect mechanisms of subpallium motor modulation. By 5 dpf, the expression of *drd1*, *drd2a* and *drd2b* appears to undergo an equally relative reduction (36.4%, 46.7%, and 37.9% respectively) in rotenone-exposed larvae relative to DMSO controls, suggesting that the regulation of their expression may be linked. The balance in expression between *drd1* and the *drd2* genes provides an interesting avenue of exploration regarding the balance of downstream post-synaptic direct and indirect pathway signaling. Our observation that dopamine receptor mRNA expression engages in a concomitant decrease rather than a compensatory increase during dopamine deficiency is consistent with observations made by Barreto-Valer *et al.* (2012). However, dopamine receptors play a critical role in anxiety-like behavior and these implications will be discussed further in section 4.5.

4.3 Ascorbic acid rescue of rotenone-exposed zebrafish

When we exposed our zebrafish embryos to rotenone, we observed that exposure to concentrations of rotenone greater than 100nM caused embryonic death. Conversely, exposure of zebrafish embryos to concentrations of rotenone less than 1nM demonstrated few to no changes in either morphology, zebrafish behavior, or dopamine neuron distribution. These observations suggest that below 1nM, rotenone does not exert an inhibitory effect sufficient to cause biologically relevant mitochondrial complex I inhibition, whereas above 100nM, rotenone causes embryonic death through inhibition of mitochondrial complex I in all cells. However, exposure of embryos to an intermediate dose of rotenone allowed us to visualize a biological effect with the loss of dopamine neurons and a subsequent behavioral phenotype, suggesting that dopamine neurons are more susceptible to ROS-mediated damage. While our data suggest that rotenone causes oxidative damage, they also demonstrate that anti-oxidant effects contribute to neuroprotection of dopamine neurons when neurons are freely permeable to antioxidant compounds. We were able to show that rotenone-induced ROS damage can be partially reversed by co-treating rotenone-exposed larvae with 200μM ascorbic acid. Co-treatment with ascorbate demonstrated a decrease in oxidative foci (figure 3.12), a partial rescue of the number of dopamine neurons lost (figure 3.29), and a partial restoration of larval locomotion (figure 3.30) in rotenone-exposed larvae.

We hypothesize that these dopamine neurons experience a higher-than-average oxidative load due to the highly oxidizing nature of dopamine synthesis (reviewed in Miyazaki and

Asanuma, 2008; Meiser *et al.*, 2013), as well as the generation of dopamine metabolites that easily form free radicals and induce neuronal toxicity (Goldstein *et al.*, 2013).

Introduction of rotenone and the inhibition of mitochondrial complex I predisposes these neurons to the formation of superoxide free radicals and other reactive oxygen species (ROS) that can overwhelm endogenous organelles that act to control oxidative stress. This accumulation of ROS leads to the depletion of the peroxisomes and lysosomes that regularly act as endogenous controls against oxidative stress damage. Addition of exogenous anti-oxidants such as ascorbic acid which are freely permeable and water soluble ameliorate the damage caused by complex I inhibitors, such as rotenone. Unfortunately, these findings do not necessarily implicate the use of ascorbate as an anti-parkinsonian medication. Pomegranate juice is a rich source of anti-oxidants, but was recently discovered to exacerbate oxidative stress and nigrostriatal degeneration in the rotenone-model of Parkinson's disease in Lewis rats (Tapias *et al.*, 2014).

4.4 Regenerative potential of adult zebrafish

Zebrafish possess a powerful regenerative ability that extends to their CNS (Reimer *et al*., 2013; Fleish *et al.*, 2011). We first observed the potential for regeneration in adult zebrafish raised from rotenone-exposed larvae when we decided to examine them for lasting deficits caused by exposure. Whilst larvae exposed to rotenone demonstrated touch insensitivity and a hypokinetic phenotype (figure 3.25), adults no longer demonstrated any significant difference in capability for locomotion. The regenerative

capacity of zebrafish appears responsible for the absence of dopamine neuron deficits in adults exposed to rotenone. We visualized frozen sections of the adult brain from zebrafish exposed to rotenone as embryos and were not able to visualize the marked differences that we had observed in the larval stages of rotenone exposure (figure 3.35). The changes that we observed to noradrenergic regions of the brain such as the locus coeruleus were no longer present (figure 3.36), and dopamine transporter mRNA levels had partially recovered (figure 3.37).

Zebrafish are unlike other mammalians with their capacity for brain regeneration. Adult zebrafish will fully recover from stab lesions (März *et al.*, 2011), and the adult zebrafish brain has a persistent population of radial glial cells with omnipotent regenerative capacity (reviewed in Alunni and Bally-Cuif, 2016). The regenerative capacity of dopamine neurons in the adult zebrafish brain has been the subject of intense study, implicating a number of transcription factors for cell signaling in the ability for adult zebrafish to regenerate lost dopamine neuron populations. The population of dopamine neurons in the adult brain appears to be maintained with a balance of TGF and Wnt signals (Lints and Emmons, 1999; Ohyama *et al.*, 2005; Castelo-Branco and Arenas, 2006) where mutant embryos lacking these signaling proteins demonstrated a loss of dopaminergic neurons, particularly in the ventral diencephalon. Conversely, overexpression studies of Wnt yielded an overpopulation of dopamine neurons in these ventral diencephalic clusters (Russek-Blum *et al.*, 2008). Delta/Notch signaling also

appears to play a critical role in dopamine neuron neurogenesis and maintenance of adult dopaminergic neuron progenitor pools (Mahler *et al.*, 2010).

Therefore, we hypothesize that rotenone will cause dopaminergic neuron loss in the larva, but these deficits will not extend into adulthood for zebrafish larva exposed to rotenone because of the powerful regenerative capacity of the adult zebrafish brain. The extent of recovery appears to manifest in the late juvenile stages, where the number of dopamine neurons appears to begin repopulating by 14 dpf. This regenerative potential does not appear to be limited to the dopaminergic neuron population, because we were also able to observe deficits to the locus coeruleus at 5 dpf recover by 14 dpf. The number of dopamine neurons does not appear significantly different in frozen sections between brains from rotenone-exposed zebrafish by 60 dpf. Furthermore, the extent of the decrease in dopamine transporter mRNA expression is not as dramatic as seen in larval stages, strongly suggesting that there is some degree of CNS recovery from rotenone exposure by zebrafish adulthood.

4.5 Dopamine receptor dysregulation results in adult zebrafish behavior phenotype

Although we were not able to visualize a decrease in the number of dopamine neurons in adult zebrafish exposed to rotenone, we were able to visualize a behavioral phenotype that we attributed to an unexpected increase in *drd1* mRNA expression. As mentioned previously, the proper regulation of both dopamine levels and dopamine receptor levels is critical to the proper function of the dopaminergic pathways in the vertebrate brain. An

imbalance in these levels may cause a variety of pathologies, and the imbalance between dopamine receptor D1 and available dopamine has been linked to the negative symptoms of schizophrenia. These symptoms include emotional withdrawal, avolition, and apathy, which are linked to a deficit in D1 dopamine receptor signaling in the prefrontal cortex of affected individuals (Okubo *et al.*, 1997). Although these manifestations of human behavior do not easily translate to specific behavioral findings in zebrafish, the behavioral profiles of dopaminergic activation between zebrafish and rats show remarkable similarities (Ek *et al.*, 2016), thus suggesting some degree of similarity between the dopaminergic control of behavior in vertebrates. We observed that adult zebrafish exposed to rotenone as embryos demonstrated a series of anxiety-like behaviors, such as tendency to avoid exploring their tank as well as avoidance of well-lit areas of the tank. We initially investigated whether we were able to attribute the anxiety-like behavior to abnormalities in the locus coeruleus. The locus coeruleus is a hindbrain structure responsible for stress and panic responses, but we were not able to visualize any changes to this structure in 14 dpf larvae (figure 3.36). However, we observed that these adult zebrafish also demonstrated a significant increase in *drd1* mRNA levels (figure 3.37).

Dopamine receptor D1 has been linked to a variety of behavioral changes in adult zebrafish, with antagonism of the D1 dopamine receptor appearing to disrupt social preferences, resulting in the avoidance of shoaling behavior in treated adults (Scerbina *et al.*, 2012). Furthermore, anxiety-like behavior was also observed in adult zebrafish

exposed to a dopamine receptor D1 antagonist (Tran *et al.*, 2015), suggesting that anxiety-like behavior manifests as a consequence of perceived low dopamine levels in the brains of adult zebrafish. An increase in *drd1* mRNA levels will yield an increased synthesis of dopamine receptor D1, and without a concomitant increase in dopamine levels in the brain, these D1 dopamine receptors will experience a paucity of dopamine, leading to similar anxiety-like behaviors. These findings are suggestive that the compensatory increase in *drd1* is responsible for the anxiety-like behavior phenotype seen in adult zebrafish exposed to rotenone.

4.6 Deep sequencing potential of dopamine neurons exposed to rotenone

Zebrafish are an excellent model organism for experiments that require a high yield of biological material. We were able to isolate and enrich a population of GFP-positive events from Tg(*dat:EGFP*) embryos, corresponding to green fluorescent dopamine neurons from these transgenic zebrafish. We were also able to successfully produce cDNA from an enriched population of dopaminergic neurons by using about 400 embryos. This isolate demonstrated an increased relative abundance of *dopamine transporter* (*dat*) mRNA, suggesting that the majority of the isolates were dopaminergic in nature. Isolates were made from embryos exposed to rotenone or DMSO, and demonstrated differences in *dat* mRNA levels. However, we were not able to examine for other transcriptional changes in gene expression. The transcriptome of dopamine neurons exposed to rotenone could subsequently be characterized by deep sequencing (RNAseq) for changes in comparison to DMSO-exposed dopamine neurons. Results from RNAseq

would highlight the transcriptional changes secondary to oxidative stress, and allow discovery and hypothesis generation for mechanisms of compensation and neuroprotection against these insults.

High quality transcriptomic sequencing is dependent on our ability to obtain a homogeneous population of cells. Therefore, in order to perform high quality deep sequencing, RNAseq should be performed on a highly homogenous cell population that has been isolated from FACS-enriched transgenic embryo tissue exposed to either rotenone or DMSO. The specificity of the isolated cell population can be increased by using embryos from a transgenic zebrafish line highly specific for dopamine neuron fluorescence. In our Tg(*dat:EGFP*) embryos, GFP is expressed in dopamine neuron clusters within the olfactory bulb, telencephalon, midbrain, and hindbrain, but a small contribution to the population of fluorescently-labeled cells originates from non-specific fluorescence in the cells of the developing jaw cartilages. This nonspecific GFP expression in jaw chondrocytes did not appear to affect our results from qPCR on FACS-enriched cells, but will present a challenge to our goal of enriching a homogeneous population of dopaminergic neurons without contamination. To address this, we could create a double-transgenic line by cross-breeding our transgenic Tg(*dat:EGFP*) zebrafish with a Tg(*elavl3:mCherry*) transgenic line. Since Elavl3 is a neuron-specific RNA binding protein that serves as a pan-neuronal marker (Kudoh *et al.*, 2001), transgenic Tg(*elavl3:mCherry*) embryos will express red fluorescent mCherry proteins in all neuronal tissue. Therefore, by adding a second transgenic marker, dopamine neurons can

be selectively identified in these double transgenic zebrafish by their combined red and green fluorescence. Cell sorting performed with two fluorescent channels will only select for double fluorescent dopamine neurons, and will exclude any cells that are non-specifically fluorescent (such as jaw cartilages or other neurons). This homogeneous population of enriched cells can then be sent for deep sequencing to highlight transcriptional changes secondary to rotenone exposure.

4.7 Translation of results to human studies

Rotenone is a pesticide that has been used extensively in commercial agriculture and aquaculture. Although the vector of environmental exposure to rotenone differs between humans and zebrafish, occupational exposure to rotenone has been associated with an increased risk of developing Parkinson's disease. However, it is not presently clear what the unsafe exposure of rotenone is for humans. Rotenone is a lipid-soluble compound, and was dissolved in DMSO before being added to the fish water in our experiments. Furthermore, the zebrafish has a permeable blood-brain barrier during early development, and exhibits a heightened biological sensitivity to compounds dissolved in their growth medium. Although humans would not find themselves constantly exposed to this pesticide, prolonged exposure may result in the rotenone becoming trapped and dissolved in adipose tissue. Our work was able to show that even at nanomolar concentrations, rotenone has a biological effect by killing dopamine neurons in zebrafish. Subsequently, although the linkage between rotenone dosing in zebrafish and the occupational exposure of humans to rotenone is not presently established, the release of low concentrations of

bio-accumulated rotenone from lipid stores secondary to occupational exposure may represent a clear risk factor for the development of Parkinson's disease.

The difficulty in translating an effective dose of a small molecule in an animal model to a biologically relevant exposure in humans remains a persistent challenge. In any animal model, a number of factors will affect our exposure parameters, namely the absorption, distribution, metabolism, excretion, and toxicity (ADMET) criteria of pharmacokinetics, which vary from molecule to molecule and organism to organism. We observed that exposing 24 hpf zebrafish to between 30nM and 100nM of rotenone was sufficient to induce apoptosis in the dopamine neurons in the ventral diencephalon by 3 dpf, and cause lasting deficits to the dopamine neuron population by 7 dpf. However, exposing zebrafish to concentrations of rotenone greater than 100nM resulted in a severe increase in larval mortality. Ideally, we can adapt our experimental procedures to account for differences in metabolism, excretion and exposure concentrations, but much work remains to be done to translate these findings into clinically relevant conclusions regarding occupational exposures of individuals to this commercially available and widely accessible complex I inhibiting agent.

Conclusions

The primary aim of this project was to develop zebrafish as a model for environmentally-induced Parkinson's disease and further characterize the physiologic changes in response to dopamine neuron loss. We initially performed a small scale screen for a dopamine neuron loss phenotype from 7 compounds that have been linked to the development of Parkinson's disease. Although this small scale screen of small molecules on zebrafish embryos presented with many challenges in execution, we were able to identify that rotenone, a commercially available compound with insecticidal and piscicidal properties preferentially kills dopamine neurons in developing zebrafish embryos. Rotenone was able to exert its neurotoxic effect at nanomolar concentrations, causing a behavioral phenotype consistent with other zebrafish models of Parkinson's disease. We were also able to confirm this rotenone-induced dopamine neuron death using molecular methods, and identify that the rotenone-induced dopamine neuron death is caused through an increase in oxidative stress. This oxidative stress disproportionately affects the dopamine neurons, inducing an apoptotic cascade through mitochondrial damage and Bax-a signaling. Furthermore, the extent of dopamine neuron loss and severity of the behavioral phenotype caused by rotenone exposure could be partially ameliorated with exposure to antioxidants such as ascorbic acid, supporting our oxidative-stress hypothesis and demonstrating that endogenous antioxidant mechanisms are being overwhelmed with rotenone exposure. We were also able to demonstrate that dopamine receptor mRNA levels were being downregulated shortly after rotenone exposure, followed by an upregulation in *dopamine receptor D1* mRNA expression 6 days after rotenone exposure.

Lastly, although we were able to demonstrate that adult zebrafish raised from embryos exposed to rotenone displayed anxiety-like behaviors, in association with abnormalities in these adult zebrafish had no lasting deficits to their dopamine neuron population.

The findings of this project allow us deeper insight into the environmental factors that influence dopamine neuron survival, and the mechanisms by which pesticides such as rotenone can cause dopamine neuron loss. We were able to show that oxidative stress saliently affects the health of dopamine-producing neurons, and we were also able to obtain some insight into regulatory mechanisms that govern the transcription of genes linked to dopamine physiology. These results will allow us to characterize the physiological mechanisms of neuroprotection against oxidative stress damage to dopamine neurons, and allow for discovery of potential neuroprotective agents against these insults.

References

Alunni A, Bally-Cuif L. 2016. A comparative view of regenerative neurogenesis in vertebrates. *Development*. **143**(5):741-53.

Anichtchik O, Diekmann H, Fleming A, Roach A, Goldsmith P, Rubinsztein DC. 2008. Loss of PINK1 function affects development and results in neurodegeneration in zebrafish. *J Neurosci.* **28**(33):8199-207.

Aschner M, Erikson KM, Herrero Hernández E, Tjalkens R. 2009. Manganese and its role in Parkinson's disease: from transport to neuropathology. *Neuromolecular Med.* **11**(4):252-66.

Bai Q, Mullett SJ, Garver JA, Hinkle DA, Burton EA. 2006. Zebrafish DJ-1 is evolutionarily conserved and expressed in dopaminergic neurons. *Brain Res.* **1113**(1): 33-44.

Barreto-Valer K, López-Bellido R, Macho Sánchez-Simón F, Rodríguez RE. 2012. Modulation by cocaine of dopamine receptors through miRNA-133b in zebrafish embryos. *PLoS One*. **7**(12):e52701.

Beaulieu JM, Gainetdinov RR. 2011. The physiology, signaling, and pharmacology of dopamine receptors. *Pharmacol Rev.* **63**(1):182-217.

Berman J, Payne E, Hall C. 2012. The zebrafish as a tool to study hematopoiesis, human blood diseases, and immune function. *Adv Hematol.* **2012**:425345.

Best JD and Alderton WK. 2008. Zebrafish: An *in vivo* model for the study of neurological diseases. *Neuropsychiatr Dis Treat.* **4**(3):567–76.

Betarbet R, Sherer TB, MacKenzie G, Garcia-Osuna M, Panov AV, Greenamyre JT. 2000. Chronic systemic pesticide exposure reproduces features of Parkinson's disease. *Nat Neurosci.* **3**(12):1301-6.

Braak H, Sandmann-Keil D, Gai W, Braak E. 1999. Extensive axonal Lewy neurites in Parkinson's disease: a novel pathological feature revealed by α-synuclein immunocytochemistry. *Neurosci Lett*. **265**(1):67-9.

Braak H, Del Tredici K, Rüb U, de Vos RA, Jansen Steur EN, Braak E. 2003. Staging of brain pathology related to sporadic Parkinson's disease. *Neurobiol Aging.* **24**(2):197-211.

Bretaud S, Allen C, Ingham PW, Bandmann O. 2007. p53-dependent neuronal cell death in a DJ-1-deficient zebrafish model of Parkinson's disease. *J Neurochem*. **100**(6):1626-35.

Bretaud S, Lee S, Guo S. 2004. Sensitivity of zebrafish to environmental toxins implicated in Parkinson's disease. *Neurotoxicol Teratol.* **26**(6):857–64.

Brette F, Orchard C. 2007. Resurgence of cardiac t-tubule research. *Physiology*. **22**:167-73.

Broughton RE, Milam JE, Roe BA. 2001. The complete sequence of the zebrafish (*Danio rerio*) mitochondrial genome and evolutionary patterns in vertebrate mitochondrial DNA. *Genome Res*. **11**(11):1958-67.

Cannon JR, Tapias V, Na HM, Honick AS, Drolet RE, Greenamyre JT. 2009. A highly reproducible model of Parkinson's disease. *Neurobiol Dis.* **34**(2):279-90.

Cachat J, Kyzar E, Collins C, Gaikwad S, Green J, Roth A, El-Ounsi M, Davis A, Pham M, Landsman S and Kalueff AV. 2013. Unique and potent effects of acute ibogaine on zebrafish: the developing utility of novel aquatic models for hallucinogenic drug research. *Behav Brain Res* **236**:258-69.

Calabresi P, Picconi B, Tozzi A, Ghiglieri V, Di Filippo M. 2014. Direct and indirect pathways of basal ganglia: a critical reappraisal. *Nat Neurosci*. **17**(8):1022-30.

Cavaco S, Gonçalves A, Mendes A, Vila-Chã N, Moreira I, Fernandes J, Damásio J, Teixeira-Pinto A, Bastos Lima A. 2015. Abnormal Olfaction in Parkinson's Disease is Related to Faster Disease Progression. *Behav Neurol.* **2015**:976589.

Chen TH, Wang YH, Wu YH. 2011. Developmental exposures to ethanol or dimethylsulfoxide at low concentrations alter locomotor activity in larval zebrafish: implications for behavioral toxicity bioassays. *Aquat Toxicol.* **102**(3-4):162-6.

Cheng HC, Ulane CM, Burke RE. 2010. Clinical progression in Parkinson disease and the neurobiology of axons. *Ann Neurol.* **67**(6):715-25.

Circu ML, Aw TY. 2010. Reactive oxygen species, cellular redox systems, and apoptosis. *Free Radic Biol Med.* **48**(6):749-62.

Clark IE, Dodson MW, Jiang C, Cao JH, Huh JR, Seol JH, Yoo SJ, Hay BA, Guo M. 2006. Drosophila pink1 is required for mitochondrial function and interacts genetically with parkin. *Nature*. **441**(7097):1162-6.

Corin MS, Elizan TS, Bender MB. 1972. Oculomotor function in patients with Parkinson's disease. *J Neurol Sci.* **15**(3):251-65.

Damier P, Hirsch EC, Agid Y, Graybiel AM. 1999. The *substantia nigra* of the human brain. II. Patterns of loss of dopamine-containing neurons in Parkinson's disease. *Brain.* **122**(8):1437-48.

Daubner SC, Le T, Wang S. 2011. Tyrosine hydroxylase and regulation of dopamine synthesis. *Arch Biochem Biophys.* **508**(1):1-12.

Davis KL, Kahn RS, Ko G, Davidson M. 1991. Dopamine in schizophrenia: a review and reconceptualization. *Am J Psychiatry.* **148**(11):1474-86.

Dodson MW, Guo M. 2007. Pink1, Parkin, DJ-1 and mitochondrial dysfunction in Parkinson's disease. *Curr Opin Neurobiol.* **17**(3):331-7.

Doty RL. 2012. Olfactory dysfunction in Parkinson disease. *Nat Rev Neurol.* **8**(6):329-39.

Eberhardt O, and Schulz JB. 2003. Apoptotic mechanisms and antiapoptotic therapy in the MPTP model of Parkinson's disease. *Toxicol Lett.* **139**(2–3):135-51.

Ek F, Malo M, Åberg Andersson M, Wedding C, Kronborg J, Svensson P, Waters S, Petersson P, Olsson R. 2016. Behavioral Analysis of Dopaminergic Activation in Zebrafish and Rats Reveals Similar Phenotypes. *ACS Chem Neurosci.* **7**(5):633-46.

Elsworth JD, Roth RH. 1997. Dopamine synthesis, uptake, metabolism, and receptors: relevance to gene therapy of Parkinson's disease. *Exp Neurol.* **144**(1):4-9.

Feng CW, Wen ZH, Huang SY, Hung HC, Chen CH, Yang SN, Chen NF, Wang HM, Hsiao CD, Chen WF. 2014. Effects of 6-hydroxydopamine exposure on motor activity and biochemical expression in zebrafish (*Danio rerio*) larvae. *Zebrafish*. **11**(3):227-39.

Fett ME, Pilsl A, Paquet D, van Bebber F, Haass C, Tatzelt J, Schmid B, Winklhofer KF. 2010. Parkin is protective against proteotoxic stress in a transgenic zebrafish model. *PLoS One*. **5**(7):e11783.

Filippi A, Mahler J, Schweitzer J, Driever W. 2010. Expression of the paralogous tyrosine hydroxylase encoding genes th1 and th2 reveals the full complement of dopaminergic and noradrenergic neurons in zebrafish larval and juvenile brain. *J Comp Neurol.* **518**(4):423–438

Filippi A, Mueller T, Driever W. 2014. *vglut2* and *gad* expression reveal distinct patterns of dual GABAergic versus glutamatergic cotransmitter phenotypes of dopaminergic and noradrenergic neurons in the zebrafish brain. *J Comp Neurol.* **522**(9):2019-37.

Fitzgerald P, Dinan TG. 2008. Prolactin and dopamine: what is the connection? A review article. *J Psychopharmacol.* **22**(2 Suppl):12-9.

Fleisch VC, Fraser B, Allison WT. 2011. Investigating regeneration and functional integration of CNS neurons: lessons from zebrafish genetics and other fish species. *Biochim Biophys Acta.* **1812**(3):364-80.

Fleury C, Mignotte B, Vayssière JL. 2002. Mitochondrial reactive oxygen species in cell death signaling. *Biochimie*. **84**(2-3):131-41

Flinn L, Mortiboys H, Volkmann K, Köster RW, Ingham PW, Bandmann O. 2009. Complex I deficiency and dopaminergic neuronal cell loss in parkin-deficient zebrafish (*Danio rerio*). *Brain.* **132**(6):1613-23.

Godoy R, Noble S, Yoon K, Anisman H, Ekker M. 2015. Chemogenetic ablation of dopaminergic neurons leads to transient locomotor impairments in zebrafish larvae. *J Neurochem.* **135**(2):249-60.

Goldstein DS, Sullivan P, Holmes C, Miller GW, Alter S, Strong R, Mash DC, Kopin IJ, Sharabi Y. 2013. Determinants of buildup of the toxic dopamine metabolite DOPAL in Parkinson's disease. *J Neurochem.* **126**(5):591-603.

Green J, Collins C, Kyzar E, Pham M, Roth A, Gaikwad S, Cachat J, Stewart AM, Landsman S, Grieco F, Tegelenbosch R, Noldus L and Kalueff AV. 2012. Automated high-throughput neurophenotyping of zebrafish social behavior. *J Neurosci Methods.* **210**:266-71.

Groenewegen HJ. 2003. The basal ganglia and motor control. *Neural Plast.* **10**(1-2): 107-20.

Gross A, McDonnell JM, Korsmeyer SJ. 1999. BCL-2 family members and the mitochondria in apoptosis. *Genes Dev.* **13**(15):1899-911.

Grossman L, Utterback E, Stewart A, Gaikwad S, Wong K, Elegante M, Tan J, Gilder T, Wu N, DiLeo J, Cachat J, Kalueff AV. 2010. Characterization of behavioral and endocrine effects of LSD on zebrafish. *Behav Brain Res.* **214**:277-84.

Haehner A, Hummel T, Reichmann H. 2014. Olfactory Loss in Parkinson's Disease. *J Parkinsons Dis.* **4**(2):189-95.

Howe K, Clark MD, Torroja CF, Torrance J, Berthelot C, Muffato M, Collins JE, Humphray S, McLaren K, Matthews L, McLaren S, Sealy I, Caccamo M, Churcher C,Scott C, Barrett JC, Koch R, Rauch GJ, White S, Chow W, Kilian B, Quintais

LT,Guerra-Assunção JA, Zhou Y, Gu Y, Yen J, Vogel JH, Eyre T, Redmond S, Banerjee R,Chi J, Fu B, Langley E, Maguire SF, Laird GK, Lloyd D, Kenyon E, Donaldson S,Sehra H, Almeida-King J, Loveland J, Trevanion S, Jones M, Quail M, Willey D, Hunt A, Burton J, Sims S, McLay K, Plumb B, Davis J, Clee C, Oliver K, Clark R, Riddle C, Elliot D, Threadgold G, Harden G, Ware D, Mortimore B, Kerry G, Heath P, Phillimore B, Tracey A, Corby N, Dunn M, Johnson C, Wood J, Clark S, Pelan S, Griffiths G, Smith M, Glithero R, Howden P, Barker N, Stevens C, Harley J, Holt K, Panagiotidis G, Lovell J, Beasley H, Henderson C, Gordon D, Auger K, Wright D, Collins J, Raisen C, Dyer L, Leung K, Robertson L, Ambridge K, Leongamornlert D, McGuire S, Gilderthorp R, Griffiths C, Manthravadi D, Nichol S, Barker G, Whitehead S, Kay M, Brown J, Murnane C, Gray E, Humphries M, Sycamore N, Barker D, Saunders D, Wallis J, Babbage A, Hammond S, Mashreghi-Mohammadi M, Barr L, Martin S, Wray P, Ellington A, Matthews N, Ellwood M, Woodmansey R, Clark G, Cooper J, Tromans A, Grafham D, Skuce C, Pandian R, Andrews R, Harrison E, Kimberley A, Garnett J, Fosker N, Hall R, Garner P, Kelly D, Bird C, Palmer S, Gehring I, Berger A, Dooley CM, Ersan-Ürün Z, Eser C, Geiger H, Geisler M, Karotki L, Kirn A, Konantz J, Konantz M, Oberländer M, Rudolph-Geiger S, Teucke M, Osoegawa K, Zhu B, Rapp A, Widaa S, Langford C, Yang F, Carter NP, Harrow J, Ning Z, Herrero J, Searle SM, Enright A, Geisler R, Plasterk RH, Lee C, Westerfield M, de Jong PJ, Zon LI, Postlethwait JH, Nüsslein-Volhard C, Hubbard TJ, Roest Crollius H, Rogers J, Stemple DL, Begum S, Lloyd C, Lanz C, Raddatz G, Schuster SC. 2013. The zebrafish reference genome sequence and its relationship to the human genome. *Nature.* **496**(7446):498-503.

Inden M, Kitamura Y, Abe M, Tamaki A, Takata K, Taniguchi T. 2011. Parkinsonian rotenone mouse model: reevaluation of long-term administration of rotenone in C57BL/6 mice. *Biol Pharm Bull.* **34**(1):92-6

Kalueff AV, Gebhardt M, Stewart AM, Cachat JM, Brimmer M, Chawla JS, Craddock C, Kyzar EJ, Roth A, Landsman S, Gaikwad S, Robinson K, Baatrup E, Tierney K, Shamchuk A, Norton W, Miller N, Nicolson T, Braubach O, Gilman CP, Pittman J, Rosemberg DB, Gerlai R, Echevarria D, Lamb E, Neuhauss SC, Weng W, Bally-Cuif L, Schneider H; 2013. Towards a comprehensive catalog of zebrafish behavior 1.0 and beyond. *Zebrafish*. **10**(1):70-86.

Kett LR, Dauer WT. 2012. Leucine-rich repeat kinase 2 for beginners: six key questions. *Cold Spring Harb Perspect Med.* **2**(3):a009407.

Kitada T, Tomlinson JJ, Ao HS, Grimes DA, Schlossmacher MG. 2012. Considerations regarding the etiology and future treatment of autosomal recessive versus idiopathic Parkinson disease. *Curr Treat Options Neurol.* **14**(3):230-40.

Koblinger K, Füzesi T, Ejdrygiewicz J, Krajacic A, Bains JS, Whelan PJ. 2014. Characterization of A11 neurons projecting to the spinal cord of mice. *PLoS One.* **9**(10):e109636.

Kokel D, Bryan J, Laggner C, White R, Cheung CY, Mateus R, Healey D, Kim S, Werdich AA, Haggarty SJ, Macrae CA, Shoichet B, Peterson RT. 2010. Rapid behavior-based identification of neuroactive small molecules in the zebrafish. Nat Chem Biol. **6**(3): 231-237.

Koonin EV, Makarova KS, Rogozin IB, Davidovic L, Letellier MC, Pellegrini L. 2003. The rhomboids: a nearly ubiquitous family of intramembrane serine proteases that probably evolved by multiple ancient horizontal gene transfers. *Genome Biol.* **4**(3):R19.

Kudoh T, Tsang M, Hukriede NA, Chen X, Dedekian M, Clarke CJ, Kiang A, Schultz S, Epstein JA, Toyama R, Dawid IB. 2001. A gene expression screen in zebrafish embryogenesis. Genome Res. **11**(12):1979-87.

Kyzar E, Collins C, Gaikwad S, Green J, Roths A, Monnig L, El-Ounsi M, Davis A, Freeman A, Capezio N, Stewart AM, Kalueff AV. 2012. Effects of hallucinogenic agents mescaline and phencyclidine on zebrafish behavior and physiology. *Prog Neuro-Psychopharmacol Biol Psychiatry.* **37**:194-202.

Lam CS, Korzh V, Strahle U. 2005. Zebrafish embryos are susceptible to the dopaminergic neurotoxin MPTP. *Eur J Neurosci.* **21**(6):1758-62.

Lang AE, Lozano AM. 1998. Parkinson's disease. First of two parts. *N Engl J Med.* **339**(15):1044-53.

Le Foll B, Gallo A, Le Strat Y, Lu L, Gorwood P. 2009. Genetics of dopamine receptors and drug addiction: a comprehensive review. *Behav Pharmacol*. **20**(1):1-17.

Li N, Ragheb K, Lawler G, Sturgis J, Rajwa B, Melendez JA, Robinson JP. 2003. Mitochondrial complex I inhibitor rotenone induces apoptosis through enhancing mitochondrial reactive oxygen species production. *J Biol Chem.* **278**(10):8516-25.

Lim SY, Fox SH, Lang AE. 2009. Overview of the extranigral aspects of Parkinson disease. *Arch Neurol.* **66**(2):167-72.

Linney E, Upchurch L, Donerly S. 2004. Zebrafish as a neurotoxicological model. *Neurotoxicol Teratol.* **26**(6):709-18.

Lulla A, Barnhill L, Bitan G, Ivanova MI, Nguyen B, O'Donnell K, Stahl MC, Yamashiro C, Klärner FG, Schrader T, Sagasti A, Bronstein JM. 2016. Neurotoxicity of the

Parkinson's Disease-Associated Pesticide Ziram Is Synuclein-Dependent in Zebrafish Embryos. *Environ. Health Perspect.* In press.

Ma C, Parng CL, Seng WL, Zhang C, Willett C, McGrath P. 2003. Zebrafish – An *in vivo* model for drug screening. *Innovations in Pharmaceutical Technologies* 38-45.

Makhija DT, Jagtap AG. 2014. Studies on sensitivity of zebrafish as a model organism for Parkinson's disease: Comparison with rat model. *J Pharmacol Pharmacother.* **5**(1):39-46.

März M, Schmidt R, Rastegar S, Strähle U. 2011. Regenerative response following stab injury in the adult zebrafish telencephalon. *Dev Dyn.* **240**(9):2221-31.

Massano J, Bhatia KP. 2012. Clinical Approach to Parkinson's Disease: Features, Diagnosis, and Principles of Management. *Cold Spring Harb Perspect Med.* **2**(6), a008870.

Mathur P, Guo S. 2010. Use of zebrafish as a model to understand mechanisms of addiction and complex neurobehavioral phenotypes. *Neurobiol Dis.* **40**(1):66-72.

McGrath P, Li CQ. 2008. Zebrafish: a predictive model for assessing drug-induced toxicity. *Drug Discov Today* **13**(9-10):394-401.

McKinley ET, Baranowski TC, Blavo DO, Cato C, Doan TN, Rubinstein AL. 2005. Neuroprotection of MPTP-induced toxicity in zebrafish dopaminergic neurons. *Brain Res Mol Brain Res.* **141**(2):128-37.

Meiser J, Weindl D, Hiller K. 2013. Complexity of dopamine metabolism. *Cell Commun Signal.* **11**(1):34.

Melo KM, Oliveira R, Grisolia CK, Domingues I, Pieczarka JC, de Souza Filho J, Nagamachi CY. 2015. Short-term exposure to low doses of rotenone induces developmental,biochemical, behavioral, and histological changes in fish. *Environ Sci Pollut Res Int.* **22**(18):13926-38.

Meredith GE, Rademacher DJ. 2011. MPTP mouse models of Parkinson's disease: an update. *J Parkinsons Dis.* **1**(1):19-33.

Miyazaki I, Asanuma M. 2008. Dopaminergic neuron-specific oxidative stress caused by dopamine itself. *Acta Med Okayama.* **62**(3):141-50.

Moisan F, Spinosi J, Delabre L, Gourlet V, Mazurie JL, Bénatru I, Goldberg M, Weisskopf MG, Imbernon E, Tzourio C, Elbaz A. 2015. Association of Parkinson's

Disease and Its Subtypes with Agricultural Pesticide Exposures in Men: A Case-Control Study in France. *Environ Health Perspect.* **123**(11):1123-9.

Mrak RE, Griffin WS. 2007 Common inflammatory mechanisms in Lewy body disease and Alzheimer disease. *J Neuropathol Exp Neurol*. **66**(8):683-6.

Mugoni V, Camporeale A, Santoro MM. 2014. Analysis of oxidative stress in zebrafish embryos. *J Vis Exp.* **2014**:89.

Navarro A, Boveris A, Bández MJ, Sánchez-Pino MJ, Gómez C, Muntané G, Ferrer I. 2009. Human brain cortex: mitochondrial oxidative damage and adaptive response in Parkinson disease and in dementia with Lewy bodies. *Free Radic Biol Med.* **46**(12): 1574-80.

Noble S, Ismail A, Godoy R, Xi Y, Ekker M. 2012. Zebrafish Parla- and Parlb-deficiency affects dopaminergic neuron patterning and embryonic survival. *J Neurochem.* **122**(1): 196-207.

Noble S, Godoy R, Affaticati P, Ekker M. 2015. Transgenic Zebrafish Expressing mCherry in the Mitochondria of Dopaminergic Neurons. *Zebrafish.* **12**(5):349-56.

Okubo Y, Suhara T, Suzuki K, Kobayashi K, Inoue O, Terasaki O, Someya Y, Sassa T, Sudo Y, Matsushima E, Iyo M, Tateno Y, Toru M. Decreased prefrontal dopamine D1 receptors in schizophrenia revealed by PET. *Nature*. **385**(6617):634-6.

Olanow CW. 2004. Manganese-induced parkinsonism and Parkinson's disease. *Ann N Y Acad Sci.* **1012**:209-23.

Pan-Montojo F, Anichtchik O, Dening Y, Knels L, Pursche S, Jung R, Jackson S, Gille G, Spillantini MG, Reichmann H, Funk RH. 2010. Progression of Parkinson's Disease Pathology Is Reproduced by Intragastric Administration of Rotenone in Mice. *PLoS ONE.* **5**(1): e8762.

Park J, Lee SB, Lee S, Kim Y, Song S, Kim S, Bae E, Kim J, Shong M, Kim JM, Chung J. 2006. Mitochondrial dysfunction in Drosophila PINK1 mutants is complemented by parkin. *Nature.* **441**(7097):1157-61.

Parng C, Roy NM, Ton C, Lin Y, McGrath P. 2007. Neurotoxicity assessment using zebrafish. *J Pharmacol Toxicol Methods.* **55**(1):103-12.

Penn AM, Roberts T, Hodder J, Allen PS, Zhu G, Martin WR. 1995. Generalized mitochondrial dysfunction in Parkinson's disease detected by magnetic resonance spectroscopy of muscle. *Neurology.* **45**(11):2097-9.

Pezzoli G, Cereda E. 2013. Exposure to pesticides or solvents and risk of Parkinson disease. *Neurology*. **80**(22):2035-41.

Pickrell AM, Youle RJ. 2015. The roles of PINK1, parkin, and mitochondrial fidelity in Parkinson's disease. *Neuron.* **85**(2):257-73.

Porras G, Li Q, Bezard E. 2012. Modeling Parkinson's disease in primates: The MPTP model. *Cold Spring Harb Perspect Med.* **2**(3):a009308.

Prabhudesai S, Bensabeur FZ, Abdullah R, Basak I, Baez S, Alves G, Holtzman NG, Larsen JP, Møller SG. 2016. LRRK2 knockdown in zebrafish causes developmental defects, neuronal loss, and synuclein aggregation. *J Neurosci Res.* **94**(8):717-35.

Radad K, Gille G, Rausch WD. 2005. Short review on dopamine agonists: insight into clinical and research studies relevant to Parkinson's disease. *Pharmacol Rep.* **57**(6): 701-12

Reimer MM, Norris A, Ohnmacht J, Patani R, Zhong Z, Dias TB, Kuscha V, Scott AL, Chen YC, Rozov S, Frazer SL, Wyatt C, Higashijima S, Patton EE, Panula P, Chandran S, Becker T, Becker CG. 2013. Dopamine from the brain promotes spinal motor neuron generation during development and adult regeneration. *Dev Cell.* **25**(5):478-91.

Ren G, Xin S, Li S, Zhong H, Lin S. 2011. Disruption of LRRK2 does not cause specific loss of dopaminergic neurons in zebrafish. *PLoS One.* **6**(6):e20630.

Ren G, Li S, Zhong H, Lin S. 2013. Zebrafish tyrosine hydroxylase 2 gene encodes tryptophan hydroxylase. *J Biol Chem.* **288**(31):22451-9.

Rihel J, Schier AF. 2012. Behavioral screening for neuroactive drugs in zebrafish. *Dev Neurobiol.* **72**(3):373-85.

Rink E, Wullimann MF. 2001. The teleostean (zebrafish) dopaminergic system ascending to the subpallium (striatum) is located in the basal diencephalon (posterior tuberculum). *Brain Res.* **889**(1-2):316-30.

Rink E, Wullimann MF. 2002. Connections of the ventral telencephalon and tyrosine hydroxylase distribution in the zebrafish brain (*Danio rerio*) lead to identification of an ascending dopaminergic system in a teleost. *Brain Res Bull.* **57**(3-4):385-7.

Rink E, Wullimann MF. 2004. Connections of the ventral telencephalon (subpallium) in the zebrafish (*Danio rerio*). *Brain Res.* **1011**(2):206-20.

Sai Y, Zou Z, Peng K, Dong Z. 2012. The Parkinson's disease-related genes act in mitochondrial homeostasis. *Neurosci Biobehav Rev.* **36**(9):2034-43.

Sallinen V, Torkko V, Sundvik M, Reenilä I, Khrustalyov D, Kaslin J, Panula P. 2009. MPTP and MPP+ target specific aminergic cell populations in larval zebrafish. *J Neurochem.* **108**(3):719-31.

Sanders LH, Greenamyre JT. 2013. Oxidative damage to macromolecules in human Parkinson disease and the rotenone model. *Free Radic Biol Med.* **62**:111-20.

Sazanov LA. 2015. A giant molecular proton pump: structure and mechanism of respiratory complex I. *Nat Rev Mol Cell Biol.* **16**(6):375-88.

Scerbina T, Chatterjee D, Gerlai R. 2012. Dopamine receptor antagonism disrupts social preference in zebrafish: a strain comparison study. *Amino Acids.* **43**(5):2059-72.

Schapira AH, Cooper JM, Dexter D, Clark JB, Jenner P, Marsden CD. 1990. Mitochondrial complex I deficiency in Parkinson's disease. *J Neurochem.* **54**(3):823-7.

Sheng D, Qu D, Kwok KH, Ng SS, Lim AY, Aw SS, Lee CW, Sung WK, Tan EK, Lufkin T, Jesuthasan S, Sinnakaruppan M, Liu J. 2010. Deletion of the WD40 domain of LRRK2 in Zebrafish causes Parkinsonism-like loss of neurons and locomotive defect. *PLoS Genet.* **6**(4):e1000914.

Sherer TB, Betarbet R, Testa CM, Seo BB, Richardson JR, Kim JH, Miller GW, Yagi T, Matsuno-Yagi A, Greenamyre JT. 2003. Mechanism of toxicity in rotenone models of Parkinson's disease. J Neurosci. **23**(34):10756-64.

Shulman JM, De Jager PL, Feany MB. 2011. Parkinson's disease: genetics and pathogenesis. *Annu Rev Pathol*. **6**:193-222

Sian J, Youdim MBH, Riederer P, Gerlach M. MPTP-Induced Parkinsonian Syndrome. In: Siegel GJ, Agranoff BW, Albers RW, et al., editors. Basic Neurochemistry: Molecular, Cellular and Medical Aspects. 6th edition. Philadelphia: Lippincott-Raven; 1999.

Simola N, Morelli M, Carta AR. 2007. The 6-hydroxydopamine model of Parkinson's disease. *Neurotox Res.* **11**(3-4):151-67.

Sulzer D, Cragg SJ, Rice ME. 2016. Striatal dopamine neurotransmission: regulation of release and uptake. *Basal Ganglia.* **6**(3):123-148.

Surmeier DJ. 2007. Calcium, ageing, and neuronal vulnerability in Parkinson's disease. *Lancet Neurol*. **6**(10):933-8.

Tapias V, Cannon JR, Greenamyre JT. 2014. Pomegranate juice exacerbates oxidative stress and nigrostriatal degeneration in Parkinson's disease. *Neurobiol Aging.* **35**(5): 1162-76.

Tay TL, Ronneberger O, Ryu S, Nitschke R, Driever W. 2011. Comprehensive catecholaminergic projectome analysis reveals single-neuron integration of zebrafish ascending and descending dopaminergic systems. *Nat Commun.* **2**:171

Taylor KM, Saint-Hilaire MH, Sudarsky L, Simon DK, Hersh B, Sparrow D, Hu H, Weisskopf MG. 2016. Head injury at early ages is associated with risk of Parkinson's disease. *Parkinsonism Relat Disord.* **23**:57-61.

Teng Y, Xie X, Walker S, Rempala G, Kozlowski DJ, Mumm JS, Cowell JK. Knockdown of zebrafish Lgi1a results in abnormal development, brain defects and a seizure-like behavioral phenotype. *Hum Mol Genet.* **19**(22):4409-20.

Thiffault C, Langston JW, Di Monte DA. 2000. Increased striatal dopamine turnover following acute administration of rotenone to mice. *Brain Res.* **885**:283-8

Tran S, Nowicki M, Muraleetharan A, Chatterjee D, Gerlai R. 2015. Differential effects of acute administration of SCH-23390, a D_1 receptor antagonist, and of ethanol on swimming activity, anxiety-related responses, and neurochemistry of zebrafish. *Psychopharmacology (Berl).* **232**(20):3709-18.

Trempe JF, Fon EA. 2013. Structure and Function of Parkin, PINK1, and DJ-1, the Three Musketeers of Neuroprotection. *Front Neurol.* **4**:38.

Tritsch, N. X., Ding, J. B., Sabatini, B. L. 2012. Dopaminergic neurons inhibit striatal output via non-canonical release of GABA. *Nature*. **490**(7419): 262-6.

Van Den Eeden SK, Tanner CM, Bernstein AL, Fross RD, Leimpeter A, Bloch DA, Nelson LM. 2003. Incidence of Parkinson's Disease: Variation by Age, Gender, and Race/ Ethnicity. *Am J Epidemiol.* **157**(11):1015-22.

Villegas R, Martin SM, O'Donnell KC, Carrillo SA, Sagasti A, Allende ML. Dynamics of degeneration and regeneration in developing zebrafish peripheral axons reveals a requirement for extrinsic cell types. *Neural Dev*. **7**:19.

Visanji NP, Brooks PL, Hazrati LN, Lang AE. 2013. The prion hypothesis in Parkinson's disease: Braak to the future. *Acta Neuropathol Commun*. **1**:2.

Wen L, Wei W, Gu W, Huang P, Ren X, Zhang Z, Zhu Z, Lin S, Zhang B. 2008. Visualization of monoaminergic neurons and neurotoxicity of MPTP in live transgenic zebrafish. *Dev Biol.* **314**(1):84-92.

Westerfield M (1995) The Zebrafish Book: A Guide for the Laboratory Use of Zebrafish (*Danio rerio*). University of Oregon Press, Eugene, OR.

Whitworth AJ, Lee JR, Ho VM, Flick R, Chowdhury R, McQuibban GA. 2008. Rhomboid-7 and HtrA2/Omi act in a common pathway with the Parkinson's disease factors Pink1 and Parkin. *Dis Model Mech.* **1**(2-3):168-74.

Xi Y, Ryan J, Noble S, Yu M, Yilbas AE, Ekker M. 2010. Impaired dopaminergic neuron development and locomotor function in zebrafish with loss of pink1 function. *Eur J Neurosci.* **31**(4):623-33.

Xi Y, Noble S, Ekker M. 2011. Modeling neurodegeneration in zebrafish. *Curr Neurol Neurosci Rep.* **11**(3):274-82.

Xi Y, Yu M, Godoy R, Hatch G, Poitras L, Ekker M. 2011. Transgenic zebrafish expressing green fluorescent protein in dopaminergic neurons of the ventral diencephalon. *Dev Dyn.* **240**:2539-47.

Xu C, Tabebordbar M, Iovino S, Ciarlo C, Liu J, Castiglioni A, Price E, Liu M, Barton ER, Kahn CR, Wagers AJ, Zon LI. 2013. A zebrafish embryo culture system defines factors that promote vertebrate myogenesis across species. *Cell*. **155**(4):909-21.

Yamamoto K, Ruuskanen JO, Wullimann MF, Vernier P. 2010. Two tyrosine hydroxylase genes in vertebrates new dopaminergic territories revealed in the zebrafish brain. *Mol Cell Neurosci.* **43**(4):394–402.

Yamamoto K, Ruuskanen JO, Wullimann MF, Vernier P. 2011. Differential expression of dopaminergic cell markers in the adult zebrafish forebrain. *J Comp Neurol.* **519**(3):576–98.

Zharikov AD, Cannon JR, Tapias V, Bai Q, Horowitz MP, Shah V, El Ayadi A, Hastings TG, Greenamyre JT, Burton EA. 2015. shRNA targeting α-synuclein prevents neurodegeneration in a Parkinson’s disease model. *J Clin Invest.* **125**(7), 2721–-5.